



Hengifoss waterfall in Iceland

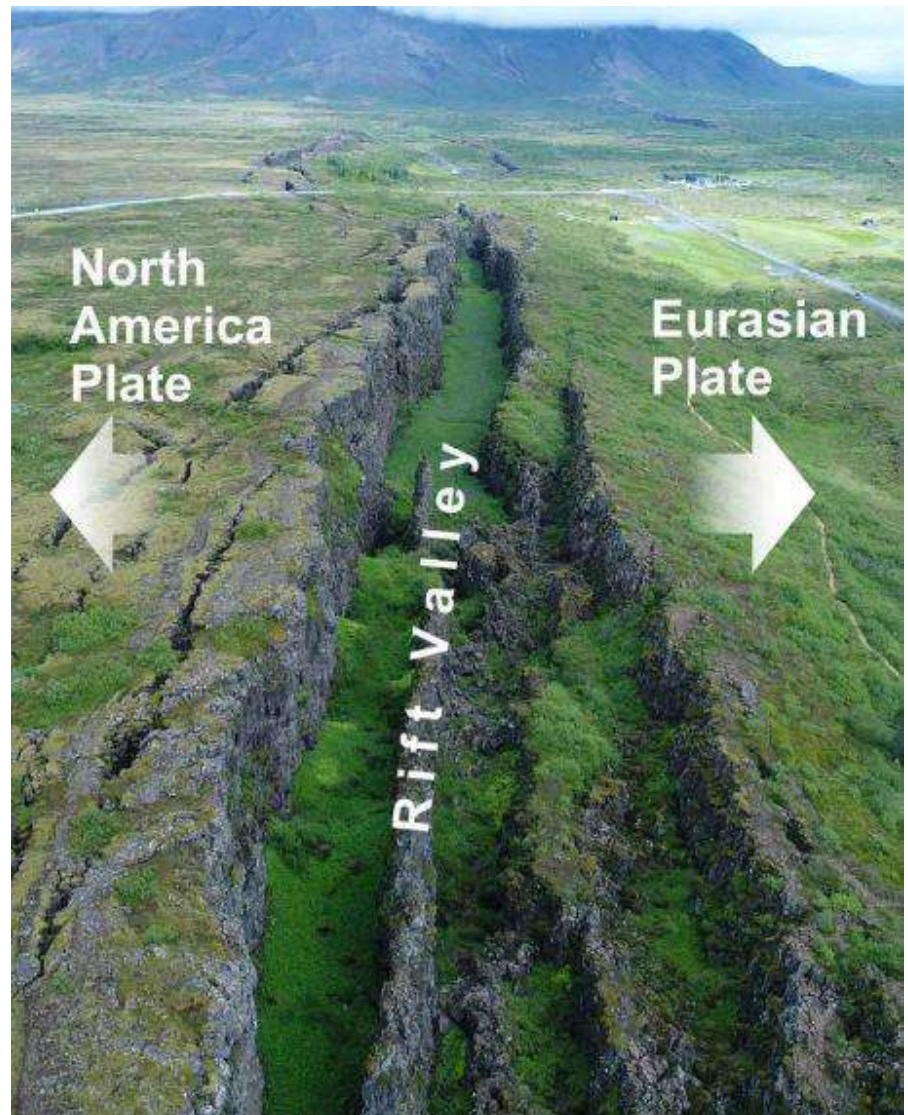


ΕΛΛΗΝΙΚΗ
ΕΠΙΣΤΗΜΟΝΙΚΗ
ΕΤΑΙΡΕΙΑ
ΕΔΑΦΟΜΗΧΑΝΙΚΗΣ
& ΓΕΩΤΕΧΝΙΚΗΣ
ΜΗΧΑΝΙΚΗΣ

Τα Νέα της Ε Ε Ε Ε Γ Μ

160

Αρ. 160 – ΦΕΒΡΟΥΑΡΙΟΣ 2022



Mid-Atlantic Ridge on Iceland
(Thingvellir National Park)

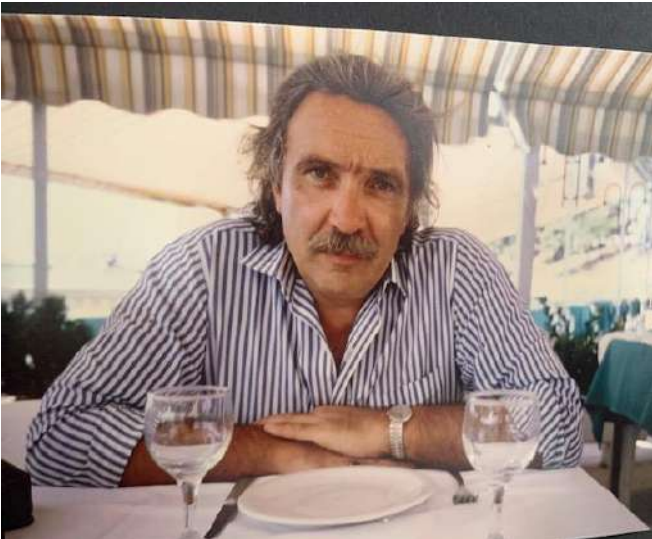


Π Ε Ρ Ι Ε Χ Ο Μ Ε Ν Α

Σπύρος Κωστόπουλος in memoriam	3
Mid-Atlantic Ridge on Iceland (Thingvellir National Park)	4
Δοκιμές εδαφομηχανικής για έργα οδοποιίας	4
Άρθρα	5
- Εκτίμηση Χαρακτηριστικών Της Ισχυρής Έκρηξης Στο Κέντρο Της Αθήνας, στις 26 Ιανουαρίου 2022	5
- Floodplain evolution and its influence on liquefaction clustering: The case study of March 2021 Thessaly, Greece, seismic sequence	8
- Detection and forecasting of shallow landslides: lessons from a natural laboratory	9
- Increased landslide activity after low-magnitude earthquakes	11
- Contractor versus consultant pile design	12
- How impact of bad roads can be worse than an earthquake	13
Could road constructions be more hazardous than an earthquake in terms of mass movement?	13
- Landslides caught on seismic networks and satellite radars	22
- Granular porous landslide tsunami modelling – the 2014 Lake Askja flank collapse	24
- M6.4 Albania Earthquake on November 26, 2019	26
- Modelling the sequential earthquake-tsunami response of coastal urban transport infrastructure	30
- Mysterious global tsunami in 2021 caused by hidden M8.2 earthquake	31
- Βαλκανατόλια: Ανακαλύφθηκε μια ξεχασμένη ήπειρος 40 εκ. ετών που συμπεριλαμβάνει την Ελλάδα	32
- G-I = Geo-Inspirational	35
- Filling the Gaps with Pressurized Tunnel Boring Machines	36
- LARGE-DIAMETER TUNNELS – An Emerging Urban Transportation Solution	38
- The Elizabeth River’s New Immersed Tube Tunnel	42
- Artificial Intelligence Applications for Tunneling	46
- Tunneling in Tight Quarters	49
- Have You Heard of Stacked Drifts?	53
- The Bearing Capacity Equation	56
Νέα από τις Ελληνικές και Διεθνείς Γεωτεχνικές Ενώσεις	57
- Εθνικό Μετσόβιο Πολυτεχνείο / Σχολή Πολιτικών Μηχανικών / Τομέας Γεωτεχνικής	57
Διαδικτυακή διάλεξη Δρ. Μαρίνας Πανταζίδου	57
- International Society for Soil Mechanics and Geotechnical Engineering	57
ISSMGE News & Information Circular February 2022	57
GeoWorld reached 25,000 registered members!	58
The urgent need for remote sensing in geotechnical engineering	58
Final draft of the Failure Paths report	59
Mid-Term TC Report TC305	59
First TC306 Geotechnical Engineering Education post	60
Announcing the 6th McClelland Lecturer – Professor Richard Jardine	60
Application of Unsaturated Soil Mechanics on the Analysis of Slopes	60

- Geoengineer	60
Geotechnical Engineers can now publish technical related content on GeoWorld, get DOIs, and reach thousands of geo-professionals	60
- International Society for Rock Mechanics and Rock Engineering	61
News	61
- International Tunnelling Association	61
Scooped by ITA-AITES #60, 1 February 2022	61
Scooped by ITA-AITES #61, 15 February 2022	61
- British Tunnelling Society – Young Members	61
Validation of Probabilistic and Artificially Intelligent Ground Models in Predicting Soil Transitions	61
- International Association of Engineering Geology	62
First Summer School of the International Association for Engineering Geology and the Environment - Impacts of Slope Instabilities on Large Infrastructures	62
- Διακρίσεις Ελλήνων Γεωτεχνικών Μηχανικών	63
Evangelia Ieronymaki, Ph.D., M.ASCE	63
Network Rail senior asset engineer Manos Tsoukalas	64
LLInterview Coming back to Europe George Gazetas	64
Προσεχείς Γεωτεχνικές Εκδηλώσεις:	65
- HYDRO 2022 Roles of hydro in the global recovery	65
- Workshop on soil erosion for Europe – Emerging challenges	66
- International Workshop on Advances in Laboratory Testing of Liquefiable Soils	67
- 9th International Congress on Environmental Geotechnics - Highlighting the role of Environmental Geotechnics in Addressing Global Grand Challenges	68
- 17th Asian Regional Geotechnical Engineering Conference	69
- IS-PORTO 2023 8th International Symposium on Deformation Characteristics of Geomaterials	70
- 9th International Offshore Site Investigation & Geotechnics Conference	71
Ενδιαφέροντα Γεωτεχνικά Νέα	73
- Brazilian expressway collapses over metro tunnel	73
- The disastrous 31 January 2022 mudflow in the La Gasca suburb of Quito, Ecuador	73
- The 1979 Nice Airport landslide and tsunami	74
- Vajont Dam, a double-curved, thin-arch dam, at 262 meters high, from above	75
- Tideway: Overcoming construction challenges at Victoria Embankment	75
- Early theories why Wiltshire road buckled and cracked	75
Ενδιαφέροντα - Γεωλογία	78
- Scientists discover lost range of 'supermountains' three times longer than the Himalayas	78
- Mysterious new substance possibly discovered inside Earth's core	79
Ενδιαφέροντα – Περιβάλλον	80
- Small artificial impoundments have big implications for hydrology and freshwater biodiversity	80
Νέες Εκδόσεις στις Γεωτεχνικές Επιστήμες	84
Ηλεκτρονικά Περιοδικά	85

Σπύρος Κωστόπουλος in memoriam



Στις 15 Ιανουαρίου έφυγε ο συνάδελφος Σπύρος Κωστόπουλος, Καθηγητής πολιτικός μηχανικός.

Γεννήθηκε το 1948 στην Αθήνα. Ήταν απόφοιτος του Κολλεγίου Αθηνών (1967). Σπούδασε στη Σχολή Πολιτικών Μηχανικών του Εθνικού Μετσόβιου Πολυτεχνείου (1971) και έγινε Διδάκτωρ Πολιτικός Μηχανικός (DrScTech) στο Ομοσπονδιακό Πολυτεχνείο της Λωζάννης (EPFL, 1981).

Ο Σπύρος είχε μακράν εμπειρία ως μελετητής και σύμβουλος Γεωτεχνικός Μηχανικός στην Ελλάδα και το εξωτερικό. Εξελέγη Αναπληρωτής Καθηγητής στο Τμήμα Πολιτικών Μηχανικών του Πανεπιστημίου Θεσσαλίας, όπου διδάξε εδαφομηχανική και γεωτεχνικές κατασκευές (1996-2008).

Είχε πάθος για την έρευνα και την καινοτομία και συμμετείχε σε πολλά ελληνικά και παγκόσμια συνέδρια, συμπόσια και ημερίδες Γεωτεχνικής Μηχανικής. Δημοσίευσε πάνω από 60 επιστημονικές εργασίες σε διεθνή περιοδικά και πρακτικά συνεδρίων ειδικότερα στα θέματα της ανάλυσης της γεωτεχνικής συμπεριφοράς μαλακών βράχων, της πειραματικής διερεύνησης των αντιστηρίξεων και της διήχνευσης της γεωμάζας και των γεωτεχνικών κατασκευών. Ήταν συγγραφέας των βιβλίων «Γεωτεχνικές Μελέτες I», «Γεωτεχνικές Μελέτες II», «Πειραματική Γεωτεχνική Μηχανική» και «Σήραγγες» (Εκδόσεις Ίων).

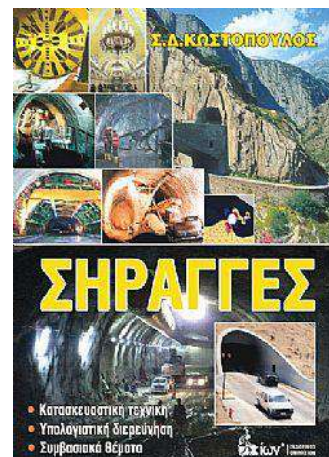
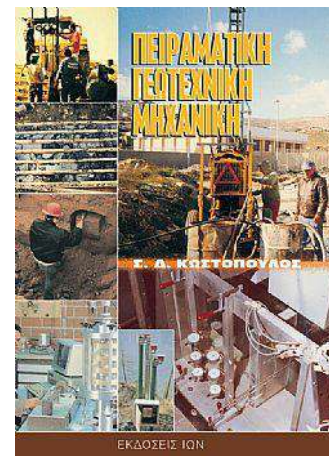
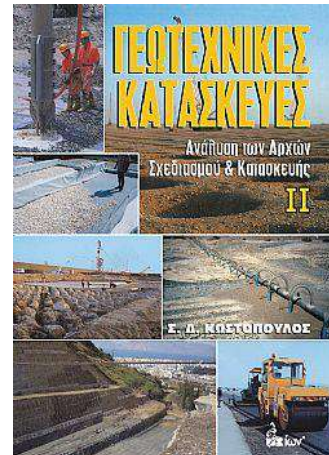
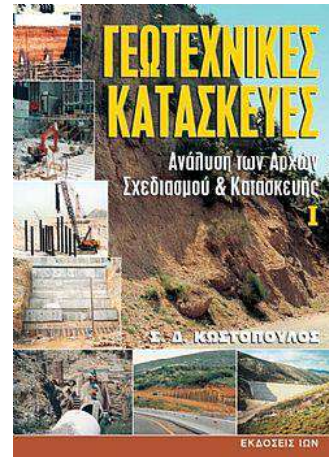
Υπήρξε εκλεκτό μέλος της Ελληνικής Επιστημονικής Εταιρείας Εδαφομηχανικής και Γεωτεχνικής Μηχανικής.

Ο Σπύρος ήταν ένας σπάνιος σε ποιότητα και πνεύμα άνθρωπος, ιδεολόγος, αντισυμβατικός με ασταίρευτο χιούμορ και περιρρέουσα τρυφερότητα. Αγαπούσε τα ταξίδια και την επαφή του με διαφορετικούς πολιτισμούς. Αγάπησε στο έπακρον την ζωή και όταν αρρώστησε τον περασμένο Οκτώβριο πάλεψε να ζήσει με οδηγό την πίστη ότι θα τα καταφέρει. Δυστυχώς η υγεία του επιδεινώθηκε και εισήχθη στο Νοσοκομείο ανήμερα των Χριστουγέννων όπου έχασε την μάχη για την ζωή. Το θλι-βερό γεγονός είναι ότι 4 μήνες πριν είχε χάσει τον μεγαλύτερο αδελφό του Κωνσταντίνο, μηχανολόγο-μηχανικό. Μια απώλεια που τον είχε κλονίσει συναισθηματικά. Η οικογένεια αποχαιρέτησε με μεγάλη οδύνη τον Σπύρο στο αποτεφρωτήριο Ριτσώνας στις 19/1/2022.

Ο Σπύρος είχε αδυναμία στην μονάκριβη κόρη του Μυρσίνη και στις τρεις εγγονές του, Χρυσάνθη, Φωτεινή και Έλλη.

Καλό ταξίδι Σπύρο!

Μυρσίνη

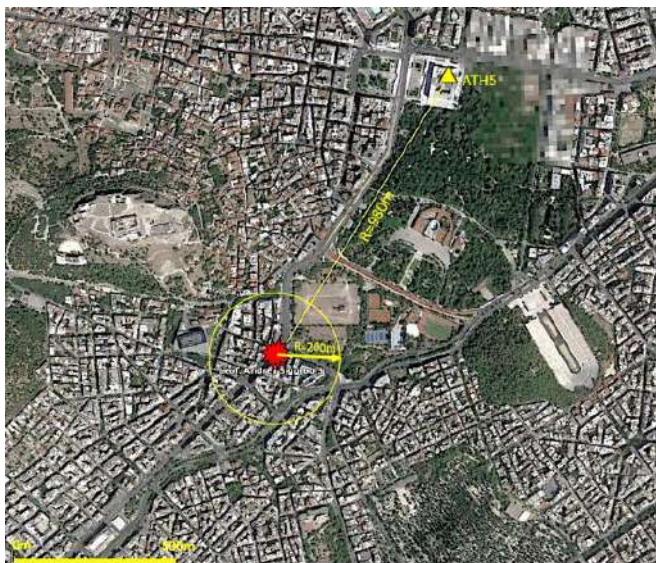


Εκτίμηση Χαρακτηριστικών Της Ισχυρής Έκρηξης Στο Κέντρο Της Αθήνας, στις 26 Ιανουαρίου 2022

Θεοδουλίδης Νίκος¹, Γρένδας Ιωάννης^{1,2}, Χατζηδημητρίου Παναγιώτης²

Η έκρηξη η οποία σημειώθηκε στον ημιώροφο εξωτερικό κτίριου επί της Λεωφόρου Συγγρού 3, κοντά στις Στήλες του Ολυμπίου Διός στην Αθήνα, στις 26 Ιαν. 2022 λίγο πριν τις 7 το πρωί, συγκλόνισε το κέντρο της πρωτεύουσας δημιουργήσε έντονο ωστικό κύμα το οποίο σε ακτίνα περίπου 200 μέτρων οδήγησε σε θραύση υαλοπινάκων πολυκατοικιών της περιοχής ενώ τραυματίστηκαν τρεις πολίτες ένας εκ των οποίων σοβαρά. Η Λεωφόρος Συγγρού έμεινε κλειστή στην κυκλοφορία οχημάτων επί 13 περίπου ώρες. Μολονότι τα ακριβή αίτια της έκρηξης δεν έχουν πλήρως εντοπισθεί οι έρευνες προσανατολίστηκαν κυρίως σε ενδεχόμενη πρόκλησή της από διαρροή υγραερίου ή φυσικού αερίου (<https://www.iefimerida.gr/ellada/ekrivi-syggroy-giati-egine-poy-strefontai-ereynes>),

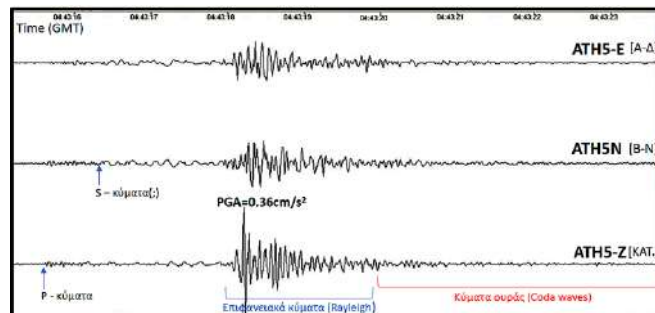
Σε απόσταση ~980m από το σημείο της έκρηξης και συγκεκριμένα σε υπόγειο του κτιρίου της Βουλής των Ελλήνων λειτουργεί σειсмоγράφος/επιταχυνσιογράφος ευρέως φάσματος και υψηλής ευαισθησίας του Ινστιτούτου Τεχνικής Σεισμολογίας & Αντισεισμικών κατασκευών (ΙΤΣΑΚ) (www.itsak.gr), με κωδικό σταθμού ATH5, ο οποίος κατέγραψε καθαρά τη συγκεκριμένη δόνηση, όπως φαίνεται στο Σχήμα 1.



Σχήμα 1. Κάτοψη της περιοχής του κέντρου της Αθήνας που περιλαμβάνει τη θέση της έκρηξης (Λεωφ. Συγγρού, 3) και το κτίριο της Βουλής των Ελλήνων όπου είναι εγκατεστημένος ο σειсмоγράφος/επιταχυνσιογράφος του ΙΤΣΑΚ (ATH5)

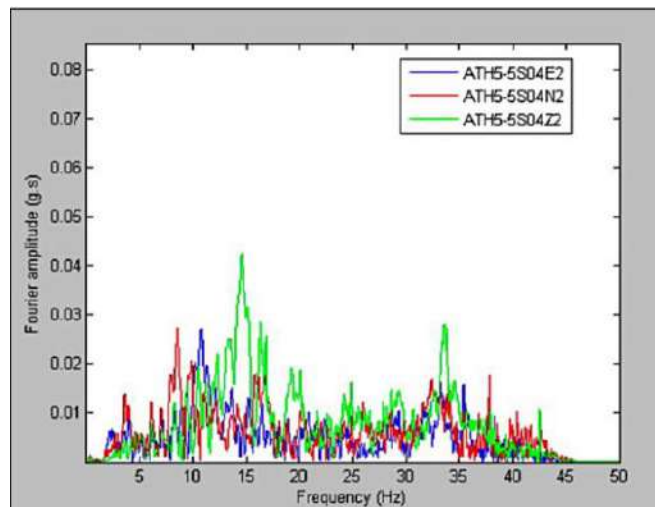
Στο Σχήμα 2 βλέπουμε την άφιξη των επιμήκων (P), των εγκάρσιων (S) κυμάτων καθώς και των επιφανειακών κυμάτων, κυρίως Rayleigh που εμφανίζονται στις περιπτώσεις επιφανειακών εκρήξεων με μεγαλύτερα πλάτη (Stein and Wysession, 2003). Στη συνέχεια, μετά τα επιφανειακά εμφανίζονται τα κύματα ουράς (coda waves) Τα τελευταία αποτελούν σκεδαζόμενα κύματα στις ετερογένειες των γεωλογικών σχηματισμών της ευρύτερης περιοχής (Aki,

1969; Aki and Chouet, 1975). Η μέγιστη εδαφική επιτάχυνση, $PGA=0.36\text{cm/s}^2$, σε απόσταση 980m από την έκρηξη, εμφανίζεται στην κατακόρυφη συνιστώσα. Αυτό το κατώφλι εδαφικής επιτάχυνσης είναι λίγο μικρότερο από το όριο ασθενούς αισθητότητας (0.5cm/s^2) (<http://shakemaps.itsak.gr>) συνάγοντας το συμπέρασμα ότι σε κοντινότερες από την έκρηξη αποστάσεις αναμένεται το ωστικό της κύμα να ήταν έντονα αισθητό ως «σεισμική» δόνηση, όπως και συνέβη στην πραγματικότητα από μαρτυρίες κατοίκων στην περιοχή γύρω από τις Στήλες του Ολυμπίου Διός.



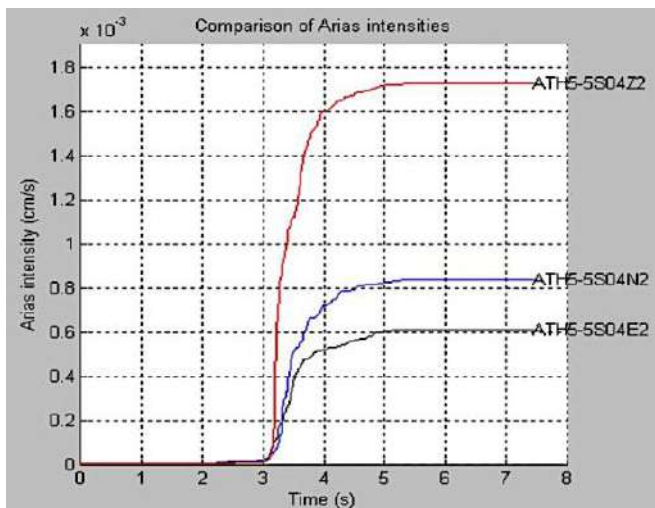
Σχήμα 2. Καταγραφή τριών συνιστωσών του σειсмоγράφου/επιταχυνσιογράφου ATH5, στο υπόγειο του κτιρίου της Βουλής των Ελλήνων.

Τα φάσματα Fourier της καταγραφής στο σταθμό ATH5 (Σχήμα 3) εμφανίζουν για την κατακόρυφη συνιστώσα της δόνησης υψηλά πλάτη σε συχνότητα ~15Hz ενώ στις οριζόντιες σε συχνότητα ~10Hz. Η υπολογισμένη ένταση κατά Arias (Arias, 1970) δείχνει σχεδόν διπλάσια ενέργεια στην κατακόρυφη δόνηση από την οριζόντια και η έκλυσή της σε ποσοστό >90% περιορίζεται σε διάρκεια ~1.5sec (Σχήμα 4).

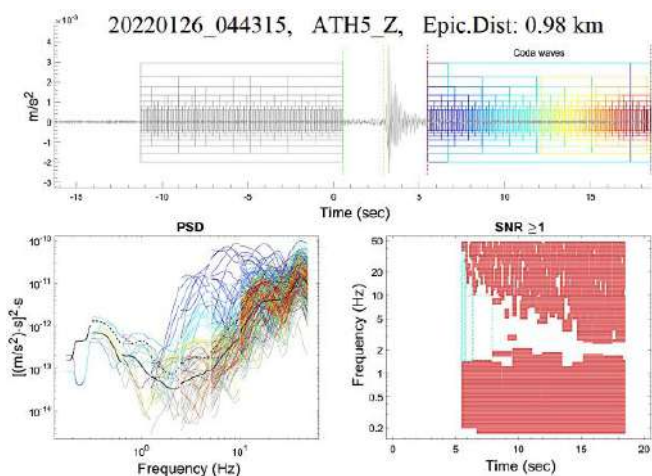


Σχήμα 3. Φάσματα Fourier των τριών συνιστωσών στον ATH5

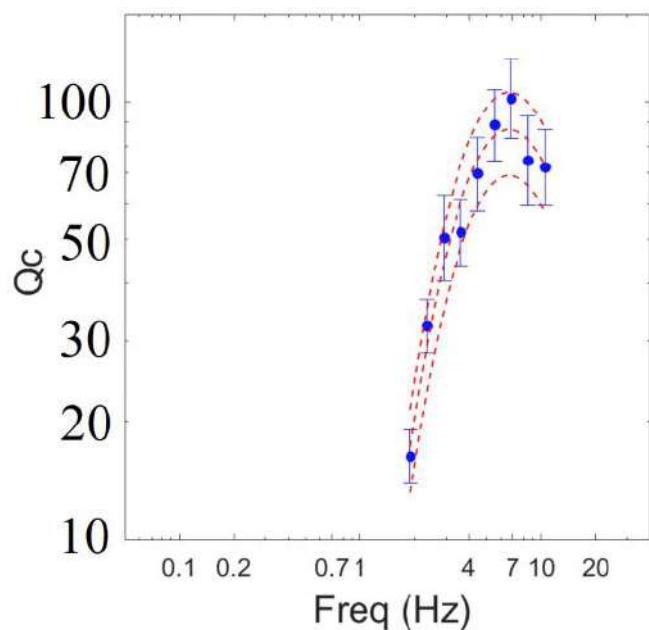
Με βάση την τεχνική που αναπτύχθηκε από τους Sebe et al. (2005, 2018) και τροποποιήθηκε από τους Grendas et al. (2022), επιλέχθηκαν τα αξιόπιστα για μελέτη παράθυρα των σκεδαζόμενων κυμάτων ουράς (scattered coda waves) της καταγραφής του ATH5 από την έκρηξη (Σχήμα 5), σε σχέση με τον εδαφικό θόρυβο. Εν συνεχεία πραγματοποιήθηκε η εκτίμηση (Σχήμα 6) και η απομάκρυνση του παράγοντα απόσβεσης της εδαφικής δόνησης, από την καταγραφή των κυμάτων ουράς, δημιουργώντας μία νέα καταγραφή αποτελούμενη θεωρητικά από στάσιμα κύματα ουράς. Από την καταγραφή αυτή κατέστη εφικτό να υπολογιστεί το φάσμα ισχύος της πηγής στο σημείο της έκρηξης.



Σχήμα 4. Ένταση Arias των τριών συνιστωσών στον ATH5

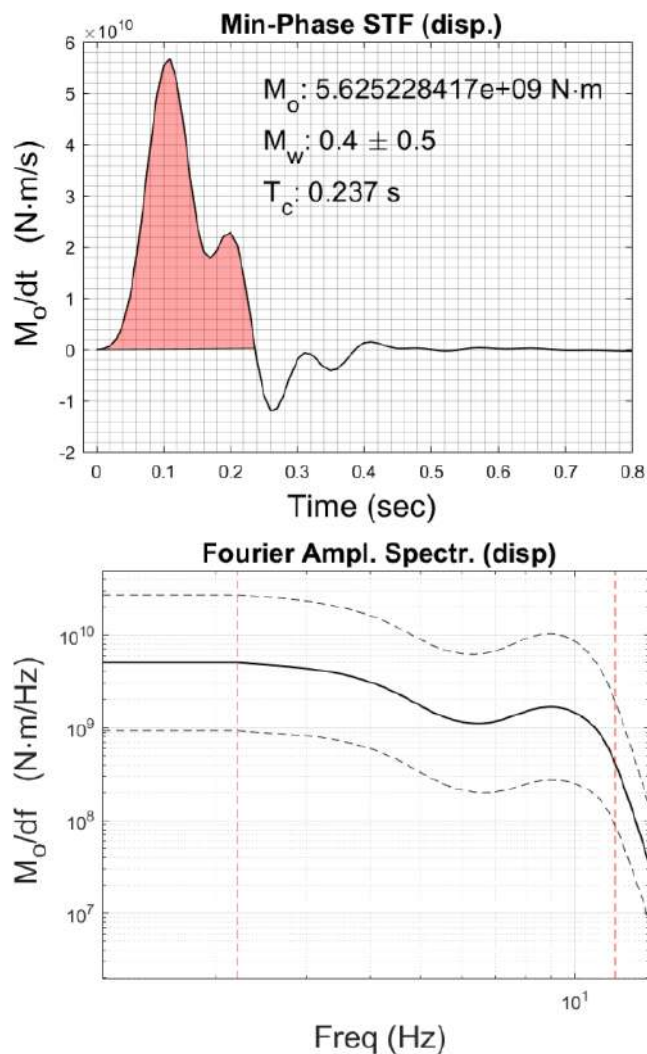


Σχήμα 5. Επιλογή παραθύρων κυμάτων ουράς (coda waves) από την κατακόρυφη συνιστώσα του σειсмоγράφου/επιταχυνσιογράφου ATH5



Σχήμα 6. Παράγοντας απόσβεσης των γεωλογικών σχηματισμών, Q_c , στην ευρύτερη περιοχή του σειсмоγράφου/επιταχυνσιογράφου ATH5.

Στη συνέχεια από το φάσμα αυτό, με χρήση της τεχνικής της φασματικής παραγοντοποίησης (spectral factorization), υπολογίστηκε το κυματίδιο ελάχιστης φάσης (minimum phase wavelet) (Σχήμα 7-αριστερά) το οποίο αντιπροσωπεύει τη χρονική συνάρτηση της πηγής (source time function) με διάρκεια ~ 0.25 sec. Το εμβαδό της χρονικής συνάρτησης της σεισμικής πηγής, που αφορά μόνο στις θετικές τιμές, αντιστοιχεί στο μέγεθος ροπής ή και στο σύνολο της ενέργειας στην πηγή, το οποίο αντιστοιχήθηκε σε μέγεθος σεισμού $M_w = 0.4 \pm 0.5$. Στο Σχήμα 7-δεξιά παρατίθεται το φάσμα Fourier της χρονικής συνάρτησης της σεισμικής πηγής, στο οποίο οι δύο κάθετες διακεκομμένες γραμμές περιλαμβάνουν το αξιόπιστο συχνοτικό του περιεχόμενο.



Σχήμα 7. Εκτίμηση της χρονικής συνάρτησης πηγής στη θέση της έκρηξης (αριστερά) και του μεγέθους ροπής αυτής (δεξιά).

Συνοψίζοντας, από την παραπάνω ανάλυση που έγινε με βάση τα σκεδαζόμενα κύματα ουράς ενός μόνον σταθμού επιταχυνσιογράφου (ATH5) και την εκτίμηση της χρονικής συνάρτησης πηγής της έκρηξης, προκύπτει ότι ο χρονική διάρκεια του κύριου παλμού της έκρηξης ήταν $T_c \sim 0.25$ sec. Επίσης εκτιμήθηκε ότι το μέγεθος της αντιστοιχούσε σε σεισμό μεγέθους $M_w = 0.4 \pm 0.5$, δηλαδή $0 < M_w < 1$.

ΒΙΒΛΙΟΓΡΑΦΙΑ

Aki, K., 1969. Analysis of the Seismic Coda of Local Earthquakes as Scattered Waves 74, 615–631.

Aki, K., Chouet, B., 1975. Origin of coda waves: Source, attenuation, and scattering effects. *J. Geophys. Res.* 80, 3322–3342. <https://doi.org/10.1029/JB080i023p03322>.

Arias, A. (1970). "A measure of earthquake intensity." R. J. Hansen, ed. *Seismic design for nuclear power plants*, MIT Press, Cambridge, Mass.

Grendas, I., Theodoulidis, N., Bard, P. Y., Perron, V., Hatzidimitriou, P., & Hollender, F. (2022). Can site effects be estimated with respect to a distant reference station? Performance of the spectral factorization of coda waves. *Geophysical Journal International* (under publication).

Sèbe, O., Bard, P.-Y., Guilbert, J., 2005. Single station estimation of seismic source time function from coda waves: The Kursk disaster. *Geophys. Res. Lett.* 32, 1–4. <https://doi.org/10.1029/2005GL022799>.

Sèbe, O., Guilbert, J., Bard, P.-Y., 2018. Spectral factorization of the source time function of an earthquake from coda waves, application to the 2003 rambervillers, France, earthquake. *Bull. Seismol. Soc. Am.* 108, 2521–2542.

Stein S. and Wysession M. 2003. *An Introduction to Seismology, Earthquakes, and Earth Structure*, Blackwell Publishing, 498p.

¹ Ινστιτούτο Τεχνικής Σεισμολογίας & Αντισεισμικών Κατασκευών (ΙΤΣΑΚ)

² Τομέας Γεωφυσικής, Τμήματος Γεωλογίας ΑΠΘ

Floodplain evolution and its influence on liquefaction clustering: The case study of March 2021 Thessaly, Greece, seismic sequence

George Papathanassiou, Sotiris Valkaniotis, Athanassios Ganas, Alexandros Stampolidis, Dimitra Rapti, Riccardo Caputo

Highlights

- This seismic sequence triggered the most extensive liquefaction phenomena in Greece the last 40 years.
- A new protocol is developed to quantitatively document liquefaction phenomena
- Remote sensing data used to delineate the liquefied areas.
- Direct influence of the floodplain's evolution to the clustering of liquefaction phenomena.
- 3D resistivity model illustrates local liquefaction-induced disruption.

Abstract

The March 2021 Thessaly, Central Greece, seismic sequence characterized by an $M_w = 6.3$ mainshock and five $M_w > 5.0$ aftershocks triggered extensive liquefaction in the floodplain of the Piniada Valley and localized phenomena along the riverbanks of the Titarissios River. In order to document these secondary effects, we carried out immediate post event surveys based on remote sensing techniques and field-based reconnaissance. The initial desktop-based approach succeeded in delineating in advance the extensive liquefaction surface manifestations and in saving time for the subsequent field survey. The field work was performed with ground-based surveys, and UAV aerial campaigns. The longest reported linear liquefaction feature was 26.7 m, while the total sand blow covered an area of 0.0325 km². Over one of the liquefaction manifestations, we performed parallel 2D electrical resistivity tomography profiles in order to reconstruct the subsoil stratigraphy. The produced 3D resistivity model successfully detects and illustrates the subsurface disruption following the generation of liquefaction. From the comparison between the spatial distribution of liquefaction phenomena and the geomorphological conditions in the area, the direct influence of the historical evolution of Pinios River in clustering liquefaction phenomena was highlighted. Thus, it is confirmed that a detailed investigation of the historical and late Holocene evolution of a floodplain i.e., location of ox-bow lakes, meanders and former river channels, can identify sites prone to liquefaction. This could result in a reduction of the area where detailed engineering geology investigations (e.g., boreholes with in-situ tests) are required for the evaluation of the liquefaction hazard.

(Engineering Geology, Volume 298, 5 March 2022, 106542, <https://doi.org/10.1016/j.enggeo.2022.106542>)

Database of liquefaction phenomena triggered by the March 2021 Thessaly, Greece, seismic sequence

Papathanassiou George, Valkaniotis Sotiris, Ganas Athanassios, Stampolidis Alexandros, Rapti Dimitra, Caputo Riccardo

This archive contains data related to the paper "Floodplain evolution and its influence on liquefaction clustering: the case study of March 2021 Thessaly, Greece, seismic sequence" by

George Papathanassiou, Sotiris Valkaniotis, Athanassios Ganas, Alexandros Stampolidis, Dimitra Rapti, Riccardo Caputo.

Submitted to *Engineering Geology, Elsevier*

Liquefaction_DB_20210303 contains shapefiles and spreadsheet for the mapped liquefaction phenomena **UAS_Liquefaction_Surveys_Larisa_EQ** contains detailed geospatial data for mapped liquefaction phenomena from UAS surveys

<https://zenodo.org/record/5634273#.YI7Tp9NBy5d>

Detection and forecasting of shallow landslides: lessons from a natural laboratory

Rupert Bainbridge, Michael Lim, Stuart Dunning, Mike G. Winter, Alejandro Diaz-Moreno, James Martin

Abstract

Rapid shallow landslides are a significant hillslope erosion mechanism and limited understanding of their initiation and development results in persistent risk to infrastructure. Here, we analyse the slope above the strategic A83 Rest and be Thankful road in the west of Scotland. An inventory of 70 landslides (2003–2020) shows three types of shallow landslide, debris flows, creep deformation, and debris falls. Debris flows dominate and account for 5,350 m³ (98%) of shallow-landslide source volume across the site. We use novel time-lapse vector tracking to detect and quantify slope instabilities, whilst seismometers demonstrate the potential for live detection and location of debris flows. Using on-slope rainfall data, we show that shallow-landslides are typically triggered by abrupt changes in the rainfall trend, characterised by high-intensity, long duration rainstorms, sometimes part of larger seasonal rainfall changes. We derive empirical antecedent precipitation (>62 mm) and intensity-duration (>10 h) thresholds over which shallow-landslides occur. Analysis shows the new thresholds are more effective at raising hazard alerts than the current management plan. The low-cost sensors provide vital notification of increasing hazard, the initiation of movement, and final failure. This approach offers considerable advances to support operational decision-making for infrastructure threatened by complex slope hazards.

1. Introduction

Shallow landslides occur where material fails in the upper layers of a soil profile, usually up to approximately 2 m depth. These landslides usually have little precursory warning and may fail rapidly (e.g., debris flow; Persichillo et al. 2016) or slowly (e.g., creep deformation; Hungr et al. 2014). Their unpredictability means they pose a significant global hazard, particularly when favourable material and fluidisation conditions transform them into debris flows (e.g., Zimmerman et al. 2020). Debris flows are extremely rapid (>5 m/s), saturated debris-rich landslides that exist along the broad spectrum of flow-like landslides (Hungr et al. 2014). Debris flow runoff potential and their capacity to entrain large quantities of water and sediment make them a significant risk where linear infrastructure traverses affected slopes (Geertsema et al. 2009; Meyer et al. 2015). Debris flows can be broadly grouped into channelized debris flows (CDFs) that are constrained for their flow path and hillslope (or open slope) debris flows (HDFs) that occur on non-incised slopes (Chen et al. 2009). CDFs and HDFs can transition into one another where HDFs meet gullies or CDFs breach channels and flow over slopes; it is this hillslope-gully coupling that can control the hazard potential (Milne et al. 2009). CDFs often occur in torrent systems, such as the Illgraben, Switzerland (Badoux et al. 2009), where the repeated flow path removes some of the spatial risk uncertainty and allows focussed monitoring of a single outflow channel.

However, at some sites historic evidence shows debris flows may occur from anywhere across wide areas with suitable topography and materials. This leads to both spatial and temporal uncertainty on triggering location and runoff. At such sites, where the risk is high, a combination of active mitigation (physically controlling site aspects using barrier, net, pit, or deflection engineering infrastructure) and passive mitigation (reducing impacts via land-use planning, closures, and warning systems) methods can be used (Huebl and Fiebigler 2005; Vagnon 2020) but can be costly given the wide area of potential source and runoff zones. In Scotland, debris flows

have repeatedly damaged roads and rail lines resulting in economic and social costs (Winter, Peeling, et al. 2019), with many valleys showing historic (and prehistoric) evidence of multiple debris flow deposits slope wide (Innes 1983; Luckman 1992; Curry 2000). Contemporary infrastructure damaging debris flows have often been linked to high-intensity rainfall (Winter, Ognissanto, et al. 2019). Climate forecasts suggest that in the future Scotland may receive more high intensity rainfall events in the winter and lower-frequency but higher-intensity rainfall during summer months (Jones et al. 2013; UKCP 2018; Finlayson 2020). Such changes in antecedent conditions and rainfall patterns may perturb hillslope sediment cascades (Bennett et al. 2014), releasing sediment from storage that is considered dormant, increasing the rapid shallow landslide hazard in mountainous areas (Winter and Shearer 2017)

Monitoring strategies for determining the level of landslide hazard posed by rainfall, in a given area or slope, vary from global to hyper-local in scale. Global determination of landslide hazard requires the combination of variables such as slope, lithology, soil wetness, antecedent rainfall, and rainfall (Stanley et al. 2021). Whilst useful for global and regional indications of landslide hazard, these global models do not allow detailed analysis of areas smaller than the resolution of the data. Input data are at coarse resolution which do not always accurately represent the real-world spatial variability (Ozturk et al. 2021), making predictions noisy or imprecise. Where a higher confidence in the level of landslide hazard is required for decision making, at linear infrastructure for example, hyper-local monitoring can be deployed. Hyper-local monitoring collects the detail required to make site specific thresholds for landslide initiation and makes significant improvements over global landslide susceptibility models (Ozturk et al. 2021).

Here we demonstrate a novel combination of near-real-time, multi-disciplinary, monitoring techniques that allow remote detection and quantification of slope changes and supplement the regional Landslide Management Plan (LMP). The objective of these techniques is to improve our understanding of shallow landslide trigger mechanisms that threaten road users and infrastructure, and thus enhance alert capabilities for road asset managers at sites that are prone to shallow-landslide/debris flow transitions. These new, relatively low-cost, monitoring techniques and analyses are essential in helping to better manage the present and future increased risk of debris flows.

...

5. Discussion

Between 2003 and 2020 there were 70 shallow landslides recorded, including 49 debris flows. Landslides come from three material types on the slope: regolith, till, and debris cones, which exert a control on source area morphology and landslide volumes. Debris cone sources are generally deeper, which likely represents thicker deposits of source material to bedrock. The failure depths sourced in the upslope surface material comprising of glacial till and regolith were significantly shallower. The total volume of source areas for debris flows and debris falls across the slope is 5,404 m³, with debris cones accounting for 18% (984 m³), regolith 15% (823 m³) and till the remaining 67% (3,597 m³). Each material type accounts for a proportion of source volumes similar to their areal coverage of the slope, indicating that no one material produces relatively more landslide volume than any other. However, debris cones produce fewer but larger landslides, whilst till and regolith sources produce smaller but more frequent landslides. Debris flows in till have closed the road seven times compared to four and three times for regolith and debris cones respectively. Debris flows in till could there-

fore be considered as the greatest risk to road closure. Similar failure plane slope angles of 30° to 31° indicate a control on landslide initiation, which may represent a critical threshold within the slope material or relate to the dip angle of the underlying bedrock – although most shallow landslides at the site are not at the bedrock-cover interface.

BEAST rainfall analysis shows that debris flows are primarily associated with abrupt rainfall trend changes, but that in some cases there is a larger seasonal signal associated with debris flow occurrence. In the 2018 study period, antecedent, and medium- to long-duration, high-intensity rainfall is shown to be an important factor in debris flows initiation. New local API and I-D rainfall thresholds, identify all landslide inducing storms and minimize false alarms, improve on the LMP and provide road authorities time to consider actions. 90% of RabT landslides occurred over a 62 mm API, indicating a critical antecedent rainfall threshold. Rainstorm I-D > 10 h is key for landslide initiation with largely higher mean rain intensity than non-landslide storms. Whilst the thresholds have been calculated locally at the RabT, the surface geology and the topography of the site are replicated in, and are representative of the surrounding mountain range, indicating that the thresholds potentially apply more regionally although there is not currently a wider, timed inventory of failures.

Time-lapse vector tracking located and quantified creeping deformation in response to rainfall drivers. I-V calculations forecast imminent failure in the initiation phase, however creep slowed when rainfall ceased and arrested despite further rainfall. This method can detect slope movement and indicate times of heightened risk of failure for management authorities.

Continuous passive seismic detection and hodograms were used to identify a HDF. In this instance, and likely others due to short RabT flow paths, the 15 second event duration is too brief for live warnings but allows for uninterrupted event detection and rapid response, outside of time-lapse image capture. Additional seismometers (now deployed) extend the range of detection and allow more traditional geo-location.

It is not yet known whether climate change has had an impact on the generation of landslides on the slope, not least as the period (2003 to 2020) over which detailed records are available is too short for such an assertion to be made. Similarly, it is not known whether rainstorms that have generated landslides have been getting more intense and longer duration on a persistent basis. It is outside of the scope of this manuscript to examine the impact of climate change. No 'relatively' complete landslide inventories (other than this one) exist for the surrounding area, and it is therefore difficult to contextualise this site in respect to increasing landslide frequency. While we cannot yet link increases in landslide frequency, or magnitude, to climate change, observations certainly indicate that the magnitude of events in 2020 was greater than in living memory and that three of the last four years at the RabT have had some of the most frequent landslide events on record.

6. Conclusions

This paper presents the results of on-site monitoring at the RabT, aimed at supplementing the existing regional LMP (Winter et al. 2009). Our novel combination of sensors and processing techniques allows near-real-time monitoring and quantification of rapid shallow landslides as demonstrated at the RabT in the west of Scotland. Results show that local sensor systems improve our understanding of triggers by allowing landslides to be attributed to specific rainstorms and therefore the conditions leading to their initiation are better quantified. Improved rainfall thresholds for periods of likely increased shallow landslide hazard have been developed for the RabT, however the techniques could be readily applied to

other sites of interest. Further, we have shown that creep deformation can be detected and then tracked in near-real time, and, that rapid debris flow failures (which may or may not have shown precursory movement) can be detected. Low-cost sensors can be replicated at high- and lower-risk sites where cost-benefit would normally prevent monitoring. Increased high-intensity rainfall due to climate warming is expected in Scotland (UKCP 2018), meaning more infrastructure and assets will have increased debris flow risk. These combined low-cost monitoring techniques are an essential advancement and now an operationally proven approach for addressing this future risk.

(**Geomatics, Natural Hazards and Risk**, Volume 13, 2022 - Issue 1, Pages 686-704, <https://doi.org/10.1080/19475705.2022.2041108>, <https://www.tandfonline.com/doi/full/10.1080/19475705.2022.2041108>)

Increased landslide activity after low-magnitude earthquakes

Over the last 25 years there has been increasing awareness and understanding of landslides triggered by high-magnitude earthquakes. Key events in generating our understanding have included the [1989 Loma Prieta earthquake in California](#), the [1999 ChiChi earthquake in Taiwan](#) and the [2008 Wenchuan earthquake in China](#), amongst many others. There has also been an increased awareness of the [elevated occurrence of landslides in earthquake affected areas for years or even decades after the main shock](#).

This understanding has raised the intriguing question as to whether low-magnitude events also have an impact on landslide occurrence in the years following the main shock, and if so, how large is the impact? This is a difficult issue to unpick as the effects are likely to be comparatively small, and will occur over a much more limited area.

A paper just published in [Nature Scientific Reports](#) ([Martino et al. 2022](#)) explores this issue in relation to the 16 August 2018 Mw=5.1 earthquake in the Molise area of central Italy. This earthquake triggered 84 landslides, primarily consisting of the movement of soil materials on comparatively low angled slopes. [I posted about this earthquake at the time](#), including this image of a landslide triggered by the event:



Slope failures triggered by the 16 August Molise earthquake in Italy. Image from Salvatore Martino, University of Roma "Sapienza".

The authors have used differential [InSAR analysis](#) to examine the movement of these slopes for the two years prior to the Molise earthquake and in the year after. Landslides in this area are primarily triggered by rainfall, which has a seasonal distribution. Thus, most slope movements occur in the autumn and winter. Over the three years of the study the seasonal rainfall totals were comparable, but in the post-earthquake year there was an increase of 118% in the number of reactivations of the landslides detected using the InSAR technique. The main effect was seen in the first three months after the main shock. Thereafter it declined over a period of about three months, and by the spring the effect had disappeared.

The authors specifically exclude the possibility that this increase in landslide activity was related to increased rainfall after the earthquake – indeed the autumn and winter was slightly less wet than in the previous two years.

The mechanical cause of this increase in landslide activity is not clear to me. There is a range of possibilities, including

weakening of the materials, with strength being regained over time; the retention of localised high pore water pressures in the slope after the earthquake, which then reduce; the effects of aftershocks that of course decline with time; temporary changes in the drainage of the slopes; or the opening of fractures that allow rainfall to infiltrate, but which then clog up.

More research is needed into this effect, both in terms of the degree to which it occurs elsewhere and the causes of it. But it is a really interesting result that is important both for our understanding of hazard and the evolution of landscapes.

Reference

Martino, S., Fiorucci, M., Marmoni, G.M. et al. 2022. [Increase in landslide activity after a low-magnitude earthquake as inferred from DInSAR interferometry](#). *Scientific Reports* **12**, 2686. <https://doi.org/10.1038/s41598-022-06508-w>

(Dave Petley / THE LANDSLIDE BLOG, 22 February 2022, <https://blogs.agu.org/landslideblog/2022/02/22/molise-aftermath>)

Contractor versus consultant pile design

Alan Willoner, Mott MacDonald

In the UK we commonly have contractor designed piled foundations. If asked why this is, the response might be "to get a more economical solution". All clients have reason to look for the most economical solution, and some put consideration into risk management, where the apparent lowest price is not necessarily the best choice.

The Institution of Civil Engineers (ICE) *Specification for Piling and Embedded Retaining Walls* provides options to choose clause B1.4 option 1 – employer design of piles – or option 2 – contractor design of piles. To get guidance on what option to use the reader may refer to the ICE *Manual of Geotechnical Engineering* 55.11, which evaluates pile group design responsibility.

Contractor designed piles may provide efficiencies for typical mid height buildings with simple load combinations. But there can be difficulties. For example, on a complex site with multiple ground risks, the piling contractor may not have the time to fully appreciate and mitigate these risks. The lead consultant typically has a year to take a building project through the early Royal Institute of British Architects stages covering the geo-environmental desk study, site visit, specification, review and interpretation of ground investigation, outline foundation design to inform pile layout drawings, and typically a D30 piling performance specification. The piling contractor's designer may look at many projects each week and produce a tender design in one day followed by a contract design with a second read of the desk study and ground investigation report within one week. Timescales dictate that the piling contractor's designer may not fully appreciate, or have opportunity to, investigate an unusual ground risk.

Consultant designed piles are required when the pile design cannot be separated from the design of the superstructure, for example new integral bridges. The same logic may be true for structures where the stiffness of the foundation is pivotal for the performance of the superstructure, such as the core of a tall slender building.

There are situations where it is difficult for a consultant to produce a performance specification for "fair tendering" of a contractor designed piling contract and be prescriptive about certain risks, such as negative skin friction, heave or lateral squeezing of soft clays. The simplest solution to these situations is generally to opt for consultant designed piles.

Contractor designed piles are generally the best option when bespoke systems such as screw piles or displacement auger piles or designs controlled by drivability rely on "in-house" case histories.

A skilled designer is needed for an economical pile design. This person could be working for a lead consultant, a contractor or a specialist consultant, so in theory any organisation could produce an economical solution if there was incentive to do so.

The UK has a system that evolved by culture rather than planning. In other countries, piles are typically designed by geotechnical engineers within or teaming up with the consultant designing the superstructure, with piling contractors providing input in the design, when needed, on methodology or practicality issues.

This talking point is about which organisation in the supply chain is best placed to carry out and own the pile design for the circumstances of a particular project. Discussions should extend to structural engineers and developers who (in the

UK) have got used to a culture of piles being contractor designed. This is so that projects with high geotechnical risks or complex pile loading have fair consideration of the advantages and disadvantages of opting for contractor or consultant designed piles.

Alan Willoner is a technical principal and the global specialist skill lead for piling and drilled shafts at Mott MacDonald. He has been involved in pile design and construction for more than 20 years via employment with piling contractors, principal contractors and consultants.

(GROUND ENGINEERING, 23 February, 2022, <https://www.geplus.co.uk/opinion/contractor-versus-consultant-pile-design-23-02-2022>)

How impact of bad roads can be worse than an earthquake

Ten-year study of a town in Turkey showed poor construction caused more than 90% of landslips

Badly built roads can generate more hazard than a significant earthquake, research shows. Hakan Tanyaş, from the University of Twente in the Netherlands, and colleagues monitored the size and number of landslips in the Arhavi area of north-eastern Turkey between 2010 and 2020. During this period several roads were constructed through the region to access a new hydroelectric scheme.

The scientists show that development had a shocking impact on the stability of the hillsides, with road construction responsible for more than 90% of the observed landslips in the region.

Their calculations, reported in the [Natural Hazards](#) journal, suggest the volume of debris created by these excess landslips is equivalent to the area being shaken by a magnitude 6 earthquake.

Because much of this sediment ends up in rivers, the scientists say it will change the way rivers flow and increase the probability and severity of flooding.

Writing in [The Landslide Blog](#), Dave Petley from the University of Sheffield, says road-induced landslides are a global issue. "The sad element of this is that these landslides almost entirely avoidable – such road-related landslide impacts are down to poor engineering practice.

"Roads do not need to be built in this way, and there are plenty of examples of good practice from around the world."

(Kate Ravillious / The Guardian, Wed 2 Feb 2022, <https://www.theguardian.com/science/2022/feb/02/impact-bad-roads-earthquake-construction-landslips>)

Could road constructions be more hazardous than an earthquake in terms of mass movement?

Hakan Tanyaş, Tolga Görüm, Dalia Kirschbaum & Luigi Lombardo

Abstract

Roads can have a significant impact on the frequency of mass wasting events in mountainous areas. However, characterizing the extent and pervasiveness of mass movements over time has rarely been documented due to limitations in available data sources to consistently map such events. We monitored the evolution of a road network and assessed its effect on mass movements for a 11-year window in Arhavi, Turkey. The main road construction projects run in the area are associated with a hydroelectric power plant as well as other road extension works and are clearly associated with the vast majority (90.1%) of mass movements in the area. We also notice that the overall number and size of the mass movements are much larger than in the naturally occurring comparison area. This means that the sediment load originating from the anthropogenically induced mass movements is larger than its counterpart associated with naturally occurring landslides. Notably, this extra sediment load could cause river channel aggregation, reduce accommodation space and as a consequence, it could lead to an increase in the probability and severity of flooding along the river channel. This marks a strong and negative effect of human activities on the natural course of earth surface processes. We also compare

frequency-area distributions of human-induced mass movements mapped in this study and co-seismic landslide inventories from the literature. By doing so, we aim to better understand the consequences of human effects on mass movements in a comparative manner. Our findings show that the damage generated by the road construction in terms of sediment loads to river channels is compatible with the possible effect of a theoretical earthquake with a magnitude greater than $M_w = 6.0$.

Introduction

Recent findings suggest that our planet has been going through a new geologic time, "Anthropocene," in which human-driven changes dominate the Earth system and its geological records instead of natural processes (Lewis and Maslin 2015; Steffen et al. 2015). The existence of the "Anthropocene" is supported by the "Great Acceleration" graphs showing proxies of growing human activities (e.g., population, water use, transportation, etc.) and their influence on natural systems (e.g., CO₂ emission, surface temperature, domesticated land, etc.), which becomes quite obvious since the mid-twentieth century (Steffen et al. 2011, 2015) and is functionally and stratigraphically distinct from the Holocene epoch (Waters et al. 2016). However, the existence of the "Anthropocene" still needs much evidence (Brown et al. 2013). Notably, soil erosion, as a geomorphologic process, has an essential role in the formation of the geological records. In fact, soil erosion in the "Anthropocene" is chiefly governed by the coupled effect of natural and human-induced soil erosion processes (Poesen 2018). In this context, we still need to better understand the interactions between these processes (Brown et al. 2017).

In seismically active mountain ranges, landslides appear as the major erosive agent (e.g., Dadson et al. 2004; Morin et al. 2018; Parker et al. 2011). Moreover, anthropogenic factors (i.e., land-use change, deforestation, hill cutting, etc.) can also be a significant contributor of landslide initiations in active mountain ranges (Maharaj 1993; Larsen and Parks 1997; Wasowski 1998; Chang and Slaymaker 2002; Guns and Vanacker 2014; Holcombe et al. 2016; Laimer 2017; Vuillez et al. 2018; Lee and Winter 2019; Li et al. 2020). In particular, road construction is reported as one of the most influential factors of mass movement and, in particular, landslide occurrence in seismically active mountainous regions such as in India (e.g., Haigh et al. 1989; Barnard et al. 2001), Nepal (e.g., Hearn and Shakya 2017; McAdoo et al. 2018), New Zealand (e.g., Coker and Fahey 1993; Fransen et al. 2001), Pakistan (e.g., Owen et al. 2008; Atta-ur-Rahman et al. 2011) and Taiwan (e.g., Chang and Slaymaker 2002; Chen and Chang 2011). This is not surprising because hillslope cutting can cause a reduction in shear strength of hillslope material, disturb water flow directions and also raised or perched water tables that lead to increase pore water pressure in case of rainfall event (e.g., Guadagno et al. 2003; Tarolli et al. 2013; Holcombe et al. 2016).

As a result, an increasing number of slope failures are observed in seismically active mountain ranges such as the Himalayan region because of road construction (Petley et al. 2007; Froude and Petley 2018). However, capturing the anthropogenic effect in landslide occurrence may not be a trivial task in such environments, because seismic shaking disturbs hillslope materials and increases landslide susceptibility irrespective of road construction (Owen et al. 2008; Tang et al. 2011). Therefore, differentiating the signal of anthropogenic effect from the seismic one can be a challenge in some cases. For instance, Khattak et al. (2010) and Khan et al. (2013) examine the post-seismic landslide evolution following the 2005 Kashmir earthquake and emphasize the possible confusion between landslides triggered by road construction and strength reduction caused by seismic shaking. The same difficulty distinguishing the contribution of anthropogenic and

seismic factors in landslide occurrence can also be valid for slope failures that occurred following the 2015 Gorkha earthquake. Rosser et al. (2021) and Jones et al. (2020) report an increased landslide rate from 2016/2017 onward, which is argued to be primarily associated with the increase in road-construction efforts. However, the disturbance induced by the earthquake is inevitably a part of the predisposing factors.

This implies that capturing the anthropogenic effect could be more convenient in an environment at which seismicity does not play a significant role in landslide occurrence. Therefore, in this study, we focus on a mountainous area located in the northeastern part of Turkey, where the site has been exposed to no significant seismicity but to multiple road construction projects. We examine not only expanding roads, but also mass movements associated with those roads over the last 11 years. To assess the role of the anthropogenic effect, we also map landslides that do not show any direct relation with roads. Ultimately, we compare our mass movement inventory triggered by hillslope cutting with landslide inventories associated with earthquakes in terms of their total surface areas. We should stress that this comparison is only valid for long-term or secondary effects of both human-induced mass movements and earthquake-induced landslides. Because, regardless of their direct consequences, both cases increase the downstream sediment loads in a river network. And this could lead not only to river channel aggregation but also to increase the probability and severity of flooding along the river channel (Fan et al. 2019). In other words, we consider the total surface area of mass movements and landslides as proxies for the long-term hazardous effects of these processes. Therefore, by this comparison, we aim to test the hypothesis that human-induced factors, in our case road constructions, could be more hazardous than an earthquake in terms of mass movements. We test this hypothesis to better assess how relevant human influence can be compared to natural processes.

We also stress that the construction projects conducted in the target area of this research are met with resistance from both non-governmental environmental organizations (e.g., WWF 2020) and geoscientific community (Akbulut and Kurdoglu 2015), because the study area is within the Caucasus ecoregion, which is one of the world's 34 biodiversity hotspots (Şekercioğlu et al. 2011a). The Kamilet Valley crossing through the study area (Sub-basins 4, 5 and 9 in Fig. 1) is one of the sites reflecting the rich biodiversity of the region. It hosts numbers of endemic and rare non-endemic plants species that need to be protected (Şekercioğlu et al. 2011b; Akbulut and Kurdoglu 2015; Yuksel and Eminagaoglu 2017). Therefore, the research question of this study—that aims at exploring the anthropogenic control on mass wasting processes—also has implications on the protection and sustainable development of a biodiversity hot spot.

Study area

The study area is located in the northeastern part of Turkey within the municipal boundaries of Fındıklı, Rize, and Arhavi, Artvin. It comprises nine catchments over approximately 195 km² (Fig. 1). Overall, the alternation of basalt-andesitic lava, pyroclastics, sandstone, marl, and clayey limestone are present throughout the area (Alan et al. 2019).

The steep topographic features of the site are coupled with a strong precipitation regime. The study area is within the zone receiving the highest precipitation measured throughout Turkey (Fig. 2a). Based on the 20 years (from 2000-06-01 to 2020-03-31) time series of the Integrated Multi-Satellite Retrievals (IMERG) Final Run product (Huffman et al. 2019), which is available through Giovanni (v.4.32) (Acker and Leptoukh 2007) online data system, the average monthly precipitation of strong events (i.e., above 0.95 quantile) is

353 ± 40 mm/month. Precipitation measurements are also available from 2012 onward (from 2012-09-04 to 2020-05-31) via three rainfall stations located nearby the study area (Fig. 2b). Based on those measurements, the average daily precipitation of strong events (i.e., above 0.95 quantile) is 30 ± 1.5 mm, whereas the maximum daily precipitation was received on September 24, 2017, as 176 mm.

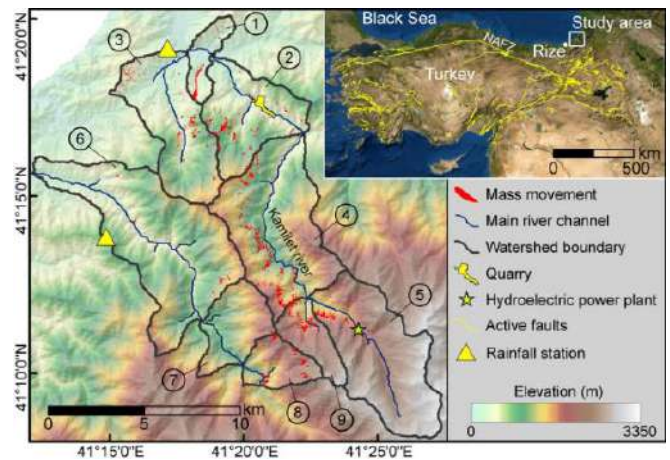


Fig. 1 Overview of the study area. The background aerial image and DEM were

The study area extends approximately 25 km from the coast-line and within the zone, elevation sharply increases to 3350 m from the sea level. This reflects the steep topography in the area. The maximum slope steepness within the examined area is 72°, whereas the average slope steepness is 29° ± 11°.

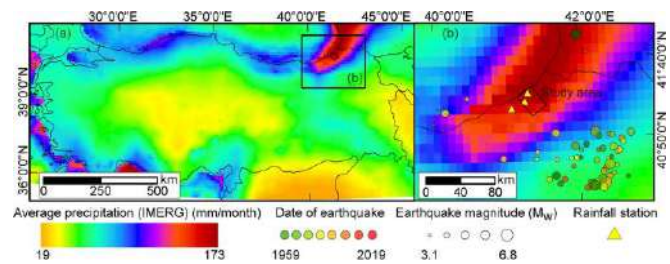


Fig. 2 Maps showing the characteristics of the study area regarding **a** the precipitation amounts that are the highest of entire Turkey (Huffman et al. 2019) and **b** the seismic record of the area for earthquakes that occurred after 1900 (U.S. Geological Survey 2017)

As for the seismicity, the study area has not been exposed to strong external forces caused by earthquakes. The study area is approximately 270 km from the North Anatolian Fault Zone (Fig. 1). The Earthquake catalog of U.S. Geological Survey (2017) shows that in the last 100 years no earthquake ($M_w > 3$) occurred within a buffer zone of 50 km radius centered within the study area (Fig. 2b). The largest earthquake ($M_w = 6.8$) occurred in 1983, approximately 120 km south-east of the study area. Except for this event, only seven earthquakes of magnitude larger than 5.0 have occurred in the near vicinity and the closest epicentral location is 70 km away from the study area.

Although the site is not seismically active, landslides are one of the main natural hazards threatening the East Black Sea region and strong precipitation, land-use change and road construction are the most common factors causing landslides (Reis et al. 2009; Nefeslioglu et al. 2011; Raja et al. 2017). Based on the fatal landslide database of Turkey (Görüm and Fidan 2021), which includes 90-year landslide records, the majority of fatal landslide (55.5%) occurred in the Black Sea.

During the last decade, an increasing number of road construction projects have been elevating the landslide susceptibility in the Black Sea Region (Raja et al. 2017). In particular, within our study area, road constructions have a significant role in landslide occurrences (Akbulut and Kurdoglu 2015). Road construction has been conducted for three main reasons: (1) to increase the accessibility to highlands to boost tourism in the region (*Green Road project*, DOKAP 2014), (2) to build a hydroelectric power plant (HEPP) in the southern part of the study area and (3) to improve the road network overall. Some of the roads constructed under the third category could be indirectly associated with the first two classes because newly constructed roads may have further stimulated the construction of others.

Among these road constructions, in particular, the *HEPP* project has affected the natural course of erosional processes since 2016 (Fig. 3). Local interviews argue that explosives were used in some parts of the road construction to facilitate the progress of the *HEPP* project. This most likely weakened the shear strength of hillslope material, increasing the landslide susceptibility of the given site and promoting the failures. In fact, the local environmental organizations (*Arhavi Doğa Koruma Platformu*) provided evidence to this claim in an early 2020 report where an increased sediment content was noted in the Kamilet River (Fig. 3).



Fig. 3 Photographs showing **a**, **b**, **c** and **d** the mass movements on hillslopes associated with road constructions of *HEPP* (The photographs were taken on June 15, 2020) and (**e** and **f**) the intersection of Kamilet and Durguna Rivers ($41^{\circ} 16' 34''$ N and $41^{\circ} 22' 32''$ E) where increased sediment content in Kamilet River caused by the *HEPP* construction is evident (The pictures were taken in May 2020). The intersection location presented in panel **e** and **f** is given in the lower right of the panel **f**

Materials and method

We map both mass movements and constructed roads from 2010 to June 2020. To create these multi-temporal inventories, we use PlanetScope (3–5 m), Rapid Eye (5 m) images acquired from Planet Labs (Planet Team 2017) and high-resolution Google Earth scenes. The details of the satellite images we used are presented in Table S1.

We create inventories based on the systematic examination of satellite images through manual mapping. We delineate mass movements as polygons and also assign a point to the crest of each polygon manually to identify some characteristics of them (i.e., slope and minimum distance of failed material to roads). We always compare two images to map mass movements that occurred and roads that were constructed within the examined time window. We do not follow a fixed temporal resolution to map mass movements or roads. In fact, we aim at using all the available cloud-free satellite images. Thus, the resulting temporal resolution of the inventories is not fixed and actually increases after 2016, following the increase in the number of available images. For instance, the temporal resolution of our inventory is approximately one year between 2010 and 2011, whereas, after 2016, it is much finer at up to one-month frequency (Table S1).

While mapping, we examine whether or not mass movements are associated with road construction. For this binary labeling, we manually go through the inventory and identify the ones having contact with roads. If the target mass movement crosses a road or is initiated right under a road cut, we label the given mass movement as a human-induced one.

Overall, during the road construction project some of the excavated materials are dumped into the river channels. The differentiation between dumped materials and human-induced landslides is challenging. Regardless, these processes initiate additional anthropogenic sediment loads to river channels. Notably, the extra sediment load could cause river channel aggregation and that could lead to an increase in the probability and severity of flooding along the river channel (Fan et al. 2019). This indicates that both dumped materials and human-induced landslides appear as factors negatively affecting the natural sediment balance of a watershed and in this regard, they are equally hazardous. Therefore, in this study, we do not differentiate the dumped hillslope materials and landslides; instead, we consider them all as human-induced mass movements.

Also, we group mass movements that occurred and roads that were constructed based on two different criteria, namely by assigning a label describing the purpose of road construction and the occurrence/construction time. For the former one, we examine the purpose of road constructions and categorize them under three headings: (1) *HEPP* project, (2) *Green Road* project and (3) others (i.e., roads constructed after 2010 for other reasons than *Green road* and *HEPP* projects). We make interviews with local people and make use of the information gathered from them to categorize roads. Using the same classification, we label not only roads but also the corresponding mass movements. We also compare mass movements associated with road constructions and the ones triggered by precipitation. We do so by examining the occurrences of mass movements for different catchments. This allows us to better investigate the anthropogenic influence by comparing two adjacent catchments exposed to different levels of external disturbances caused by road construction.

For the second criterion, we label mass movements/roads using one year of fixed temporal windows. As a result, we create 11 temporal categories that we can use to examine the evolution of both mass movements and roads from 2010 to June 2020 with one-year temporal resolution. If the existing mass movements expand over time, we only map the new surface in the examined time window.

To examine the landscape characteristics and precipitation regimes, we use Shuttle Radar Topography Mission (SRTM) digital elevation models (approximately 30-m resolution) (NASA JPL 2013), and the Global Precipitation Measurement (GPM), the Integrated Multi-Satellite Retrievals (IMERG) Final Run product (Huffman et al. 2019) and rainfall data provided by the Turkish State Meteorological Service (TSMS

2020) for three stations located nearby the study area (Fig. 2b).

Ultimately, we compare our human-induced mass movement inventory with a sample of earthquake-induced landslide inventories, available via the U.S. Geological Survey Science-Base platform (Schmitt et al. 2017; Tanyaş et al. 2017). We make this comparison to assess how hazardous road construction could be compared to naturally occurring landslides. For the comparison, we examine the landslides' size statistics, which has been used as a basis to identify landslide-event magnitude scale (m_{LS}) and provides a measure to quantify the severity of landslide events (Malamud et al. 2004). We calculate m_{LS} using the code provided by Tanyaş et al. (2018). We also calculate the slope of the power-law distribution (β , power-law exponent) that the frequency-density distribution of landslides exhibits (Guzzetti et al. 2002; Malamud et al. 2004; Tanyaş et al. 2019) using the method proposed by Clauset et al. (2009). To estimate an earthquake magnitude for an equivalent earthquake-induced landslide inventory with our human-induced one, we use the empirical relation between earthquake magnitude (M) and landslide-event magnitude scale (Malamud et al. 2004).

$$m_{LS} = 1.29 \times M - 5.65 \quad (1)$$

Results

Mapping of roads and landslides

We identified the roads associated with "HEPP" and "Green Road" projects (Fig. 4a) based on information from our local contacts and interviewees. They informed us about other expansion work conducted along the route of the Green Road project. We could not identify the time of these expansions, but we know the sections where the engineering work was carried out. We labeled the roads that already exist as of January 2010 as "Pre-2010" based on our analyses of satellite scenes. We labeled the rest of the roads constructed after 2010 as "Others." Based on the identified roads, we also mapped and labeled corresponding mass movements, which are mostly characterized by shallow, rotational slides (Fig. 4b).

To create these road and mass movement inventories, first, we mapped both roads and mass movements associated with HEPP (Fig. 4). Mapping mass movements was particularly challenging because of the short-term interactions between mass movements and engineering activities. Specifically, local people indicated that the excavated hillslope materials were mostly dumped into the river channels during the construction, and also down the slope of the road cut. This may have also induced some landslides further down the hillslope because of the additional load. Notably, this makes the identification of landslides difficult because the dumped hillslope materials and landslides triggered by the construction are mostly mixed and have a similar appearance in satellite scenes. For instance, Fig. 5a and b shows a segment of the road excavation conducted as part of the HEPP project. This satellite image clearly shows that dumped materials are mixed with landslides triggered by road construction. We can both see mass movements that were initiated from the upper or lower hillslopes. For the former ones, we can be sure that these are human-induced landslides. However, for the latter cases, we cannot differentiate whether they are solely dumped materials or human-induced landslides. In fact, most likely, their genesis is the result of the coupled effect of both processes. Therefore, as we also stressed in Sect. 3, we considered them all as human-induced mass movements as they are equally harmful as anthropogenic sediment sources.

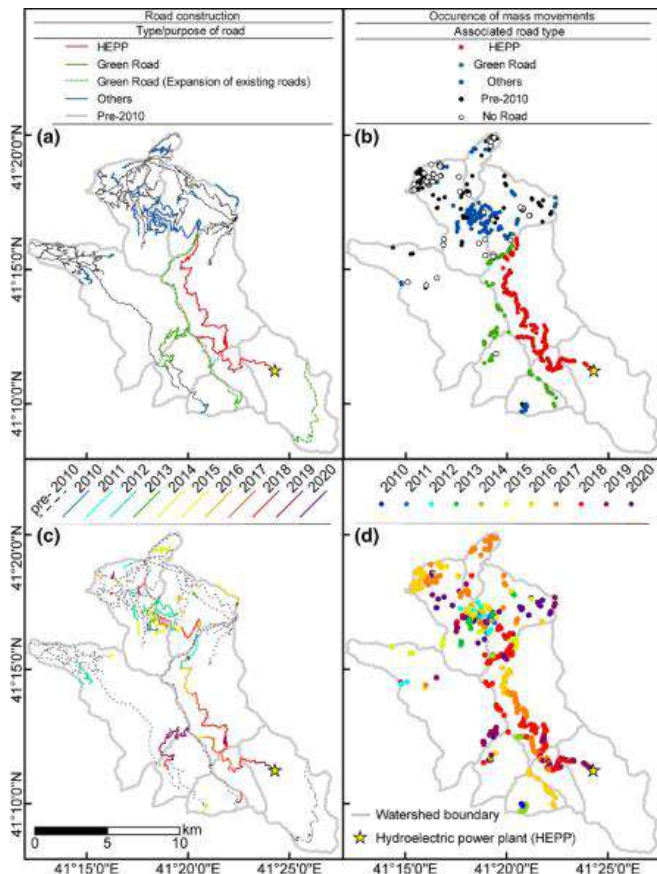


Fig. 4 Maps showing the distribution of **a** the roads constructed for different purposes and **b** the associated landslides as well as **c** the temporal evolution of the roads and **d** the associated landslides



Fig. 5 Google Earth scenes showing the pre- and post-excavation landscape in a selected area (**a–b**) along the route excavated for the HEPP project ($41^{\circ} 13' 56''$ N and $41^{\circ} 20' 18''$ E). The examined segment of the road was constructed between July 17, 2016, and September 6, 2016. Within the same period, mass movements widely occurred. We also identified some mass movements enlarged between September 6, 2016, and July 9, 2017. Another pre- and post-images (**c–d**) showing mass movements at a selected site ($41^{\circ} 15' 37''$ N and $41^{\circ} 20' 24''$ E) along the route excavated for the Green Road project. Mass movements occurred between September 18, 2017, and May 27, 2018. The locations of these mass movements were given in the lower right of panel (**a**) and (**c**)

We also mapped mass movements that occurred along with the Green Road project (Fig. 4a). Some of the mass movements occurred along existing roads, which were expanded in relation to the Green Road project. Similar to the HEPP case, dumped hillslope materials might also play a role in these mass movements. However, Fig. 5c and d shows that the crests of some mass movements extend backward from the road and therefore, we argue that there must be a mixture of both dumped materials and human-induced mass movements if they are not purely human-induced mass movements.

Moreover, we mapped mass movements that occurred along other roads (i.e., *Others*) that were excavated during the same period (Fig. 4 and Fig. S1). These are mostly secondary and private roads opened to access agricultural sites or houses and therefore, they were created without the use of explosives. Consequently, excavated materials are expected to be less compared to HEPP and Green Road, which were designed for higher traffic loads that require a wider road section and cut.

Ultimately, we mapped landslides that occurred along the existing roads (*Pre-2010*) (Fig. S2) and the ones triggered by natural agents irrespective of roads (*No Road*) (Fig. S3). Precipitation is the most likely triggering factor for these landslides. However, for the *Pre-2010* case, road works should have played a crucial role in the failure mechanism by disturbing both resisting forces against sliding and hydrological conditions. As for the *No Road* case, in addition to precipitation as a triggering factor, some anthropogenic factors might have played a role, albeit to a much lesser extent. We will elaborate on the possible contribution of those indirect anthropogenic factors in Sect. 5.

Analyses of mass movements

We mapped 557 mass movements and a 267.2 km long road network. Overall, 33.9% of the roads were developed during the last 11 years, for various purposes (Tables 1 and 2). Among them, 10.8% is associated with the HEPP project and 4.4% is related to the *Green Road* project. Also, some of the existing roads have been extended in relation to the Green Road project and this contribution refers to 11.4% of all roads in the study area. Moreover, 18.7% of the roads constructed after 2010 are not directly associated with the HEPP nor the *Green Road* projects, but some indirect connections could exist (*Others*).

Table 1 Characteristics of different road types

Type/purpose of road	Length (km)	(%)	Average steepness of the terrain that the road is crossing (degree)
HEPP	28.8	10.8	33.0
Green Road	11.9	4.4	26.0
Green Road (Expansion of existing roads)	30.6	11.4	22.0
Others	49.9	18.7	20.0
Pre-2010	146.1	54.7	22.0
Total	267.2		

We also examined mass movements in relation to road work. Our findings show that 90.1% of them occurred after 2010 while being in immediate proximity to the roads (Table 2). As

for the cumulative area of mass movements, the anthropogenic influence is also significant: 90.7% of total size is associated with road constructions. Roads constructed as part of the HEPP project have the most substantial contribution to mass movement occurrences. In the study area, 1.3 km² of mass movements were solely caused by the HEPP project, which refers to 50.6% of the total size identified in the study area. During the last 11 years, 9.9% of mass movements occurred with no direct relationship with roads. In terms of total size, the influence of these mass movements constitutes 9.3% of the total area of mass movements.

Table 2 Characteristics of mass movements associated with different road types

Associated road type	Count	(%)	Total area (km ²)	(%)	Average slope (degree)	Average landslide size (m ²)	Average minimum distance of landslide to road (m)
HEPP	196	35	1.3	51	34	6396	20
Green Road	75	13	0.3	13	31	4449	22
Others	148	27	0.5	21	29	3230	60
Pre-2010	83	15	0.2	6.1	24	1829	41
No Road	55	9.9	0.2	9.3	28	3453	65
Total	557		2.5				

This static summary is complemented below by examining the variation in both road construction and mass movement occurrence on a temporal basis (Figs. 4c, d and 6). For instance, we noticed a peak value in road construction in 2012 (Fig. 6a). However, the peak in the constructions does not correspond to a significant number of mass movements. This is mainly because of the morphologic conditions encountered through the route. In fact, most of the roads we mapped between 2011 and 2012 are associated with roads categorized as *Others* (Fig. 6b). The mean slope steepness observed through these roads is 20°, which is the lowest steepness of the terrain that the road is crossing among different construction projects (Table 1). The highest slope steepness is observed through the roads associated with the HEPP project (33°), whereas the two other categories (i.e., *Pre-2010* and *Green Road*) both cross relatively smooth topography compared to the HEPP project (Table 1). Specifically, the *Green Road* project mainly follows the existing old road path, which passes through ridges. Therefore, a predominant part of these roads did not require any hillslope cut in our study area. This explains why the mass movements triggered in response to the activities of the HEPP project gave the largest damage among different construction projects (Table 2).

Figure 6a also shows that the total length of constructed roads per year continuously increases between 2013 and 2019. However, the increase in the number of mass movements associated with road construction does not follow the same trend with the road constructions. The largest mass movement rates are observed between 2015 and 2019 and this refers to the period that the HEPP project-related road constructions were carried out. Therefore, as we stressed above, the steepness of the terrain, which is quite steep along the route of the HEPP project, also plays a major role in these observations.

The increase in the mass movement trend could also be linked to strong precipitation (Fig. 6d). For instance, between 2015 and 2018 where high mass movement rates exist, the study area was exposed to the strongest rainfall events of the examined period. However, the precipitation component does not solely explain the variation in mass movement rates. For instance, in 2014, mass movement rate is significantly lower than 2017 level, although the amount of precipitation is quite similar to 2017 level (Fig. 6d).

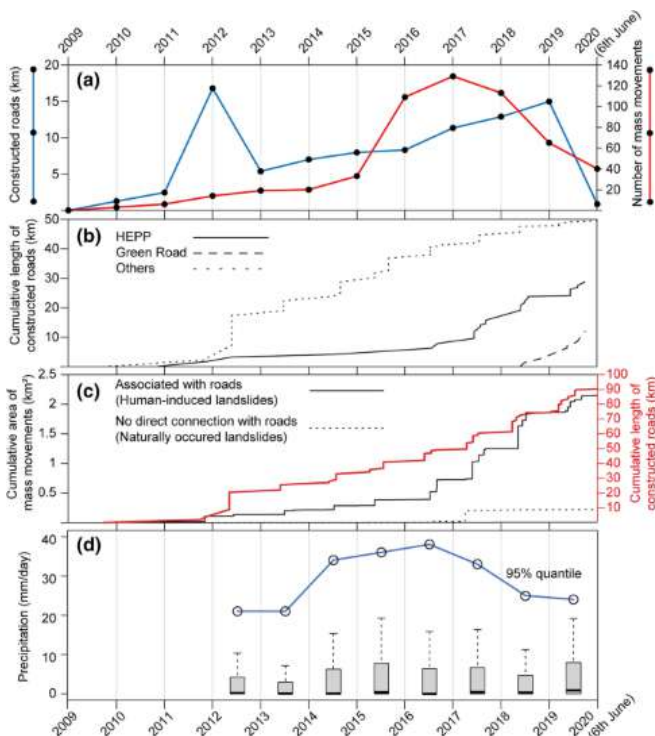


Fig. 6 Plots showing the yearly variation in road constructions and mass movement occurrences from 2010 to 2020 in terms of **a** the number of mass movements against the entire length of constructed roads, **b** the roads constructed for different purposes, **c** the cumulative trend in total mass movement size and road length and **d** the variation in rainfall regime expressed by precipitation amounts above the 0.95 quantile and boxplots excluding outliers. Precipitation data gathered from the rainfall stations (TSMS, 2020) are available from 2012 onward

The findings presented above imply that the road construction is the main factor governing mass movement rates and precipitation could be considered as a predisposing factor elevating its susceptibility. To elaborate on this issue, we examined the spatial distribution of mass movements and the variation in the total mass movement population in relation to distance to roads (Fig. 7). Our findings show that 88% of the total mass movement population occurred within a zone bounded by a 100 m road-buffer zone. This confirms that the increase in mass movement rate is mostly due to road constructions.

We also examined how the road constructions evolved after 2010 in each catchment and, consequently, how this affected the occurrences of mass movements per hydrological unit. Figure 8 shows the summary of these temporal evolutions. For this analysis, we excluded the naturally occurring landslides. Our findings show that if there is no significant road construction, the number of mass movements is relatively low. For instance, catchments 1, 2, 3 and 4 are adjacent catchments. Among them, catchment 1 is the only hydrological unit where the total length of constructed roads in the last 11 years is less than 5 km. The associated total mass movement size in catchment 1 is 0.02 km², whereas, in the

three other catchments (2, 3 and 4), it ranges from 0.24 to 0.82 km². We observed a similar situation in catchments 5, 8 and 9, where we identified a relatively low amount of road constructions (< ~ 5 km) associated with a limited number of mass movements (Fig. 8). In catchments 6 and 7, the total length of the road (~ 10 km) is in between two other sets we mentioned above, but we identified 28 and 9 mass movements in these catchments. These roads are mostly associated with the *Green Road* project and thus the limited number of mass movements is most likely because of the steepness of the topography along the route followed during the construction (Table 1).

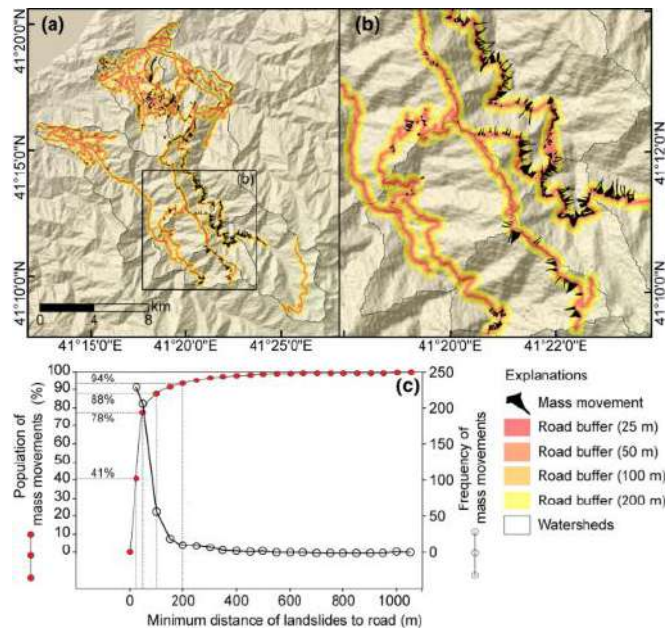


Fig. 7 Plots showing **a** the areal extent of the examined area and spatial distribution of mass movements with respect to road buffer zones, **b** a closer view of mass movements and buffer zones and **c** variation in mass movement population and frequency of mass movements in relation to distance to roads

We also compared human-induced mass movements with naturally occurred ones in terms of slope steepness and size of mass movements. Figure 9 shows that slope steepness of human-induced mass movements varies quite broadly compared to naturally occurring landslides. Hillslopes where the slope steepness ranges from 15° to 50° are associated with a minimum of 20 and a maximum of 100 human-induced mass movements. Conversely, the frequency of naturally occurring landslides increases up to 30° (with a minimum of five and a maximum of 15 landslides), and then sharply decreases for steeper slopes. This large difference is undoubtedly induced by road excavations performed on steep slopes, as demonstrated by the much more numerous mass movements that occurred under anthropic disturbance. In fact, the same slope ranges appear to be mostly stable under natural conditions. Also, there is a large difference in average mass movement size triggered by road constructions and natural agents. The average size of human-induced mass movements is approximately ~ 20,000 m² in the steepest slopes (i.e., 55°–60°), whereas the maximum average size of naturally occurring landslides is ~ 1000 m².

To assess the consequences of human effects on mass movements, we also compared our mass movement inventory (i.e., only the mass movements associated with road constructions) with nine earthquake-induced landslide-event inventories sharing similar landslide-event magnitude and total mass movement area. Figure 10 shows that the human-induced mass movement inventory we mapped is compatible

with landslide events triggered by earthquakes having magnitudes varying from $M_w = 5.9$ to $M_w = 7.2$. This observation is made regardless of climatic and morphologic conditions.

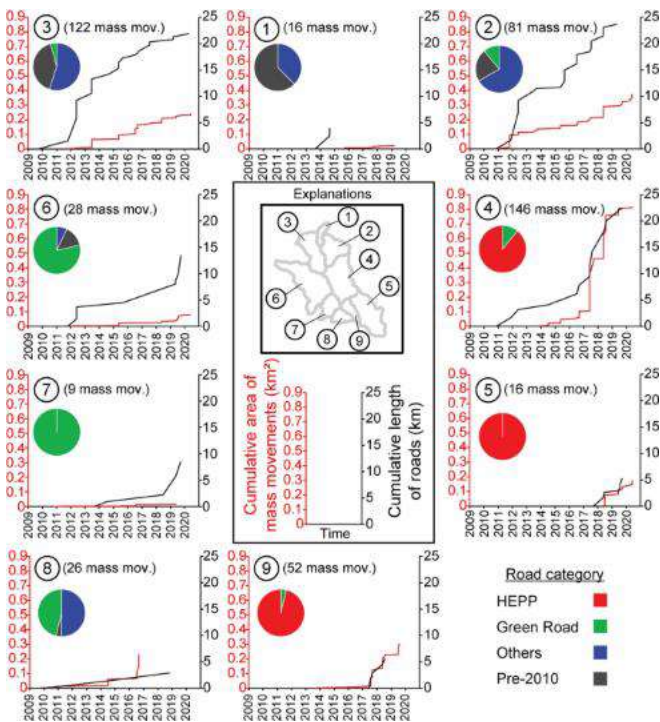


Fig. 8 Figure showing the temporal evolution of both roads and mass movements within each catchment from 2010 to June 2020. Catchments 2, 3 and 4 appear as hydrological units exposed to the highest road construction and consequently, the largest number of mass movements

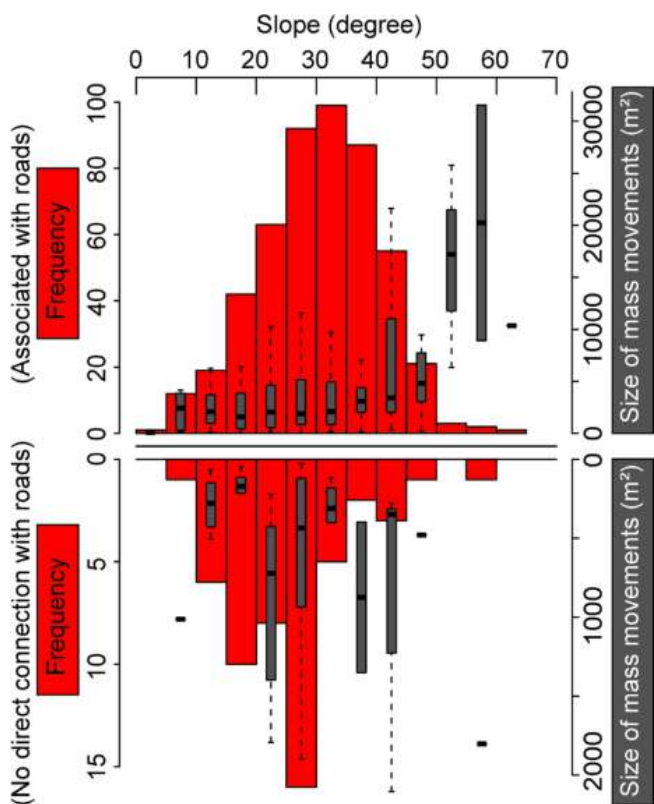


Fig. 9 The comparison of human-induced mass movements (top panel) with naturally occurring (bottom panel) ones in terms of slope steepness and mass movement size characteristics

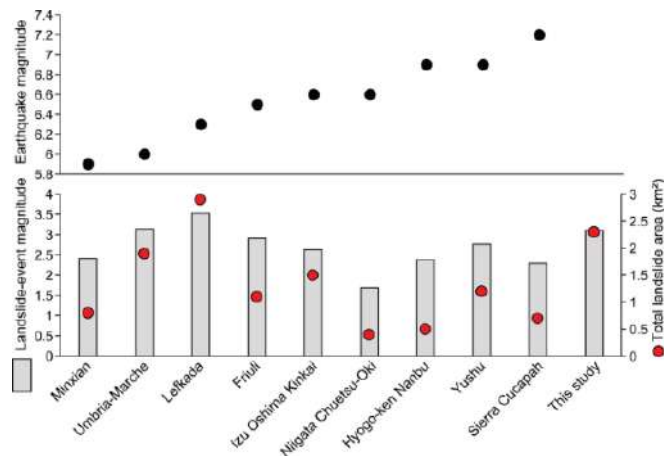


Fig. 10 Comparison between our human-induced mass movement inventory and nine earthquake-induced landslide inventories. Landslide-event magnitudes were calculated based on Tanyaş et al. (2018)

Among the ten examined cases, the total surface affected by landslides changes significantly from one case to another, with many cases showing a much larger spatial extent compared to our study site. Therefore, for a better comparison, we further investigated the landslide inventory associated with the 2013 Minxian earthquake ($M_s = 6.6$ based on the China Earthquake Network Center and $M_w = 5.9$, according to USGS), where the extent of the region affected by landslides is equivalent to our study area. Specifically, the earthquake occurred between Minxian and Zhangixian (in the Gansu Province, China) on a thrust fault and triggered 2330 co-seismic landslides covering $\sim 200 \text{ km}^2$ (Xu et al. 2014), which is also compatible with our study area where the examined catchments cover approximately 195 km^2 .

The cumulated extent of all the landslide polygons associated with the Minxian earthquake is 0.8 km^2 , whereas the total size of our human-induced mass movements is 2.3 km^2 . This shows that even the mass movements solely related to the HEPP project (total mass movement area is 1.3 km^2) can significantly surpass the total co-seismic landslide size induced by the Minxian earthquake.

Before comparing the two inventories in terms of their size statistics, we first analyzed in terms of climatic and morphologic conditions. To collate the climatic information, we used the 20 years (from 2000-06-01 to 2020-03-31) precipitation time series accessed via the IMERG Final Run product, for both sites. Figure 11a shows that both sites have similar precipitation regimes, although the precipitation is relatively higher in our study area. Also, slope and local relief (derived from the SRTM DEM at $\sim 30 \text{ m}$) observed in our study area indicate rougher terrain within the landslide-affected area compared to those affected by the Minxian earthquake (Fig. 11b and c).

We recognize that the two different sites cannot be thoroughly compared, because a much more thorough assessment should be made accounting for detailed geological, geotechnical and hydrological data. However, on the basis of the simplified overview we provide, we can hypothesize that if an earthquake with comparable magnitude to Minxian would occur in our study area, the resultant landslide event should be more significant because our study area is associated with higher precipitation and steeper terrain conditions.

We also calculated the magnitudes of our human-induced mass movement inventory ($m_{LS} = 3.1$) and the Minxian inventory ($m_{LS} = 2.4$). The difference between the two cases is consistent with our initial assumption that if a similar earth-

quake occurred in our study area, it would be more hazardous. In fact, based on the empirical relation between earthquake magnitude (M) and landslide-event magnitude scale proposed by Malamud et al. (2004), the earthquake magnitude for an equivalent earthquake-induced landslide inventory would be 6.8. This shows how destructive the anthropogenic effect on geomorphological processes could be compared to natural processes. The destruction caused by the sediment supply produced by the road constructions conducted in the last 11 years is compatible with the possible effect of a theoretical earthquake with a magnitude greater than 6.0.

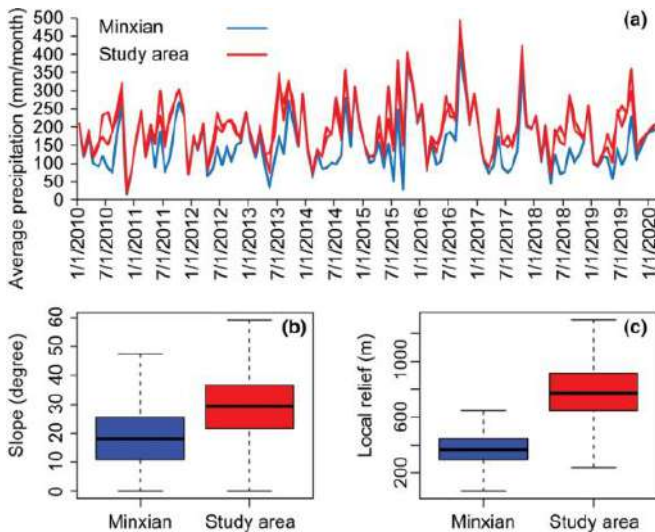


Fig. 11 Plots comparing our study area with the landslide affected area of 2013 Minxian earthquake regarding **a** precipitation amounts, **b** slope steepness and **c** local relief

The comparison between the probability- and frequency-area distributions of the human-induced mass movements we mapped and those naturally triggered by the 2013 Minxian earthquake shows that larger mass movements were triggered in our Turkish site (Fig. 12). The power-law exponents calculated for both our inventory ($\beta = -2.7$) and the Minxian inventory ($\beta = -2.3$) are close to each other and align well with distributions documented in the literature. Power-law exponents of naturally occurred landslide inventories fall in the range 1.4–3.4, with a central tendency 2.3–2.5 (Van Den Eeckhaut et al. 2007; Stark and Guzzetti 2009; Tanyaş et al. 2018).

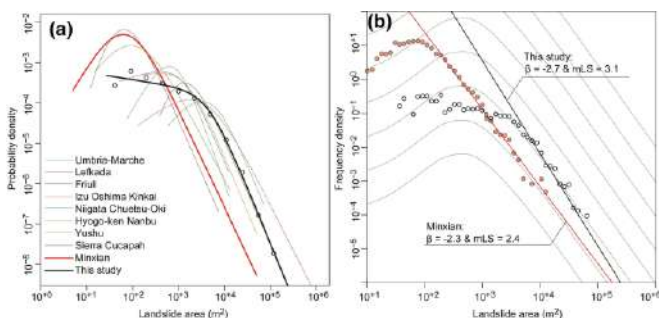


Fig. 12 Plots showing **a** the probability-area and **b** frequency-area distributions of selected landslide inventories as well as the mass movements associated with roads in our study area. The probability density curves presented in the panel (a) are fitted by a double-Pareto distribution using the code of Rossi et al. (2012). Power-law exponents (β) were calculated based on the method proposed by Clauset et al. (2009), whereas power-law fits and landslide-event magnitudes were identified based on Tanyaş et al. (2018)

Discussion

In this study, we provide quantitative, thorough systematically mapping mass movement rate after major road constructions in a mountainous region that is exposed to strong precipitation regimes. We specifically chose this region because seismicity does not play an active role here and therefore, capturing the anthropogenic effect on slope stability is more evident than in tectonically active mountainous regions such as Nepal, India or Pakistan. In tectonically active areas, the legacy of previous earthquakes could last for a long period, increasing the landslide susceptibility (Parker et al. 2015). In particular, after strong earthquakes, the elevated susceptibility is noticeable in the following years (up to nine years) and it decreases over time (Fan et al. 2018). Consequently, in such environments, it would be challenging to decompose the signal of earthquake legacy from anthropic disturbances. Precipitation could also add another layer of complexity. In fact, the occurrence of a landslide or a population of landslides is always controlled by multiple predisposing and triggering factors (e.g., geotechnical properties, hydrologic conditions, land cover, external loads, etc.) (e.g., Jaboyedoff et al. 2018). Capturing the relative contribution of each conditional factor requires not only highly detailed temporal landslide inventories—where we can assess the exact date of occurrence of each landslide—but also quantitative measurements of the predisposing factors at a given time. Notably, we lack such detailed datasets in this paper, and this is often the case in many landslide susceptibility studies, even when multi-temporal models are built (e.g., Guzzetti et al. 2005).

Despite the complexity we faced and the limited temporal information on other controlling factors, we could still investigate whether a relationship exists between slope failures and anthropogenic effects. To address this issue, we made a binary classification distinguishing human-induced and naturally occurring mass movements on the basis of satellite images. However, in some cases, this identification was challenging, as well. For instance, the largest landslide we mapped within the region occurred on November 7, 2016, following a strong precipitation event (Ersoy 2017). This event was a shallow earth-slide flow that affected an area of approximately 0.2 km² within the Kireçli village (Fig. 13). Satellite images show that the crest of the landslides is precisely aligned with an existing road. Some parts of the road failed as a result of this landslide (Ersoy 2017). The complexity in the interpretation arose because this landslide could also be linked to natural landscape evolution processes. In fact, the landslide initiated at the ridge of the slope where the susceptibility is generally higher. Thus, the shallow landslide might have been triggered regardless of the possible influence of the road.

In such cases, we labeled mass movements as naturally occurring ones since we do not have adequate support to argue that they are human-induced. We did this to implement a conservative approach in our analyses. However, emphasis should still be given to the possible direct or indirect anthropogenic effects. In fact, the road could have a direct implication by increasing the pore water pressure at the crest of the landslide. Also, the external loads associated with traffic might be another likely contributor to the landslide initiation. This event is a very interesting example also because of the existence of an active rock quarry approximately 3 km east. There, to dig into the slope and collect the material explosives are commonly used. Our local contacts informed us that some damages had been observed at houses in villages close to the quarry (i.e., Dikyamaç, Güneşli, Dereüstü villages). Among them, the Dereüstü village is located approximately 2.5 km northwest of the quarry, at a comparable distance to the mudflow location (Fig. 13). Therefore, the disturbance exerted by activities related to the quarry might have also played a role in triggering the landslide mentioned above.

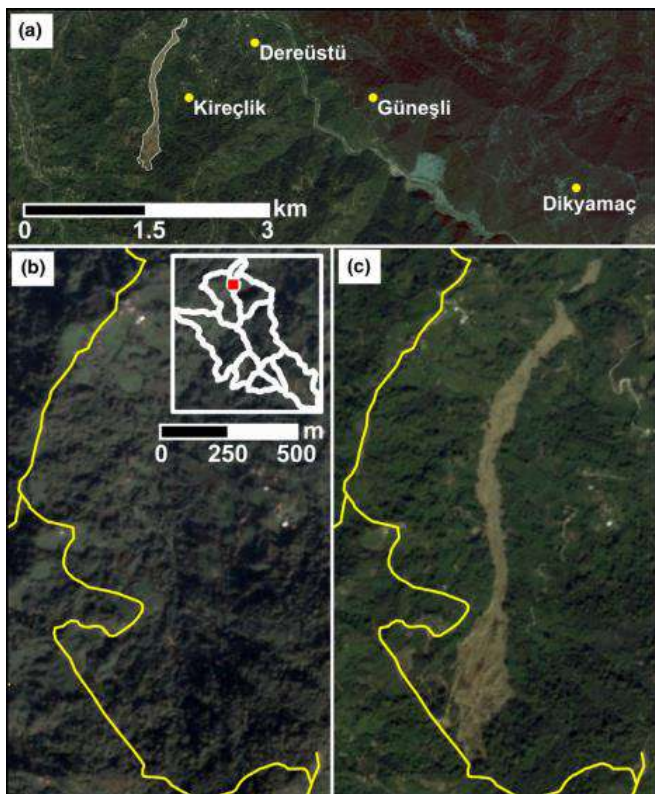


Fig. 13 PlanetScope scenes showing the pre- and post-landslide landscape of the largest landslide mapped within the study area ($41^{\circ} 17' 37''$ N and $41^{\circ} 18' 27''$ E). This landslide occurred on November 7, 2016. The location with respect to our study area is given in the upper right of the panel (b). Yellow lines in the panel (b) and c indicate roads

A similar anthropogenic effect, if not even stronger, could also be valid for mass movements triggered along the roads constructed as part of the HEPP project, because of the explosives directly used to cut the hillslope. In fact, apart from hillslope cuts, explosives have been used in the last segment of the road approaching the HEPP site. In this section, approximately 620 m of the route passes through a tunnel. In such steep terrain, any time a new road is constructed, the damage to the slope is almost inevitable unless extreme precautions are taken. This is also reported in the literature. For instance, Froude and Petley (2018) report that from 2004 to 2016, 30% and 43% of fatal landslides occurred in India and Nepal are associated with road constructions. In these cases, the high landslide rates are not due to the lack of engineering solutions. In fact, landslides triggered in response to road construction projects are a well-known issue for both India and Nepal. The required and appropriate engineering practices necessary to minimize environmental damage have already been documented (e.g., Hearn and Shakya, 2017). The observed landslide hazard associated with road construction is mostly due to neglected engineering solutions (Hearn and Shakya 2017). Therefore, road construction in mountainous regions should not be envisioned unless the required investment in road design is available (Valdiya 2014; Hearn and Shakya 2017). Notably, the site we examined is a good example where road construction has widely damaged the landscape, and it is clear that better precaution or stabilization investments should have been put into practice.

Conclusions

In this study, we report a distinct correlation of mass movements and major road constructions that explicitly shows human impact on mountainous environments which are under anthropogenic disturbance recently. Our results further suggest that slope instabilities increased drastically after major

service road constructions for hydroelectric power plants and as well as other road extension works. Despite the high precipitation amounts in the region, naturally occurring landslides represent a minor percentage both in number and landslide-size-characteristics when compared to the equivalent human-induced mass movements. Regardless of the natural hillslope processes at play, the poor implementation of engineering practices able to ensure stable slope conditions in co- and post-construction phases not only resulted in dangerous widespread mass movements but also caused a substantial change in the sediment transport along with the river network. We could not access enough information on the potential effects of this to quantify increases in sediment loads. However, in the long term, the coarse nature of the material removed from the slopes could also clog narrow river passages, potentially damming small sections of the river network and could cause river-channel aggradation leading to flooding. Therefore, these extra sediments originating from human-induced mass movements could further induce a chain of hazardous events, which could affect not only people living nearby but also the rich biodiversity of the region that needs to be protected. This actually means that all endemic-rare plant and animal species that exist in Kamilet Valley are in danger now because of the poor engineering practice. Specifically for our study area, the results of this work emphasize the need to consider erosion and post-changes in hillslope processes and sediment flux that further lead to additional threats to the local community and biodiversity in response to poor engineering practices and any other anthropogenic disturbances.

We also stress that the impact of road construction can disturb the natural slope equilibrium to an extent comparable with moderate (larger than $6 M_w$) earthquakes. For a seismically inactive area as we examine, this observation is crucial to understand how hazardous the anthropogenic effects could be in terms of landsliding. Such an observation implies that human activities can have a large, if not even dominant, impact on landscape evolution and the natural regime of surface processes. This is part of the definition of "Anthropocene," an age where our society shapes nature for our purposes, frequently at the risk of damaging ourselves.

References

1 ÷ 73

[Natural Hazards](#) (2022)

<https://link.springer.com/article/10.1007/s11069-021-05199-2#Tab1>

Landslides caught on seismic networks and satellite radars

Andrea Manconi, Alessandro C. Mondini, and the AL-PARRAY Working Group

Abstract. We present a procedure to detect landslide events by analysing in sequence data acquired from regional broadband seismic networks and spaceborne radar imagery. The combined use of these techniques is meant to exploit their complementary elements and mitigate their limitations when used singularly. To test the method, we consider a series of six slope failures associated to the Piz Cengalo rock avalanche recently occurred in the Swiss Alps, a region where we can benefit from high spatial density and quality of seismic data, as well as from the high spatial and temporal resolution of the ESA Copernicus Sentinel-1 radar satellites. The operational implementation of the proposed approach, in combination with the future increase in availability of seismic and satellite data, can offer a new and efficient solution to build and/or expand landslide catalogues based on quantitative measurements, and thus help in hazard assessments and definition of early warning systems at regional scales.

1 Introduction

Landslides cause globally fatalities and devastation, with remarkable effects especially on low-income and/or developing countries (Froude and Petley, 2018). While the spatial occurrence of landslides is related to intrinsic geo-morphological, and climatic characteristics (Stead and Wolter, 2015), catastrophic failures arise when slope materials reach a critical damage state (Petley, 2004). In many cases, the ultimate trigger towards failure events is related to anthropic activities, extreme meteorological events, and earthquakes (Bayer et al., 2018; Huang et al., 2017; Lacroix et al., 2019).

Quantitative and accurate data on timing, location and size of landslide events are crucial to study the relationships between local and regional preconditioning factors, to recognize potential causes, as well as to identify the potential effects of climatic forcing. Moreover, efficient early warning systems at regional scale rely on the availability of accurate and complete landslide catalogues (Gariano and Guzzetti, 2016). Despite recent efforts, the knowledge on spatial and temporal landslide distribution is incomplete. The information about landslide volume, runout, velocity, etc. is usually available only when the events threaten life or damage infrastructures, as well as when they are associated with large earthquakes or exceptional meteorological occurrences. These catalogues, however, deliver only a partial picture of the impact of such events on the landscape. In addition, many landslide events are unreported because they occur in remote regions and do not have immediate and/or relevant impacts on human activities. This strongly hinders the completeness of inventories used for hazard assessment and for calibration of early warning systems at regional scales (Guzzetti et al., 2019).

In recent years, two methods have emerged in the panorama of landslide event detection, i.e. satellite remote sensing and seismic data analyses. This is mainly due to the increased availability and quality of these datasets at global scale, as well as to the open data access policies. In particular, Earth Observation (EO) data acquired through different satellite missions are more and more exploited by systematic visual interpretation, as well as supervised and unsupervised automatic classification methodologies, in order to build catalogues of landslide events triggered by large earthquakes and/or extreme meteorological events (Mondini et al., 2019; Tanyaş et al., 2017). These methodologies strongly depend on the availability of the images, which are usually not adequate for systematic early landslide detection. Further, despite the identification of signatures of landslide events in

seismic networks deployed for earthquake monitoring is not a new observation (Govi et al., 2002; Weichert et al., 1994), technical advances and diffusion of broadband seismic sensors have increased the possibility to detect and locate also landslide events of small-moderate size at regional scales. Automatic or semi-automatic procedures adapted from earthquake location routines have demonstrated fair performances (Chao et al., 2017; Dammeier et al., 2011; Ekstrom, 2006; Fuchs et al., 2018); however, while uncertainties of several km can be tolerated in case of earthquake epicentral locations, landslides are extremely confined phenomena affecting a single slope (or only small portions of it). A more accurate location of the events can be achieved with local networks specifically designed to identify mass movements (Dietze et al., 2017; Cook and Dietze, 2022). Despite, such procedures are impractical at the scales of a mountain chain.

In this work, we jointly use broadband seismic data and spaceborne radar imagery to show a procedure allowing for a systematic detection and location of landslides, as well as an initial definition of their area of impact, and their magnitude. We present results over the region recently affected by the Piz Cengalo, a steep granitic massive located in the central Alps at the border between Switzerland and Italy (see Figure 1), The area was repeatedly affected by large (> 1 Mm³), rock slope failure processes in the past decades, with the main event on August 23, 2017, being the largest (>3 Mm³) and most catastrophic reported in recent years, causing 8 fatalities as well as damages in the range of 50M\$. A detailed description of the event, its preconditioning factors, potential causes, the dynamics of the rock slope failure and the subsequent debris flow reaching the village of Bondo, is beyond the scope of this work. Thus, the readers are referred to the recent literature for more information on these specific topics (Mergili et al., 2019; Walter et al., 2019).

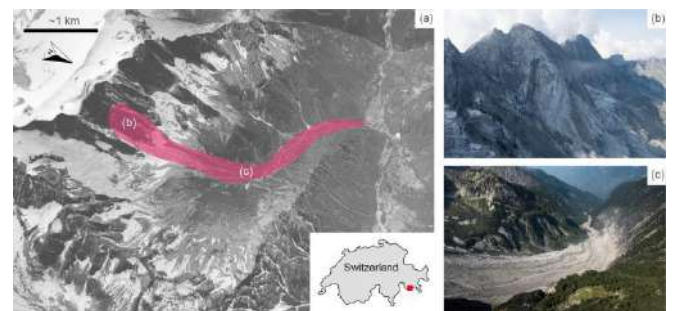


Figure 1: Overview of the area of investigation. (a) View of the Val Bondasca, with approximate outline of the area affected by the Piz Cengalo (46.29475° N, 9.602056° E) rock avalanche and subsequent debris flows, © Google Earth 2021; (b) Detail of the release area, August 25, 2017; (c) Detail of the deposits, August 30, 2017. © Photos VBS swisstopo Flugdienst.

...

5. Conclusions

The key take-home message of this study is to show how the systematic combination of seismic and remote sensing data can be useful for identification and mapping of landslide events. The use of SAR satellites shows the advantages of all weather, day and night, and systematic acquisitions at global scale. When available, optical imagery and/or SAR imagery acquired with different bands, full polarimetric, or with higher spatial resolution can eventually contribute to an increase the quality and the quantity of the information. We believe that combining seismic and spaceborne data is a viable approach for a future operational monitoring system at the scale of the Alps, and for this reason this work can be the starting point

to raise awareness in the community, as well as to foster co-operation and the funding necessary for such an endeavour. We conclude remarking that our approach is not intended to be used for early recognition of landslides or as early warning tool. The main goal of an operational implementation could be to systematically populate landslide catalogues relying on quantitative and accurate information on timing, magnitude, and frequency also in remote areas. Improved catalogue completeness is very important for the calibration of regional early warning systems based on rainfall thresholds, as well as on regional hazard assessments (Guzzetti et al., 2019). The availability of remote sensing imagery with daily or sub-daily revisit times could lead to an employment in early detection of landslide events and possibly also in disaster response scenarios, but these potential applications have to be evaluated in future studies.

European Geosciences Union / Natural Hazards and Earth System Sciences, Preprint nhess-2022-34, <https://doi.org/10.5194/nhess-2022-34>, <https://nhess.copernicus.org/preprints/nhess-2022-34>

Granular porous landslide tsunami modelling – the 2014 Lake Askja flank collapse

Matthias Rauter, Sylvain Viroulet, Sigríður Sif Gylfadóttir, Wolfgang Fellin & Finn Løvholt

Abstract

Subaerial landslides and volcano flank collapses can generate tsunamis with devastating consequences. The lack of comprehensive models incorporating both the landslide and the wave mechanics represents a gap in providing consistent predictions of real events. Here, we present a novel three-dimensional granular landslide and tsunami model and apply it to the 2014 Lake Askja landslide tsunami. For the first time, we consistently simulate small-scale laboratory experiments as well as full scale catastrophic events with the same model. The model captures the complete event chain from the landslide dynamics to the wave generation and inundation. Unique and complete field data, along with the limited geographic extent of Lake Askja enabled a rigorous validation. The model gives deep insights into the physical landslide processes and improves our understanding and prediction capabilities of frequent and catastrophic landslide tsunamis.

Introduction

Tsunamis induced by giant landslides impacting water bodies can be catastrophic^{1,2}, as recently manifested by the 2018 Anak Krakatau volcanic sector collapse that caused 430 fatalities in the Sunda Strait^{3,4,5}. More than six other events during the last 15 years with tsunami run-up as high as 150 m^{6,7,8,9,10} show that such powerful tsunamis happen relatively frequently. Further, a variety of other fatal events from volcanic sector collapses (1792 Mount Unzen tsunami¹¹) to subaerial land- (e.g. 1963 Vajont landslide¹²) and rockslides (e.g. three Norwegian events from 1904–1936²) underpin their destructive potential. Paleotsunami evidence from ancient volcano sector collapses shows that these events may scale up to an even larger magnitude^{13,14} and that they might have oceanic reach¹⁵.

Despite recent progress in modelling coupled landslide and tsunami dynamics^{16,17,18,19,20,21,22}, realistic landslide tsunami modelling is still a major hurdle in understanding and predicting future events. Fundamental properties of landslide tsunamis have been studied extensively in the laboratory²³, but this is yet to be matched with predictive mathematical models^{16,17}. Simplifications of either landslide dynamics (e.g. simplified rheologies^{19,24}) or wave generation (e.g. depth-integration^{16,25}) have prevented real progress in this field for more than a decade and it has become clear that a paradigm shift is necessary²⁶. A key issue has been the inability to explain both the landslide dynamics and the tsunami at various scales with a unified model and parametrisation. Without validated continuum-mechanical models, a deeper understanding of the process is hardly possible and predictions cannot be scaled up to forecast real events.

In this work, we provide a significant leap forward, and demonstrate, for the first time, a model that is equally applicable to laboratory and real case events. The novel multiphase granular flow and tsunami model is based on the $\mu(I)$, $\phi(I)$ -rheology, complemented by critical state theory and pore fluid flow²⁷. This is a logical extension of the classic $\mu(I)$ -rheology for dry granular material proposed by Jop et al.²⁸ and allows mixing of the granular material with fluids that represent the tsunami. Accuracy and scalability are demonstrated through laboratory data²³, but more importantly, through a unique dataset obtained from the 2014 Lake Askja (Iceland) landslide and tsunami (see Fig. 1), covering in detail both the landslide footprint and the tsunami run-up across the entire periphery of the lake⁶. The limited geographical extent of Lake Askja renders it reminiscent of a

large-scale laboratory, suitable for testing models at a full-scale and appropriate resolution. The insight obtained from this event shows promise on how predictive granular multiphase models with very few assumptions are within reach for even the largest events (e.g. Anak Krakatau, Mount Unzen). We use the multiphase Navier–Stokes equations to simulate the porous landslide and the pore fluid (see the Methods section for more details). The pore fluid is composed of air and water and extends beyond the slide to represent the lake and the tsunami. The unknown variables of the model are the granular velocity \mathbf{u}_g , the combined velocity of water and air \mathbf{u}_c , and the volumetric phase fractions of granules ϕ_g , water ϕ_w and air ϕ_a . The phase fractions range from 0 to 100% and describe the local mixture of constituents as shown in Fig. 2. The granular rheology is described in terms of the $\mu(I)$, $\phi(I)$ -rheology²⁷ and the permeability is described by a drag model. While this model is computationally expensive, it is within reach even for full three-dimensional simulations of real cases and a good trade-off between simplicity and accuracy.



Fig. 1: Lake Askja landslide tsunami. **a** Photo of Lake Askja including the landslide scar and deposition from the 2014 landslide event (Picture: Kristinn I. Pétursson). **b** Rendered simulation of this event, showing the wave in the middle of the lake and the displaced landslide mass, highlighted in red.

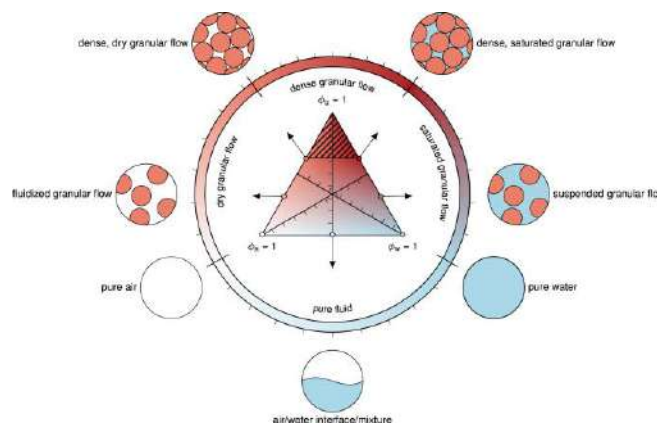


Fig. 2: Phases and the corresponding flow regimes.

The multiphase Navier–Stokes equations allow the representation of various fluids and flow regimes by combining the phase fractions as shown in the diagram. Phases differ in densities and stress models and can thus represent the behaviour of the various flow regimes. The striped area is excluded, accounting for the pore space that is always present in granular material. The coloured ring represents a reduced colour map of limiting cases. The relevant part of this ring is used as colour map in this paper to visualise the local phase fractions.

Results and discussion

...

Discussion

This work represents a major step forward in modelling subaerial landslide tsunamis. Hindcasting the small-scale experiment of Viroulet et al.²³ demonstrates remarkable accuracy of wave kinematics and landslide run out, without the

need for optimised parameters. Other observable details, such as the water intrusion and the frontal vortex appeared naturally in the simulations. The numerical results further compare well with the 2014 Lake Askja landslide tsunami at full scale, predicting tsunami run-up heights and landslide run-out as deduced from field observations⁶. Again, phenomena such as vertical granular jets occurred naturally in the simulations. However, the simulations are computationally expensive (see method section) and uncertainties of various nature (numerical, geological, constitutive parameters) are present. Differences between observations and simulations are small and improved agreement can most likely be obtained with a more careful estimation of the constitutive parameters, higher grid resolutions or by including additional processes, such as turbulence or surface tension. A long-standing problem of granular flow models, the apparent reduction of the friction coefficient for very large events^{42,43}, remains unsolved in the presented model and it will be a major challenge to identify the responsible processes in the future. The presented model might be helpful in this endeavour as well, providing a strong platform for further developments.

The model is sufficiently complex to accurately predict the landslide dynamics and wave generation, but still efficient enough to tackle full three-dimensional problems. It is presently too computationally expensive for parametric studies or probabilistic analyses³⁹, but provides fundamental new insight into the physics of landslide tsunamis. This model may hence be used operationally, to build an understanding of the involved processes or as a benchmark for a new generation of more efficient models. Calibrating and developing depth-integrated models with porous and granular character^{7,44,45} represents a possible path forward, while dynamic coupling with depth-integrated tsunami models for the far-field propagation^{15,46} represents another promising approach, deemed necessary for resolving problems where the tsunami propagates over long distances. Notably, the discrete element method (DEM)⁴⁷ provides an alternative to continuum-mechanical models, however, for a substantially higher computational cost that scales unfavourable with the size of the event.

Full three-dimensional methods are relatively rare in the tsunami community but their application and the respective publications have been rising consistently in the last few years. In the present paper, we show that such models may provide the necessary paradigm shift to understand and predict landslide tsunamis. The $\mu(I), \phi(I)$ -rheology plays a central role in this endeavour, because it allows to include the granular and porous nature of the slide. With the increasing computational capabilities expected in the near future, utilisation of fully three-dimensional models can become mainstream. This represents a unique opportunity to improve the protection of coastal communities and our understanding of devastating landslide tsunamis.

...

Data availability

The geographic data is available upon request from Sigríður Sif Gylfadóttir (siggasif@vedur.is). The data generated in this study and the respective measurements are provided in the [supplementary information](#). [Source data](#) are provided with this paper.

Code availability

The code is available upon request from Matthias Rauter (matthias@rauter.it).

References

1 ÷ 65



EERI Earthquake Reconnaissance Report:

M6.4 Albania Earthquake on November 26, 2019

Volume 1: Executive Summary



Anton Andonov, Markel Baballëku, Georgios Baltzopoulos, Nikola Blagojević, Jitesdra Bothara, Stéphane Brûlé, Svetlana Brzew, Panayotis Carydis, Llambro Duni, Edmond Dushi, Fabio Freddi, Roberto Gentile, Christos Giarlelis, Federica Greco, Merita Guri, Brisid Isufi, Rexhep Koçi, Efthymios Lekkas, Marko Marinković, Olga Markogiannaki, Spyridon Mavroulis, Chiara McKenney, Ivan Miličević, Viviana Novelli, Anastasios Sextos, Chungwook Sim, Despoina Skoulidou, Sotiria Stefanidou, Nikolaos Theodoulidis, Fred Turner, and Enes Veliu.

Reviewers: Fred Turner and David Wald

January 2022

A product of the EERI Learning from Earthquakes Program

1 INTRODUCTION

1.1 Organization of the EERI Earthquake Reconnaissance Report

...

1.2 Overview of Reconnaissance Teams

1.3 Overview of earthquake

On the morning of Tuesday, November 26, 2019, at 3:54 local time, an MW 6.4 earthquake struck 16 km north of Durrës, a port city on the Adriatic coast and the second largest city in Albania. The epicenter was 33 km northwest of Tirana, the largest city and capital of Albania. Deaths and injuries were concentrated in Durrës and the village of Thumanë, though Tirana and several smaller municipalities in north-western Albania were also affected. With 51 fatalities, the earthquake was the deadliest worldwide in 2019. At least 913 people were injured, including 255 individuals who were injured during the aftershock sequence.

The earthquake was preceded by an MW 5.6 foreshock on September 21, 2019, at 14:04 local time, 12 km north of Durrës. The period after the November 26, 2019, earthquake was characterized by a great number of aftershocks. During the period from November 26, 2019, to June 30, 2020, over 2,000 events were recorded by the Albanian Seismological Network, including five aftershocks greater than M5.

The September 21, 2019, and the November 26, 2019, earthquakes are the strongest earthquakes that have affected Albania in the last 40 years. The strongest event to affect Albania in the 20th century occurred on April 15, 1979 (MW 6.9). This event had an epicenter on the southern coast of Montenegro (approximately 75 km from Durrës), but it

caused loss of life and building damage in the northern part of Albania.

2 SEISMOLOGY AND GROUND MOTION

Albania is located in southeastern Europe on the Balkan Peninsula. The Durrës region is situated in the Periadriatic Fore-deep, an area where the Adriatic microplate subducts under the Eurasian Plate. The Outer Albanides geological structure, where the Durrës region is located, is characterized by an active and complicated geologic-tectonic structure (Aliaj et al., 1996).¹ The MW 6.4 earthquake on November 26, 2019, was caused by an east dipping, blind, thrust fault located under the Durrës syncline. It is estimated that the subsurface fault rupture length was about 19 km.

The epicenter of the earthquake was 16 km from Durrës. The earthquake ground shaking lasted around 50 seconds; however, the strong motion recording in Durrës lasted only 15 seconds due to a loss of electricity. The peak acceleration measured was approximately 0.2g (192 cm/s²), and the maximum Intensity estimated in Durrës was VIII (severe) based on the Medvedev–Sponheuer–Karnik scale; see Figure 1. The Durrës basin has characteristics that amplify ground motion, and for periods between 0.3 seconds and 1.0 seconds, the spectral acceleration in Durrës was high with values around 0.5g, which contributed to the damage of mid-rise buildings (5 to 10 stories) in downtown Durrës (Figure 2).

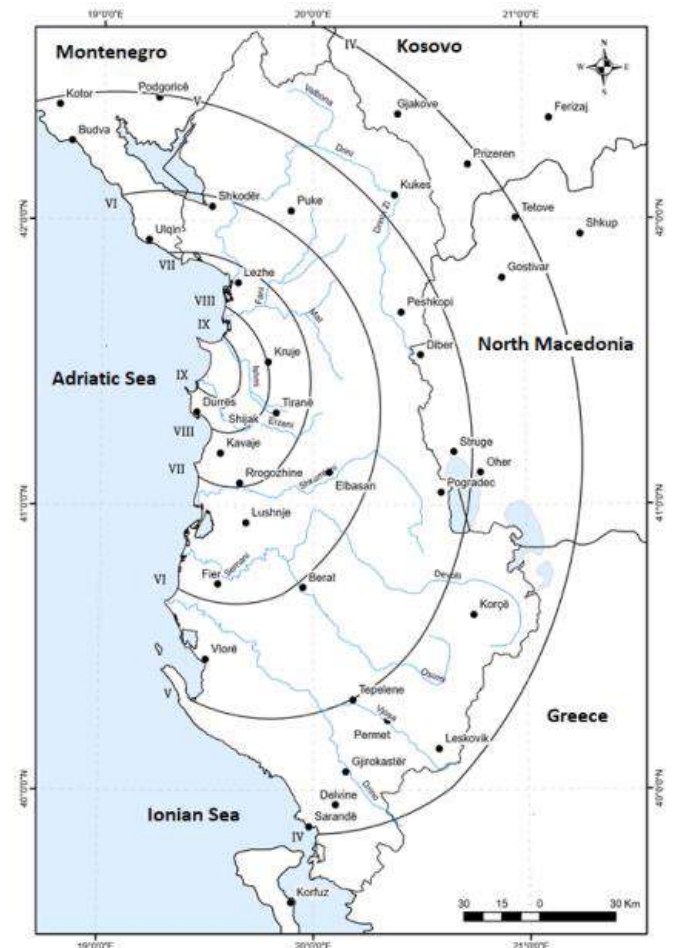


Figure 1. Observed MMI distribution related to the November 26, 2019, (MW6.4) earthquake (source: Koci et al., 2019).²

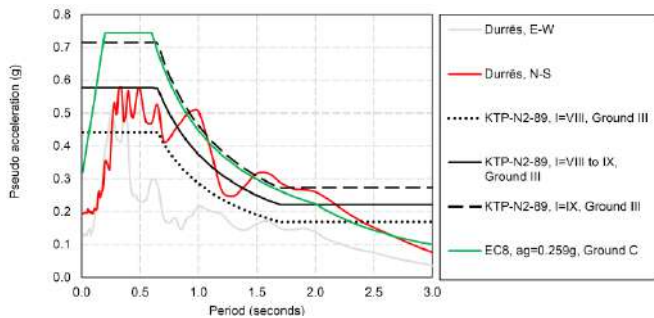


Figure 2. Elastic spectra according to KTP-N.2-89 and EC8 codes and the 5% damped horizontal pseudoacceleration response spectra for recorded motions at the Durrës station during the November 26, 2019, mainshock.

Figure 2 presents the 5% damped pseudoacceleration response spectra corresponding to the north-south and east-west oriented components of the recorded ground motion at the station in Durrës, along with the spectra corresponding to the 1989 Albanian seismic design code KTP-N.2-89 (Academy of Sciences and Ministry for Construction, 1989)³ for seismic intensities VIII, between VIII and IX, and IX, and soft soil conditions (category III) corresponding to the station site. Although KTP-N.2-89 is still the official code in Albania, in recent years, Eurocode 8 has been increasingly used for design applications on a voluntary basis. For comparison, a Eurocode 8 (European Committee for Standardization, 2004)⁴ elastic spectrum is also plotted for ground type C (based on the average value of propagation velocity of S waves in the upper 30 m of the soil profile at a shear strain of 10⁻⁵ or less, $v_{s,30} = 202$ m/s, for the Durrës station) and the reference peak ground acceleration on rock equals 0.259g for a return period of 475 years based on recent seismic hazard studies (IGWE, 2021).⁵

It can be seen from Figure 2 that the spectral accelerations in the north-south direction are close to the KTP-N.2-89 spectra values for the frequency range corresponding to mid-rise buildings. The Eurocode 8 elastic spectrum developed for peak ground acceleration levels based on recent studies is close to the KTP-N.2-89 spectrum for intensity IX, but ground conditions are even worse in other parts of the city of Durrës, which indicates that the Eurocode 8 requirements combined with recent seismic hazard studies are more demanding for the structures in Durrës. For all periods except for those around 1s and those between 1.4s and 2.2s, it can be observed that the spectra corresponding to recorded ground accelerations are within the range of elastic spectra based on KTP-N.2-89 code for seismic intensity between VIII and IX corresponding to the epicentral area of the earthquake. The KTP-N.2-89 spectrum for the highest intensity (IX) envelops the recorded spectra for almost the entire range of periods, except for localized spikes in spectral values near 1s and 1.5s.

3 GEOTECHNICAL EFFECTS

Northwestern Albania is highly susceptible to geotechnical effects, including liquefaction and slope movement. This susceptibility has been assessed by relevant studies on the landslide and liquefaction susceptibility and the history of the Periadriatic Depression. The slope movements and liquefaction phenomena observed after the November 26, 2019 mainshock and the September 21, 2019 foreshock were characteristic of the region.

Liquefaction phenomena were triggered by the November mainshock in several sites, including the coastal part of southern Durrës, the Rinia-Fllakë Lagoon, the Erzen River estuary, and the area west of the town of Thumanë. The main

characteristic of these liquefaction-affected sites is the occurrence of recent Holocene deposits, including marshy, lagoonal, and river deposits. The main types of phenomena observed in the liquefaction-affected sites included individual sand boils, the ejection of liquefied material from ground cracks, the arrangement of sand boils along ground cracks, and water and sand fountains in still waters. The liquefaction observed in coastal Durrës affected an urban area at sites in close proximity to totally or partially collapsed hotels (Figure 3). In the Rinia-Fllakë Lagoon, liquefaction caused slight damage to the electric power supply system.



Figure 3. The liquefaction site in the southern part of Durrës was close to three hotels that experienced extensive structural damage: the totally collapsed Mira Mare Hotel, the partially collapsed Vila Verde hotel, and the Lubjana hotel (drone source: Lekkas et al., 2019).⁶

Slope movements were triggered in both the November mainshock and the September foreshock. Landslides and liquefaction in the Shkëmbi i Kavajës area affected the local road network.

4 LIFELINES AND TRANSPORTATION

The earthquake caused limited damage to infrastructures such as bridges, railways, airports, the power sector, telecommunication, water supply, and irrigation systems. Services and functions were restored shortly after the earthquake. The damage caused by the earthquake immediately triggered emergency response. Most services were restored within 24 hours after the earthquake, which shows the capability of local authorities in mobilizing manpower, materials, and equipment to cope with the impacts of a major earthquake disaster. Distributed infrastructure systems experienced limited damage, as the earthquake shaking was not severe enough to test their resilience or the infrastructure management systems.

The transport network suffered limited damage and disruption due to the earthquake despite the presence of a well-distributed transportation network in the area. The road network only suffered minor damage to road pavement due to

cracking, which caused damage to the secondary elements of the two overpass bridges near Durrës (Figure 4) and damage to bridge deck seating. Similarly, in Durrës, a wagon repair workshop, one railway station, and one railway bridge suffered moderate to severe damage. Albanian civil aviation, including air transportation operations, did not report any damage.

Post-earthquake observations show that the water, sanitation, and solid waste management facilities/systems suffered minimal damage or losses, though there was an extensive network of piped supply and sewer systems in the area. The earthquake caused damage to a sewage treatment plant and water supply pipes near Durrës (Figure 5) and one pumping

station in Lezha. The damage to the pipeline was fixed within a day. Four water supply depots also suffered damage in Tirana.



Figure 4. A damaged highway overpass near Durrës (photo: J. Bothara)

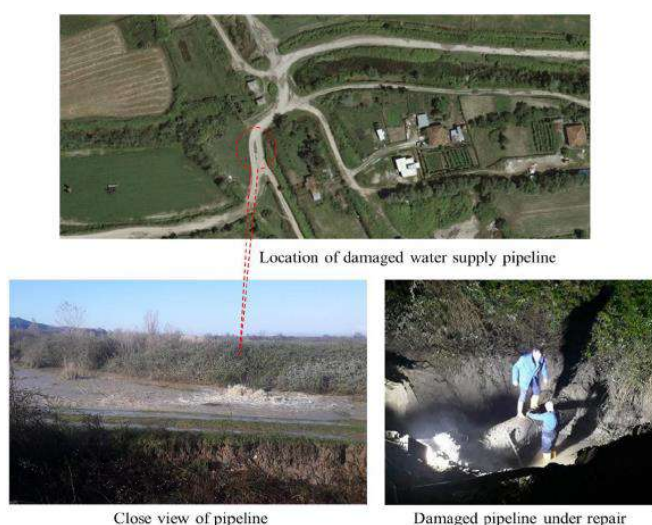


Figure 5. Damage to a water supply pipeline near Ishem, Durrës (photos: M. Baballëku).

5 RESPONSE AND RECOVERY

...

8 CLOSING REMARKS

The November 26, 2019 earthquake was the strongest to hit Albania since 1979. The earthquake put to test the emergency response capabilities of Albania and the seismic safety of the building stock and critical infrastructure.

With regards to seismology, the level of earthquake shaking was within the expectations of the seismic hazard studies conducted over the years for the Durrës region. Unfortunately, a strong motion recording station was not available close to the Thumanë village that suffered significant damage and casualties, and the strong motion record from the Durrës station was not available for the full duration of ground shaking. These records would have been useful for gaining a better understanding of the earthquake and its consequences. For this reason, further investments into the Albanian Seismological Network are recommended. In addition, updated seismic hazard maps need to be approved and used for seismic design purposes in the near future.

The earthquake highlighted the importance of geotechnical aspects related to the seismic response of buildings and other engineering structures. The earthquake damage was widespread in soft-soil areas, and clustering of damaged buildings was observed near liquefaction sites, particularly in the Durrës area.

The housing sector suffered the most significant damage and losses, whereas lifelines, transportation, and critical infrastructure systems remained generally functional. A major issue related to housing, especially in suburban areas, is the informal construction during the post-1990 period, which resulted in a large stock of nonengineered low-rise buildings. Among taller reinforced concrete buildings, those with inadequately engineered renovations or extensions (e.g., the addition of stories, floor extensions, and demolition or addition of structural and nonstructural walls) experienced more extensive damage compared to other buildings. These issues need to be addressed by relevant authorities to mitigate the risk in existing building stock from the effects of future earthquakes.

Low-strength multifamily unreinforced masonry buildings with prefabricated hollow core slabs of the pre-1990 vintage proved to be life-threatening during this earthquake; hence, existing buildings of this type need to be urgently identified and retrofitted.

The damage patterns in reinforced concrete buildings include extensive cracking of infills and partition walls, interaction of infills with concrete frames, and the hazards associated with infills due to out-of-plane failures. The damage can be attributed to excessive lateral drifts due to flexible frame systems with shallow beams, inadequate amount of shear walls, irregularities in plan and elevation (even when shear walls are present), interaction with infills, inadequate detailing of reinforced concrete elements, and substandard quality of materials. It is important to review current construction practices associated with these buildings and provide guidance to prevent similar damage from occurring during future earthquakes.

It is recommended to pay more attention to the seismic safety of school facilities alongside the improvement of their condition. It is particularly important to evaluate the seismic safety of facilities that were not initially designed as schools with the appropriate "importance factor". It is also very important to create a detailed database of the condition of existing school buildings, a program for continuous monitoring of the condition of these buildings, and detailed studies on the seismic vulnerability and risk of school buildings.

Most reinforced concrete hospital buildings have masonry infills that were not considered in seismic design and were not detailed for in-plane and out-of-plane seismic actions. As a result, even though the buildings did not experience any structural damage due to the earthquake, these damaged infills limited the functionality of these hospital buildings. Special attention is needed to mitigate this issue in hospital buildings and protect them from future earthquakes.

Response and recovery are areas where important lessons were learned by the local authorities. Significant assistance from several European countries, including the neighboring countries, was received during the immediate response stage. The damage assessment process was initially challenging due to the lack of standardized damage assessment procedures. Challenges during the preparation of detailed structural assessment reports for damaged buildings arose due to the differences between Eurocode 8 (Part 3), which was required by the government decree, and the Albanian design codes and practice.

Finally, it should be noted that the current seismic design code in Albania KTP N.2-89 (issued in 1989) is outdated because it was developed at a time when the construction typologies and technology were quite different from today. In this context, it is urgently needed to either update the Albanian seismic design code or adopt Eurocodes. In addition, measures need to be taken to ensure the enforcement of the building design codes in practice and to minimize or eliminate altogether future informal construction developments.

https://www.researchgate.net/publication/358107750_EERI_Earthquake_Reconnaissance_Report_-_M64_Albania_Earthquake_on_November_26_2019

Modelling the sequential earthquake-tsunami response of coastal urban transport infrastructure

Azucena Román-de la Sancha, Rodolfo Silva, Omar S. Areu-Rangel, Manuel Gerardo Verduzco-Zapata, Edgar Mendoza, Norma Patricia López-Acosta, Alexandra Ossa, and Silvia García

Abstract

Transport networks in coastal, urban areas are extremely vulnerable to seismic events, with damage likely due to both ground motions and tsunami loading. Most existing models analyse the performance of structures under either earthquakes or tsunamis, as isolated events. This paper presents a numerical approach that captures the sequential earthquake-tsunami effects on transport infrastructure in a coastal area, taking into consideration the combined strains of the two events. Firstly, the dynamic cyclical loading is modelled, applied to the soil-structure system using a finite difference approximation to determine the differential settlement, lateral displacement, and liquefaction potential of the foundation. Next, using a finite volume method approach, tsunami wave propagation and flooding potential are modelled. Finally, the hydrostatic and hydrodynamic loads corresponding to the wave elevation are applied to the post-earthquake state of the structure, to obtain a second state of deformation. The sequential model is applied to an embankment in Manzanillo, Mexico, which is part of a main urban road, the response is analysed using ground motion records of the 1995 Manzanillo earthquake-tsunami event.

<https://nhess.copernicus.org/preprints/nhess-2021-381/>

Mysterious global tsunami in 2021 caused by hidden M8.2 earthquake

Scientists have uncovered the source of a mysterious 2021 tsunami that sent waves around the globe in August 2021 when a magnitude 7.5 earthquake hit near the South Sandwich Islands. The epicenter was 47 km (29 miles) below the Earth's surface — too deep to initiate a tsunami — and the rupture was nearly 400 km (250 miles) long, which should have generated a much larger earthquake. This case represents an extreme example of the broad spectral behaviors of subduction zone earthquakes and calls for attention in the research and warning of similar events.

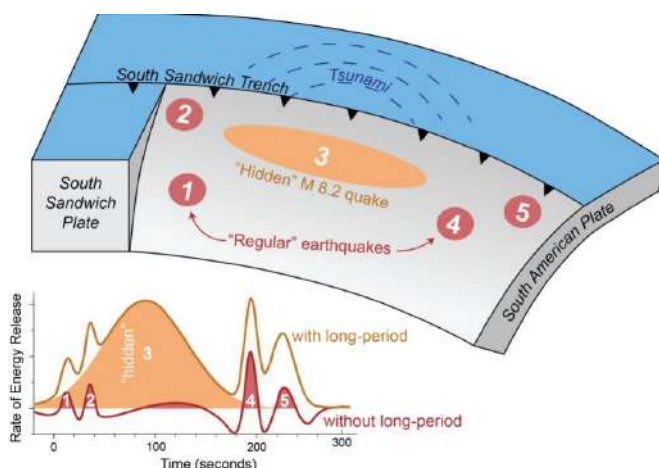
Now, a new study¹ published in AGU Geophysical Research Letters revealed the quake wasn't a single event, but five, a series of sub-quakes spread out over several minutes. The third sub-quake was a shallower, slower M8.2 quake that hit just 15 km (9.3 miles) below the surface. That unusual, 'hidden' earthquake was likely the trigger of the worldwide tsunami.

"The 2021 August South Sandwich Island Mw 8.2 earthquake was a surprise, because it was initially reported as a magnitude 7.5 event at a deep depth but generated a global-spreading tsunami that would only be expected for a larger and shallower event," researchers said.

"By using seismic data with period as long as 500 seconds, we revealed a hidden Mw 8.16 shallow slow event that happened between clusters of regular ruptures in the beginning and end. Although the slow event contributed 70% of the seismic moment, lasted three minutes, and ruptured a 200 km (124 miles) section of the plate interface, it is essentially invisible at short or intermediate periods, which explains its anomalously low body-wave and surface-wave magnitudes."

"The third event is special because it was huge, and it was silent," said lead author Zhe Jia, a seismologist at the California Institute of Technology.² "In the data we normally look at [for earthquake monitoring], it was almost invisible."

Predicting hazards for complex earthquakes can be difficult, as the South Sandwich Islands quake demonstrates. The USGS initially reported the magnitude 7.5 quake and only added the M8.2 the following day, as the surprise tsunami lapped on shores up to 10 000 km (6 200 miles) away from its point of origin.³



A magnitude 8.2 earthquake was 'hidden' within a magnitude 7.5 earthquake in 2021, sending a mysterious tsunami around the world, according to a new study in Geophysical Research Letters. Credit: Zhe Jia and AGU

"We need to rethink our way to mitigate earthquake-tsunami hazards. To do that, we need to rapidly and accurately characterize the true size of big earthquakes, as well as their physical processes," Jia said.

Because this type of earthquake can result in an unexpected tsunami, it's critical to improve our predictions.

"With these complex earthquakes, the earthquake happens and we think, 'Oh, that wasn't so big, we don't have to worry.' And then the tsunami hits and causes a lot of damage," said Judith Hubbard, a geologist at the Earth Observatory of Singapore who was not involved in the study.

"This study is a great example of how we can understand how these events work, and how we can detect them faster so we can have more warning in the future."

Both Jia and Hubbard noted a long-term goal is to automate the detection of such complex earthquakes, as we can for simple earthquakes. For the 2021 quake, the tsunami was small by the time it reached shores, and most of the permanent residents of the remote, volcanic islands are penguins. But complex earthquakes can pose significant hazards if they generate larger tsunami or strike in a densely populated region.

References:

¹ The 2021 South Sandwich Island Mw 8.2 Earthquake: A Slow Event Sandwiched Between Regular Ruptures - AGU Geophysical Research Letters - Zhe Jia et al. - February 8, 2022 - <https://doi.org/10.1029/2021GL097104>

² Hidden magnitude-8.2 earthquake source of mysterious 2021 global tsunami - [AGU](https://www.agu.org)

³ Complex earthquake: USGS says M7.5 in South Sandwich Islands was foreshock of M8.1 - [The Watchers](https://www.usgs.gov)

(Teo Blašković / THE WATCHERS, February 10, 2022, [Mysterious global tsunami in 2021 caused by hidden M8.2 earthquake \(watchers.news\)](https://www.watchers.news))

Βαλκανατόλια: Ανακαλύφθηκε μια ξεχασμένη ήπειρος 40 εκ. ετών που συμπεριλαμβάνει την Ελλάδα

Πολλές από τις γεωλογικές αλλαγές που οδήγησαν στη Βαλκανατολία δεν έχουν ακόμη γίνει πλήρως κατανοητές



Μια ήπειρος που υπήρχε πριν από περίπου 40 εκατομμύρια χρόνια που φιλοξενούσε εξωτική πανίδα μπορεί να «άνοιξε το δρόμο» στα ασιατικά θηλαστικά για τον «αποικισμό» προς νότια Ευρώπη, σύμφωνα με νέα έρευνα.

Σφηνωμένη μεταξύ Ευρώπης, Αφρικής και Ασίας, αυτή η ξεχασμένη ήπειρος - την οποία οι ερευνητές έχουν ονομάσει «[Βαλκανατόλια](#)» - έγινε πύλη μεταξύ Ασίας και Ευρώπης όταν η στάθμη της θάλασσας έπεσε και σχηματίστηκε μια χερσαία γέφυρα, περίπου 34 εκατομμύρια χρόνια πριν.

«Το πότε και πώς το πρώτο κύμα ασιατικών θηλαστικών έφτασε στη νοτιοανατολική Ευρώπη παραμένει ελάχιστα κατανοητό», γράφουν ο παλαιοντολόγος Αλέξης Λιχτ και οι συνεργάτες του στη νέα τους μελέτη.

Πριν από περίπου 34 εκατομμύρια χρόνια, στο τέλος της εποχής του Ηώκαινου*, μεγάλοι αριθμοί γηγενών θηλαστικών εξαφανίστηκαν από τη Δυτική Ευρώπη καθώς εμφανίστηκαν νέα ασιατικά θηλαστικά. Το γεγονός αυτής της ξαφνικής εξαφάνισης τώρα είναι γνωστό ως [Grande Coupure](#).

Πρόσφατα βρέθηκαν ευρήματα απολιθωμάτων στα Βαλκάνια υποδεικνύοντας μια «ιδιόμορφη» βιοπεριοχή που φαίνεται ότι επήλθε στα ασιατικά θηλαστικά να «αποικίσουν» τη νοτιοανατολική Ευρώπη από 5 έως 10 εκατομμύρια χρόνια πριν συμβεί το Grande Coupure.

Για τη διερεύνηση, ο Λιχτ, του Γαλλικού Εθνικού Κέντρου Επιστημονικής Έρευνας, και οι συνεργάτες του επανεξέτασαν τα στοιχεία από όλες τις γνωστές τοποθεσίες απολιθωμάτων στην περιοχή, η οποία καλύπτει τη σημερινή Βαλκανική χερσόνησο και την Ανατολία, τη δυτικότερη προεξοχή της Ασίας.

Η ηλικία αυτών των τοποθεσιών αναθεωρήθηκε με βάση τα τρέχοντα γεωλογικά δεδομένα και η ομάδα ανακατασκεύασε τις παλαιογεωγραφικές αλλαγές που εντόπισε, η οποία έχει ένα «σύνθετο ιστορικό επεισοδιακής βύθισης και επανεμφάνισης».

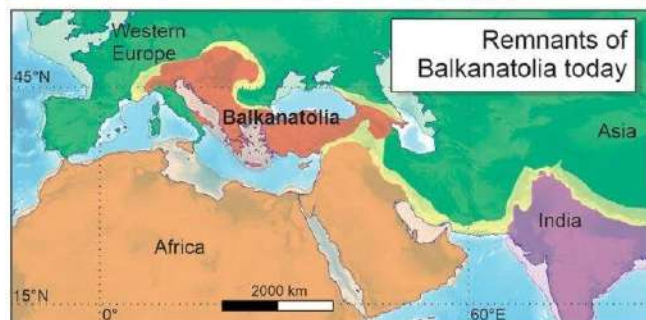
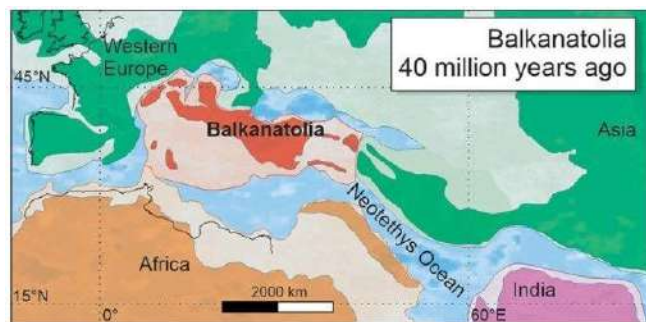
Αυτό που βρήκαν υποδηλώνει ότι η «Βαλκανατολία» χρησίμευσε ως σκαλοπάτι για τη μετακίνηση των ζώων από την Ασία στη δυτική Ευρώπη, με τη μετατροπή της αρχαίας ξηράς από αυτόνομη ήπειρο σε γέφυρα ξηράς - και επακόλουθη εισβολή με ασιατικά θηλαστικά - που συμπίπτουν με κάποιες «δραματικές παλαιογεωγραφικές αλλαγές».

Πριν από περίπου 50 εκατομμύρια χρόνια, η Βαλκανατολία ήταν ένα απομονωμένο αρχιπέλαγος, χωριστό από τις γειτονικές ηπείρους, όπου άκμασε μια μοναδική συλλογή ζώων διαφορετική από εκείνες της Ευρώπης και της ανατολικής Ασίας, σύμφωνα με την ανάλυση.

Στη συνέχεια, ένας συνδυασμός πτώσης της στάθμης της θάλασσας, αυξανόμενων στρωμάτων πάγου της Ανταρκτικής και τεκτονικών αλλαγών συνέδεσαν την ήπειρο της Βαλκανατολίας με τη Δυτική Ευρώπη, μεταξύ 40 και 34 εκατομμυρίων ετών πριν.



Αυτό επέτρεψε στα ασιατικά θηλαστικά, συμπεριλαμβανομένων των τρωκτικών και των τετράποδων οπληφόρων θηλαστικών (γνωστοί και ως οπληφόρα) να μεταναστεύσουν προς τα δυτικά και να εισβάλουν στη Βαλκανατολία, δείχνει το αρχείο απολιθωμάτων.



Ο Λιχτ και οι συνεργάτες του ανακάλυψαν επίσης θραύσματα οστού γνάθου που ανήκει σε ζώο που μοιάζει με ρινόκερο σε μια νέα τοποθεσία απολιθωμάτων στην Τουρκία, την οποία χρονολόγησαν περίπου 38 έως 35 εκατομμύρια χρόνια πριν.

Το απολιθωμα είναι, αναμφισβήτητα, το αρχαιότερο ασιατικό οπληφόρο που ανακαλύφθηκε στην Ανατολία μέχρι σήμερα και προηγείται του Grande Coupure κατά τουλάχιστον 1,5 εκατομμύριο χρόνια, υποδηλώνοντας ότι τα ασιατικά θηλαστικά «αποίκισαν» προς την Ευρώπη μέσω της Βαλκανατολίας.

Αυτό το νότιο μονοπάτι προς την Ευρώπη κατά μήκος της Βαλκανατολίας ήταν ίσως πιο ευνοϊκό για τα αυτά τα ζώα από το να διασχίζουν περιοχές μεγαλύτερου γεωγραφικού

πλάτους μέσω της Κεντρικής Ασίας που εκείνη την εποχή ήταν πιο ξηρές αναφέρει ο Λιχτ και οι συνεργάτες του.

Πολλές από τις γεωλογικές αλλαγές που οδήγησαν στη Βαλκανατολία δεν έχουν ακόμη γίνει πλήρως κατανοητές.

Η μελέτη δημοσιεύτηκε στο [Earth-Science Reviews](#).

* Το Ηώκαινο είναι γεωλογική εποχή η οποία διήρκεσε από 56 έως 33,9 εκατομμύρια χρόνια πριν και είναι η δεύτερη εποχή της Παλαιογενούς περιόδου του Καινοζωικού αιώνα. Το Ηώκαινο βρίσκεται χρονικά ανάμεσα στο Παλαιόκαινο και το Ολιγόκαινο. Η έναρξη του Ηώκαινου χαρακτηρίζεται από μια σύντομη περίοδο κατά την οποία η συγκέντρωση άνθρακα-13 ήταν ιδιαίτερα χαμηλή σε σχέση με τον άνθρακα-12 στην ατμόσφαιρα. Το τέλος της χαρακτηρίζεται από συμβάν εξαφάνισης, το οποίο μπορεί να σχετίζεται με τη σύγκρουση αστεροειδών στη Σιβηρία και στον κόλπο Τσέζαπικ.

(Στέφανος Νικήτας / Huffington Post, 23/02/2022, https://www.huffingtonpost.gr/entry/valkanatolia-anakaleftheke-mia-xechasmene-epeiros-40-ek-eton-poe-semperilamvanei-ten-ellada_gr_6215dce3e4b0ef74d727e8ef)

Balkanatolia: The insular mammalian biogeographic province that partly paved the way to the Grande Coupure

Alexis Licht, Grégoire Métais, Pauline Coster, Deniz İbilioğlu, Faruk Ocakoğlu, Jan Westerweel, Megan Mueller, Clay Campbell, Spencer Mattingly, Melissa C. Wood, K. Christopher Beard

<https://doi.org/10.1016/j.earscirev.2022.103929> [Get rights and content](#)

Abstract

The Grande Coupure corresponds to a major episode of faunal turnover in western Europe around the Eocene-Oligocene boundary that is generally attributed to the influx of multiple clades of Asian mammals. However, Asian mammal clades begin to appear in the fossil record of southeastern Europe during the middle [Eocene](#), 5–10 million years prior to the Grande Coupure. How and when these Asian mammal clades colonized southeastern Europe remains poorly understood, partly because the fossil record of mammals from nearby Anatolia is characterized by marked [endemism](#) and very limited exchanges with Asia during most of the [Eocene](#). We resolve this apparent paradox by reviewing the age of existing paleontological sites from the Balkans to the Caucasus and documenting the oldest Asian perissodactyls found so far in central Anatolia, which date to the lower or middle Priabonian, 38 to 35 million years ago, on the basis of geochronological, magnetostratigraphic and biostratigraphic data. We show that the Eocene distribution of mammals across Eurasia supports a previously unrecognized biogeographic province, designated here as Balkanatolia, spanning the eastern and central segment of the Neotethyan margin. Isolated from mainland Eurasia during the early and middle Eocene, Balkanatolia formed a low-topography [archipelago](#) where endemic and anachronistic mammals thrived. We show that the Eocene fossil record supports Balkanatolia having been colonized by Asian ungulates and rodents by the late Bartonian (mammalian [Paleogene](#) biohorizon MP16), following the establishment of a continuous terrestrial dispersal corridor across the central segment of the Neotethyan margin. This colonization event was facilitated by a drop in global eustatic sea level and a tectonically-driven sea retreat in eastern Anatolia and

the Lesser Caucasus during the late middle Eocene. These paleogeographic changes instigated the demise of Balkanatolia as a distinct biogeographic province and paved the way for the dispersal of Asian endemic clades before and during the Grande Coupure in western Europe.

Introduction

The mammalian biogeography of Eurasia during the Paleogene is commonly described as two distinct biogeographic provinces, western Europe and eastern Asia, separated by several epicontinental seaways acting as barriers (Brikiatis, 2014). For most of the Paleocene and Eocene, both regions display significantly different mammalian faunas with some level of intra-provincial endemism (Franzen, 2003; Menecart et al., 2021), punctuated by episodic long-distance exchanges with North America (Beard and Dawson, 1999; Beard, 2008) and Gondwana (Gheerbrant and Rage, 2006), and gradually increasing exchanges between eastern Asia and the Indian subcontinent (Klaus et al., 2016). The biotic provincialism shown in eastern and western Eurasia ended abruptly in the earliest Oligocene, 33.9 to 33.4 million years ago, with the decline of endemic Eocene animals in western Europe, such as adapiform primates, palaeotheriid perissodactyls and nyctitheriid laurasiatherians, and the rapid appearance of invasive taxa from eastern Asia, including crown clades of rodents (such as cricetids and castorids), perissodactyls (such as rhinocerotoids) and artiodactyls (such as anthracotheriids and hornless ruminants; Vianey-Liaud, 1991; Hartenberger, 1998; Hooker et al., 2004). This faunal turnover is often referred to as the “Grande Coupure” (Stehlin, 1909) and is roughly synchronous with the Oi-1 glaciation 33.5 million years ago (Hooker et al., 2004; Costa et al., 2011), the most dramatic episode of ice-sheet growth, eustatic sea level drop, and global cooling associated with the fall into the Oligocene Icehouse (Miller et al., 2009). However, this simple picture of two biogeographic provinces has been challenged by recent paleontological findings emphasizing the peculiarity of a third mammalian biogeographic region spanning from southeastern Europe to Anatolia, characterized by high endemism and earlier dispersal events (Tissier et al., 2018; Métais et al., 2018).

The discovery several decades ago of Eocene perissodactyls (amynodontids, hyracodontids, and bronthotheriids) and artiodactyls (anthracotheriids) in southeastern Europe showing Asian affinities had already underscored a clear biogeographic separation between western and southeastern European faunas prior to the Grande Coupure (Koch, 1897; Kretzoi, 1940; Nikolov and Heissig, 1985). Recent discoveries of additional Eocene mammals of Asian affinity such as anthracotheriids in Italy (Grandi and Bona, 2017), amynodontids, bachitheriids (Menecart et al., 2018; Tissier et al., 2018) and cricetid rodents (de Bruijn et al., 2018) in the Balkans indicate that invasive mammals from Asia began to colonize southeastern Europe sometime between the Lutetian and the Priabonian, potentially as much as 10 million years before the Eocene-Oligocene Transition (Tissier et al., 2018). However, when and how the first wave of Asian mammals made it to southeastern Europe remains poorly understood, because the ages of most of these fossil localities are associated with large uncertainties, as they are based on mammalian biostratigraphy and distant correlations between European and Asian fossil sites.

The geographic distribution of these early Asian immigrants spans a mosaic of Gondwana-derived and Laurasia-derived terranes assembled throughout the upper Cretaceous and lower Paleogene (van Hinsbergen et al., 2020). This amalgamation of terranes, designated here as Balkanatolia (Fig. 1), formed a low-elevation landmass from the Alpine region to the Lesser Caucasus for much of the Eocene. Balkanatolia has a complex history of episodic drowning and emergence

during the Eocene (Barrier et al., 2018), and it has been depicted either as a discontinuous archipelago (Böhme et al., 2013) or a wide and continuous island (the Balkanian-Anatolian Island of Franzen, 2003). It has thus been proposed that Asia-derived mammals dispersed to southeastern Europe along a "southern route" through Balkanatolia, via island hopping and/or during episodes of quasi-complete emergence (Becker, 2009; Böhme et al., 2013; Mennecart et al., 2018, Mennecart et al., 2021).

The past connectivity between individual Balkanatolian islands and the existence of this southern dispersal route remain debated because of the striking differences between Eocene mammal faunas on opposite sides of Balkanatolia, in southeastern Europe and Anatolia, respectively. Previously documented Eocene Anatolian mammal faunas from the Pontides and Anatolide-Tauride terranes indicate longstanding physical isolation from the rest of the world, because they comprise a unique mélange of endemic mammals including embrithopods (large afrotherian herbivores from Gondwana; Erdal et al., 2016; Gheerbrant et al., 2018), metatherians of Gondwanan origin (Métais et al., 2018), anachronistic survivors of an otherwise Paleocene European ungulate clade (Métais et al., 2017), with only bats (Jones et al., 2019) and primates (Beard et al., 2020) showing likely biogeographic affinities with Asia. Rodents have yet to be documented in Anatolia before the Eocene-Oligocene Transition (EOT; de Bruijn et al., 2003), and Asian ungulates remain undocumented before the late Oligocene (Métais et al., 2016). Yet the southern dispersal route through Anatolia cannot be ruled out because the temporal relationships among the endemic Eocene Anatolian faunas and the various Asia-derived fossils from Eocene sites in southeastern Europe remain poorly understood due to the poor geochronological resolution of many of the relevant fossil sites. That is, it remains unclear if these different faunal assemblages reflect biogeographic provincialism within Balkanatolia or different temporal stages within a single biogeographic province, before and after the establishment of a southern dispersal route linking Balkanatolia with adjacent parts of Asia.

This paper provides a synthesis of the biogeographic history of Balkanatolia and investigates the chronology of mammalian dispersal along the Neotethys margin preceding the Grande Coupure, based on new fossil material and an exhaustive review of Eocene fossil sites from central Europe to the Caucasus. We report here the discovery of the oldest ungulates from Anatolia showing clear biogeographic affinities with Asia, which constrain the arrival of invasive terrestrial vertebrates from Asia to Anatolia no later than the early to middle Priabonian, at least 1.5 million years prior to the Grande Coupure. We show that current paleontological data from Balkanatolia do not require faunal provincialism to explain its various assemblages; regional fossil site chronology is consistent with an initial episode of colonization from Asia achieved by the late Bartonian, signaling the end of endemism in Balkanatolia. We show that this dispersal event possibly coincides with precursor faunal turnovers in western Europe predating the Grande Coupure, and thus indicates the initiation of a southern route for Eurasian dispersal as early as the late middle Eocene. The dispersal event is synchronous with a regional marine regression in Anatolia and the adjacent Caucasus, attributed to a combination of global eustatic drop and collisional tectonics along the central segment of the Neotethyan margin. This sea retreat established a continuous corridor for the dispersal of land mammals along the Neotethyan margin, triggering the demise of Balkanatolian endemism.

Section snippets

Regional context

Balkanatolia is defined as a semi-continuous strip of land during the Paleocene and Eocene between the western European craton and the Cimmerian terranes of the Middle East (Sanandaj-Sirjan, Lut and Afghan Blocks). To the north, the basement of Balkanatolia comprises Laurasia-derived terranes (Tisza, Dacia, Rhodope and Standja Massif, Pontides) that were separated from the core of Laurasia by back-arc spreading between the Late Jurassic and Late Cretaceous (Stephenson and Schellart, 2010). To ...

Results

Two taxa of fossil mammals, both of which pertain to Asian perissodactyl clades, have been recovered from basal red beds of the İncik Formation in the Yerköy Syncline. The first of these is documented by maxillary fragments (width x length: ca. 70 × 70 cm) with erupted molars (Fig. 3a) that pertain to a large brontothere, identified here as *Embolotherium* aff. *andrewsi* (see Appendix A1). The second taxon (Fig. 3b) is represented by an isolated upper molar pertaining to a hyracodontid ...

A 2 stage-scenario for the biogeographic history of Balkanatolia

The discovery of late Eocene Asian ungulates in Anatolia provides a minimum age of middle Priabonian (>35 Ma) for the end of Anatolian biogeographic isolation. It shows that, like southeastern Europe, Asian ungulates reached Anatolia at least 1.5 million years before the Grande Coupure. In order to evaluate the relationship between Anatolian and southern European fossil localities, we compiled all published Balkanatolian sites with land mammals (all mammals excluding fossil sirenians, cetaceans ...

<https://www.sciencedirect.com/science/article/abs/pii/S0012825222000137?via%3Dihub>

(Τα άρθρα που ακολουθούν προέρχονται από πρόσφατο αφιέρωμα του περιοδικού Geostrata του Geo-Institute / ASCE στα υπόγεια έργα)

G-I = Geo-Inspirational



Robert B. Gilbert

I am inspired by tunnels. My dad was a mining engineer, and his passion for geology and the underground clearly rubbed off on me. I got excited about geotechnical engineering as a student at the University of Illinois, learning about tunnel case histories and visiting the Tunnel and Reservoir Plan, aka "Deep Tunnel," project in Chicago. My wife designs and builds tunnels for a living and is honored to be a member of The Moles. To this day, I enjoy making tunnels and arches in sand castles whenever I'm at a beach.

The importance of tunnels and underground construction is growing. Tunnels for water, wastewater, energy, and transportation are needed more and more to support population growth. Climate change is increasing the demands on tunnels in coastal cities to protect infrastructure from rising water levels. The new Infrastructure Bill will motivate the construction of many new tunnels and the rehabilitation of existing tunnels across the United States. Even Elon Musk thinks tunnels have a bright future!

Tunnels also pose one of the most challenging and interesting geotechnical problems. They require a substantive understanding of geology, geomechanics, structures, hydraulics, ground improvement, ventilation, mechanical systems, monitoring networks, and construction means and methods. The risks of delays, cost increases, and damage to surrounding infrastructure during construction are significant. And, critically, the consequences of a collapse can be catastrophic. But when all goes well, tunnels are magnificent feats of engineering and construction.

The Geo-Institute is working to serve the tunneling and underground construction community. The G-I Underground Engineering and Construction technical committee has collaborated with the Society of Mining, Metallurgy and Exploration through the Underground Construction Association, the Deep Foundations Institute, The Moles, and the Beavers on the *Down for That* (undergroundcareers.org) initiative.

This collaboration created a *Down for That* website to provide information about a career in the underground as well as informational resources for students, educators, and professionals. *Down for That* puts together tunnel tours around the

country and gets experienced tunneling people in the classrooms for students and others interested in learning more. *Down for That* is currently developing a new Geo-Challenge Underground Engineering student competition in time for Geo-Congress 2023 in Los Angeles, a city with its share of tunnels and challenging tunnel projects.

There's more the G-I can do to support the demand for tunnels and underground construction in the future. We can partner with SME to host a Geo-Congress that includes either a North American Tunneling Conference or a Rapid Excavation and Tunneling Conference.

We can encourage and support the inclusion of underground engineering and construction topics in undergraduate and graduate curricula. We can foster more research into improving the efficiency and effectiveness of underground construction. We can let the public, and especially youngsters who might become future geoprosessionals, know how important and cool tunnels are.

In summary, the G-I serves an important umbrella role in supporting underground (yes, pun intended) engineering and construction, in leading efforts to improve the state of practice, and in inspiring young engineers to seek a future in the underground community. If the new Geo-Challenge involves tunnels in moist beach sand, count me in!

Robert B. Gilbert, Ph.D., P.E., D.GE, NAE, M.ASCE

President, ASCE Geo-Institute

bob_gilbert@mail.utexas.edu

[Geostrata - February/March 2022 - G-I = Geo-Inspirational \(readgeo.com\)](#)

Filling the Gaps with Pressurized Tunnel Boring Machines

Edward J. Cording



Figure 1. Alaskan Way Viaduct Replacement tunnel: 57.5-ft-diameter TBM cutterhead in the exit shaft.

A revolution is here: the ability to tunnel deep beneath waterways without continually using compressed air, and at shallow depth in urban areas without damaging surface settlement. It began about 50 years ago with pressure-face (slurry balance and earth pressure balance) tunnel boring machines that prevented inflow and large ground loss into the tunnel face.

Previously, most tunnel shields had open faces and were hand-mined, and then, in the mid-20th century, were mechanized using diggers or rotating cutterheads. It was a continual struggle to prevent inflow of water and soil into the open tunnel face. Furthermore, loss of ground into the open overcut gaps around the tunnel shield, resulting in surface settlements in the range of 1 to 2 in., could not be prevented.

Filling the gaps. In recent decades, the revolution has continued with electronically monitored, fully pressurized TBMs that consistently prevent loss of ground, not only into the face of the TBM but into the gaps around the shield and tail of the TBM so that settlements are reduced to levels that do not damage overlying structures (Gap #1).

But there are other gaps that need to be filled in organizing and controlling pressurized TBM tunneling.

- Gap #2: between the control of the TBM and the geotechnical monitoring
- Gap #3: between the assessment of building protection measures and the required capabilities of the pressurized TBM

Gap #1: Filling the Gaps around TBMs to Prevent Loss of Ground

Unfilled gaps around the shield and tail of TBMs are the primary cause of regular loss of ground and surface settlement. They include:

The tail gap between the ground and the segmental lining at the tail of the shield. The approximate 4- to 6-in.-wide gap around the segmental lining is filled by continuously injecting grout, usually a fast-gelling, two-component grout, through the tail as the TBM advances. Injection pressures and volumes are monitored throughout the advance. Over the past few decades, continuous injection through multiple ports in the tail of the shield has largely eliminated loss of ground into the tail gap.

The overcut gap behind the cutterhead. The overcut (steering gap) on the shield body behind the cutterhead must be filled and pressurized to prevent loss of ground into the gap. Injecting bentonite slurry through the shield during the TBM shove more consistently fills and pressurizes the gap than can be achieved by relying solely on the flow of conditioned muck around the cutterhead to fill the gap, particularly in coarse soils. The volume injected and the pressures on the shield perimeter are monitored during and between advances. Injecting bentonite slurry is particularly needed and required for large-diameter TBMs and when tunneling below structures and at shallow depths.

An example of the ground control achieved with pressurized TBM is the Alaskan Way Viaduct Replacement (AWVR) tunnel, which was driven with a 57.5-ft-diameter earth pressure balance machine, or EPBM (Figure 1). The drive was completed in April 2017 beneath downtown Seattle in glacio-lacustrine clays, silts, outwash sands and gravels, and tills. The 1.2-in. overcut gap around the shield body was filled and pressurized with bentonite slurry throughout the entire drive. Polymers were added when sands were above the tunnel crown. Face and shield pressures were maintained between advances by automatic injection of bentonite slurry into the cutterhead chamber and shield gap.

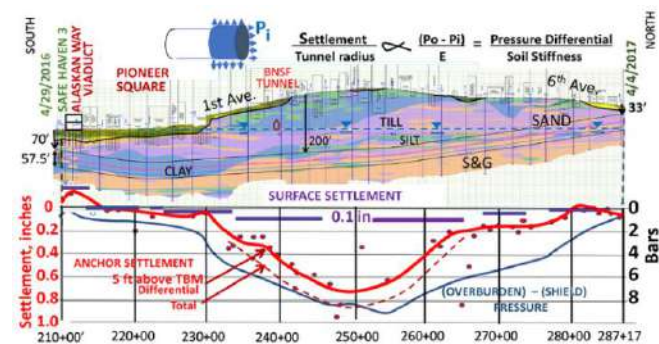


Figure 2. Alaskan Way Viaduct Replacement tunnel pressurized TBM controls settlement.

During the design and proposal stages, requirements for building protection were evaluated assuming ground loss percentages in the range of 0.35 to 0.50 percent, which resulted in estimated settlements exceeding the 0.5- to 1-in. settlement criteria and led to a series of mitigation measures. Prior to tunneling, closely-spaced micropiles were installed between the Viaduct pile foundations and the tunnel crown. Their installation resulted in Viaduct settlements exceeding the 1 in. criterion, whereas the pressurized TBM caused no settlement when it was advanced 15 ft below the foundations. Compensation grouting through multiple, closely spaced, horizontal-sleeve port pipes was to be conducted as the TBM advanced beneath historic Pioneer Square buildings, but was eliminated when early test section results showed that the pressurized TBM was causing less settlements than the 0.5 in. settlement criterion for those buildings.

In fact, prevention of ground loss into the gaps resulted in actual surface settlements throughout the tunnel alignment that were an order of magnitude less than those estimated from the assumed ground loss percentages. Surface settlements were 0.1 in. when tunneling at depths of 200 ft (Figure 2). Surface settlements were even less — not measurable with automated total station — when tunneling at depths less than 100 ft because the difference between overburden pressure and the TBM face/shield pressure was much less. Settlement of extensometers located 5 ft above the TBM (shown in red) was proportional to the difference between overburden pressure and the pressure around the shield body (shown in blue), confirming that settlements were essentially elastic. Postconstruction, 2D and 3D finite element analyses

correlated closely with the measured settlements, confirming that filling and pressurization of the gaps prevented ground loss.

Gap #2: Filling the Gap between Geotechnical Monitoring and Pressurized TBM Operation

A gap often exists between the geotechnical monitoring program and the TBM operation. The TBM team is focused on tunneling operations, not the geotechnical instrumentation data, particularly when it's provided in a form that's difficult to relate to the TBM advance. Conversely, the instrumentation specialist's scope and experience often does not include the review and evaluation of TBM operating parameters related to ground control.

Both the owner and TBM contractor should provide within their teams a construction monitoring lead or team to coordinate the geotechnical monitoring program and correlate the data with the key TBM operating parameters. Real-time plots of piezometric pressures and ground movements around the advancing TBM should be correlated with TBM parameters such as face/shield pressures, injection and conditioning volumes, and muck volumes. These results should be provided and evaluated regularly with the owner's project management and TBM operations teams.

Such a team was part of the contractor's joint venture on the AWVR tunnel project. A summary was emailed after each shove. Contract documents called for the establishment of a Construction Monitoring Task Force consisting of the owner, the contractor, operations, and construction monitoring. These parties met daily to review and evaluate ground movement and TBM operating parameters.

On a current LA Metro tunnel, regular summaries and time plots of TBM operating parameters are prepared by a tunnel engineer on the Metro construction management team. Shield gaps are filled and pressurized with bentonite slurry. Surface and building settlements have been held to 0.1 and 0.2 in. after passage of the twin 21-ft-diameter TBMs in the alluvial sands and clays.

Gap #3: Filling the Gap between Building Protection Study and Pressurized TBM Requirements

A gap often exists between the pre-construction building protection investigation and the requirements for controlling the pressurized TBM. Typically, the building protection report is prepared by the tunnel designer or the geotechnical consultant, but it's not coordinated with requirements for control and monitoring of the TBM. In building protection studies, the lateral strain and angular distortion imposed on a structure and the potential for damage can be determined from estimated surface settlement. However, an assumed percentage of ground loss is often used to estimate the settlement rather than considering the requirements for controlling the TBM to prevent ground loss.

The building protection report may recommend mitigation measures to reduce damage to structures (e.g., deepening the tunnel alignment) or ground improvement or ground replacement (e.g., compensation grouting beneath structures). But the primary mitigation for an estimated ground loss should be to consistently monitor and control the TBM to prevent the ground loss. Building protection studies should be coordinated with the criteria for controlling the TBM and monitoring its performance at start up, throughout the drive, at hold points, and approaching critical structures to confirm that control is consistently achieved.

The Revolution Continues

Today's technology has reached the point where pressurized

TBMs can be consistently controlled, monitored, and relied upon as the primary means for protecting overlying structures and preventing damaging settlement. By necessity, much of the progress in ground control has been led by projects with large-diameter TBMs. It has been demonstrated that ground can be controlled at tunnel depths shallow enough so that a single, large-diameter TBM can be used on transit systems to mine both the double track and station platforms at depths shallow enough for efficient access, such as with escalators. There are many opportunities for improvement, and there's much work to be done, including:

- More interaction and coordination among parties monitoring and controlling the TBM and ground movement, whatever the contract form
- Continued progress on TBM design and operation for consistent ground control in variable ground profiles
- Development of monitoring and data management systems, from planning through construction to post-construction, that provide comprehensible summaries and correlations of construction and ground monitoring data in real time, as well as permanent, accessible files for future analyses and design

The focus is on the geotechnical/tunnel engineer, who has a key role to play in filling the gaps:

- During design, to assess geotechnical properties, ground behavior, and building protection based on requirements for monitoring and control of the pressurized TBM
- During construction, to observe and report on both ground behavior and its cause — the key operating parameters of the advancing TBM that control ground movement

The model was established 80 years ago with the pioneering work of Karl Terzaghi and Ralph Peck on the Chicago Subway. They conducted "squeeze tests," measuring displacement of the clay into the liner plate tunnels, which showed that ground loss equaled the volume of the surface settlement trough. Most importantly, they observed construction and compared and correlated results on a single blueprint. In one case, as the tunnel went deeper into the soft clay, surface settlements increased to 5 in. Peck observed the delays in filling the gap between the clay and the lining, which, when corrected, reduced the settlement to 2 in. These lessons are still invaluable today as we observe the ground and the construction events, often through the lens of thousands of data plots in electronic data files.

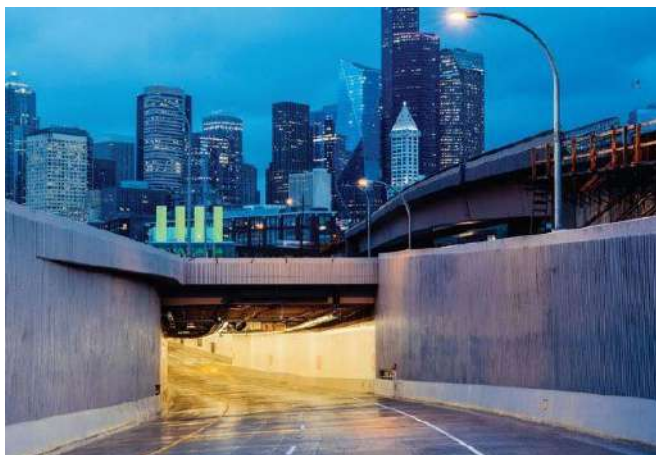
EDWARD J. CORDING, PH.D., F.ARMA, F.GSA, NAE, M.ASCE, is professor emeritus at the University of Illinois at Urbana-Champaign, where he served on the Civil and Environmental Engineering faculty for 35 years. His research and engineering practice has focused on the stability and ground control around TBM tunnels and mined caverns in rock and soil, and impacts on existing structures in urban areas. He can be reached at cordovaconsult@gmail.com.

[Geostrata - February/March 2022 - Filling the Gaps with Pressurized Tunnel Boring Machines \(readgeo.com\)](#)

LARGE-DIAMETER TUNNELS – An Emerging Urban Transportation Solution

Overcrowded Cities Say "NO" to Disruption while Solving their Mobility Issues

Sanja Zlatanic, Mike Wongkaew, Yang Jiang, Anthony Bauer, P.E., and Paul Hetu



View of downtown Seattle at the south portal SR 99 Tunnel.

Cities are becoming very dense, and the use of surface space is usually at a premium. Efficient infrastructure and transportation solutions are becoming an absolute necessity, and sustainable, planned use of both surface and underground spaces is now critical. As cities develop infrastructure and mobility solutions to keep up with increased population and economic growth, the issues of livability, quality of life, community preservation, and effectiveness of infrastructure become of special concern.

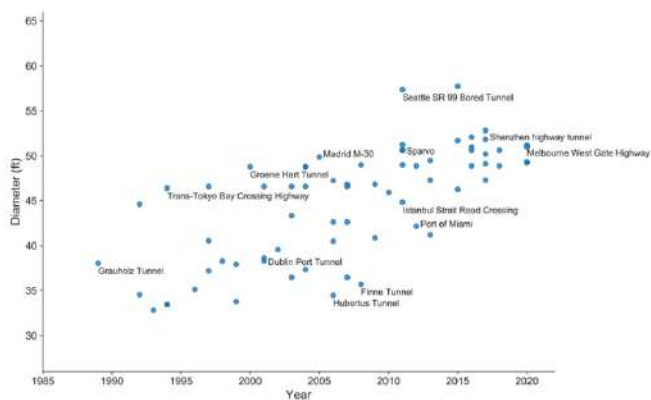


Figure 1. Growth of TBM diameter over time.

Benefits of Underground Transportation Solutions

The use of underground space has proven beneficial to solving urban mobility needs and addressing another challenge — disruption of communities, businesses, traffic, utilities, and services. For the most part, tunnel construction takes place out of sight of the public and minimizes surface disruptions within densely built urban environments. Construction-related impacts, including vibrations, noise, and dust, are also lower than for similar at-grade transportation solutions.

Using tunnels for transportation promotes preservation of existing communities, environmentally sensitive areas, and parks, as well as historical structures and cultural heritage. In contrast to at-grade or above-ground alternatives, underground transportation increases the property values along a

corridor. Because they're not affected by inclement weather, tunnels also have longer service life due to lower exposure to deicing chemicals and freeze-thaw cycles. Tunnels conform to imposed ground deformation limits and are safer in seismically active areas. As cities and their conscientious citizens become ever more cognizant of these benefits, they increasingly embrace underground transportation solutions.

Enhanced Benefits of Large-Diameter Tunnels for Use in Cities

Large-bored tunnels further enhance the benefits of underground infrastructure by significantly reducing surface disruption during construction of cut-and-cover work in public right of way, generally associated with constructing rail or transit stations within dense urban zones. Figure 1 demonstrates the growth of large-tunnel boring machine diameter over time. To date, there are at least 45 projects around the world that have been constructed using TBMs larger than 46 ft in diameter.



Figure 2. SR 99 tunnel section showing traffic lanes, emergency exits, exhaust air plenums, and utility pathway below the roadway.



Figure 3. SR 99 bored tunnel cross section.

Advancements in large-bore TBM technology have enabled new types of projects that would have previously been considered infeasible. For example, the 38.1-ft-diameter Grauholz Tunnel in Switzerland was the first to break the 30-ft mark in the late 1980s, enabling a dual-track, high-speed rail line within a single-bored tunnel. In the mid-1990s, the 46.4-ft-diameter Trans Tokyo Bay Tunnels were the first to accommodate a two-lane highway within each bore. In Madrid, Spain, the record tunnel diameter grew to 49.9 ft in the late 2000s to accommodate three lanes of the M-30 highway housed within each of the two bores.

Large "Bertha" Excavates a Four-Lane Highway Beneath Downtown Seattle

The record was broken again in mid-2010 with the completion of Washington State Department of Transportation's 57.5-ft-diameter SR 99 tunnel. This large-bore tunnel was used to replace the aging and seismically vulnerable double-deck Alaskan Way Viaduct without disrupting the heavy traffic flow or the adjacent congested business district during construction. Following completion of the tunnel and demolition of the existing above-grade state highway, the tunnel reconnected the downtown community to the Seattle waterfront.

The tunnel cross section, as illustrated in Figure 2, was designed to maximize the horizontal roadway envelope and improve the driver's sight distance, tunnel safety, and traffic operations, while optimizing the tunnel diameter and space allocation within the bore. With a 53-ft internal diameter, the tunnel accommodates two, 11-ft-wide travel lanes and 8-ft (west) and 2-ft (east) shoulders in each direction, with 15.5-ft vertical clearance. The west shoulder is wide enough for first-responder access or parking of a disabled vehicle, and also allows for routine maintenance and repairs without closing traffic lanes.

This tunnel incorporated an innovative fire life safety solution: during a fire emergency, ventilation dampers at the incident location open to extract smoke into the exhaust air plenum on the outer side of the roadway wall, which is connected to emergency fan plants at the north and south portals. While vehicles ahead of the incident would continue to travel and exit the tunnel, motorists behind the incident would safely evacuate into the fire-rated and pressurized egress corridor located on the opposite side of the roadway wall. The space above each roadway is used for lighting, signs, fire suppression sprinklers, and other tunnel systems. The space below the lower roadway is used for utilities and sump pumps.

Large-Diameter TBM Connects Europe and Asia Beneath the Bosphorus Strait

The Istanbul Strait Road Tube Crossing (also called the Eurasia Tunnel), which provides a transportation connection between Asia and Europe, represents another innovative use of a large-bore tunnel, as shown in Figure 3 (see "Connecting Continents — Challenges of the Eurasia Tunnel, Istanbul," by Ray Castelli and David Smith, in the November/December 2019 issue of *GEOSTRATA*, pp. 54-59). The tunnel was designed to ease traffic congestion caused by light vehicles, such as cars and minibuses, traveling across the Bosphorus Strait. It improves connections to a wide network of highways, increases capacity across the Bosphorus by approximately 100,000 vehicles a day, and saves motorists up to 45 minutes of commuting time — all without disturbing the historically significant area within which it was built.

The 2.1-mi-long subsea bored tunnel, constructed using a 44.9-ft-diameter slurry TBM (Figure 4), accommodates stacked roadways and houses two lanes on each level with a

vertical clearance of 9.8 ft. The region's variable geology, hydrology, and propensity for seismic activity, combined with high water pressure and the large-diameter double-deck configuration, make the Eurasia Tunnel one of today's most challenging projects. The TBM alignment control was exceptional, arriving at the receiving portal within 2 in. of the design target.



Figure 4. The Eurasia Tunnel TBM, designed for 13-bar hydrostatic pressure cross section.

Advancements in Large-Diameter TBM Technologies

Pressurized-face TBMs work by balancing the external soil and groundwater pressure with the internal pressure in the excavation chamber at the front of the TBM. This internal pressure is provided by pressurized slurry, in the case of slurry TBMs, or by a screw conveyor that controls the extraction of the excavated soil as the TBM advances forward, in the case of earth pressure balanced TBMs.

As the TBM diameters grow larger, the ability to control the ground and protect buildings, utilities, and other structures above the tunnel excavation becomes increasingly important. There are three primary sources of ground loss that could propagate up and outward to cause surface settlement:

- Face loss occurs when the imbalance of the external and internal face pressures causes longitudinal extrusion of soil into the tunnel.
- Shield loss occurs where the surrounding ground converges into the annular gap created by the differential diameters of the excavation and the TBM shield (this small overcut reduces friction between the shield and the ground).
- Tail loss occurs behind the TBM — as the TBM thrusts forward against the installed tunnel lining, the thickness of the TBM shield leaves behind a gap outside the tunnel lining into which the ground could converge.

Typically, ground loss of 0.5 percent of the theoretical excavation volume is considered tolerable for smaller (up to 20-ft-diameter) TBMs. However, using this volumetric ratio for large-bore TBMs is not practical or realistic.

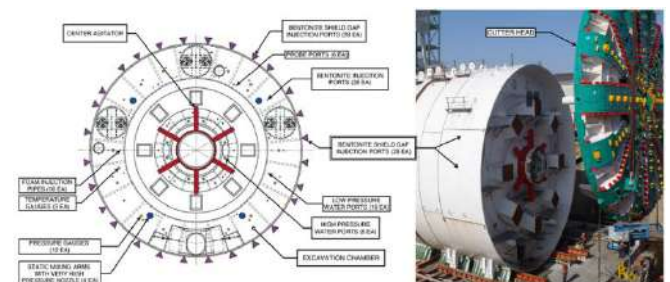


Figure 5. Shield gap injection ports on "Bertha" TBM used to excavate SR 99 in Seattle, Wash.

Large-diameter TBMs control the face pressure differential by injecting air bubbles (in the case of slurry TBMs) or bentonite slurry (in the case of EPB TBMs) into the excavation chamber. For EPB TBMs, two screw conveyors or two-stage screw conveyors are also used. To mitigate the shield loss for EPB TBMs, bentonite slurry is injected into the overcut gap through ports outside the TBM shield, as shown in Figure 5. For slurry TBMs, the slurry used to support the tunnel face generally flows around the shield and fills the overcut; therefore, in both cases the TBM face and shield are "pressurized," and with the proper selection of TBM manufacturer and operator, the machine would be able to control the ground fully. To mitigate the tail loss, a two-component grout comprised of hydration-stabilized cementitious grout and an accelerator are injected through ports behind the TBM into the tail gap. The accelerator activates the grout to create an engineered bedding for the tunnel lining, thereby arresting further ground convergence. Check grouting is also used through the segment ports to further compensate for any ground deformation caused by potential unfilled voids around the segments, as required.

State-of-the-art TBMs utilize big data. Real-time measurements from pressure cells and hundreds of other sensors inside and around the TBM, together with readings from external borehole instruments and settlement monitoring points on utilities and structures above the alignment, are fused and processed through data analytics to fine-tune the ground control measures and TBM operations. Other key technological advances unique to large-diameter TBMs include powerful electric motors to deliver the torque required to excavate a larger tunnel face, better seals for the TBM main bearing and the tail shield to cope with immense pressure sustained by deeper and larger tunnels, as well as improved tunnel-lining gaskets that minimize water infiltration of the installed tunnel lining. Advancement in the structural design of the TBM and the use of wear sensors in TBM cutting tools, cutter head, and shield body increase the predictability of the TBM performance and the intervals of maintenance cycles. The distance and speed that the cutter head and the cutting tools travel increase with the tunnel diameter, causing faster wear. Nowadays, advances in TBM design permit replacement of cutting tools from within the TBM under atmospheric pressure condition.

The Next Big Wave: Using Large-Diameter Single Bores to Optimize Mass Transit

The traditional configuration for subway projects relies on two, single-track tunnels for bidirectional transit. As noted, this arrangement frequently requires cut-and-cover construction for the stations and crossovers, which could be highly disruptive to the community and may bring the benefits of underground mass transit into question. The availability of large-diameter TBM tunneling technologies now allows station platforms and crossovers to be housed within a single bore, thereby eliminating cut-and-cover excavations and reducing surface impacts. In addition to civil, architectural, and structural requirements, single-bore tunnels also accommodate fire and life safety requirements, such as emergency ventilation and egress, as well as wayside track equipment, including practically all rail and facility systems required by modern transit facilities.

The single-bore arrangement for mass transit has been successfully implemented in Spain for the Barcelona Metro Line 9 and is currently being planned by other transit agencies. In the U.S., the Santa Clara Valley Transportation Authority is considering a single-bore tunnel with in-tunnel station platforms as part of the Bay Area Rapid Transit Silicon Valley Phase II project, known as VTA's BSV Phase II, in San Jose, Calif. As shown in Figure 6, station platforms are stacked inside the 48-ft-diameter tunnel. Station entrance shafts would

be located off the public right of way to reduce surface disruption. Adits will be constructed using the sequential excavation method to provide passenger connections between the station entry and the train platforms. Additional adits will be used to create pathways for ventilation, emergency egress, and other systems.



Figure 6. A single-bore subway station design being considered for the VTA's BSV Phase II project. (Courtesy of the Santa Clara Valley Transportation Authority.)

Construction Planning for Large-Bore Tunnels: Not a "Smooth Sailing"

Planning for large-diameter TBM tunneling must consider logistics and special construction operations. Generally, 3 to 5 acres are needed at the tunneling portal to support a large-diameter EPB TBM, and 5 to 7 acres for a slurry TBM. Developing the portal site layout is especially challenging and must consider the following activities:

- TBM power, assembly, service, and disassembly
- Precast concrete tunnel-lining segment delivery, handling, and storage
- Tunnel support equipment, such as segment carriers, muck cars, and personnel transporters
- Crane access and swing radius
- Slurry plant
- Muck conveyor
- Muck processing, storage bins, disposal, and haul routes in and out of the site
- Supporting utilities, such as ventilation, power, compressed air, water supply, and water discharge
- Laydown areas for tunnel utilities, slurry pipe, and conveyor belts
- Water treatment plants
- On-site batch plants for grout, material silos, and aggregate bins
- Field office space, crew parking, and crew dry houses

Larger TBMs present high electrical loads, which must be coordinated with local utility providers. It's not uncommon for a large TBM and its supporting equipment to require more than 25 megavolt-ampere power. In some cases, a new power substation and distribution lines may be required to bring power to the TBM launch site.

The delivery and assembly of the TBM also need careful planning. TBMs may be fabricated and shipped to the project site on freight lines or cargo ships in pieces, spread out over many truckloads. The maximum dimensions and weights for the haul route, from the ship port crane capacities to the project-site entrance width, are needed to determine how the components are packaged at the TBM factory. Vertical clearances at overpasses, lane width restrictions, bridge weight limits, permit load routes, and other factors are all used to develop the logistical plan.

Solving Urban Mobility with Minimum Disruption — A Way to Go

Geo-professionals and allied partners in the tunneling and civil engineering industries have risen to the challenge of solving urban mobility by developing and delivering large-bore transportation tunnels that minimize disruption to communities, businesses, and services both during construction and in service. While citizens and cities have increasingly embraced large-bore solutions and benefited from the large-diameter TBM technologies, the trajectory of tunnel-diameter growth has not plateaued. The technological boundary and innovation will continue to expand, equipping the engineering communities and transportation agencies with continually bigger and better tools to serve mobility needs, while preserving livability, quality of life, and the effectiveness of infrastructure.

SANJA ZLATANIC, P.E., is the chair of HNTB's national tunnel practice and has led multibillion-dollar tunnel projects that have won many industry awards. She served as technical expert for the SR 99 project, project manager for independent design verification of the Eurasia Tunnel, and technical task lead for a study that devised single bore option for VTA's BSV Phase II project. She can be reached at szlatanic@HNTB.com.

MIKE WONGKAEW, Ph.D., P.E., S.E., is the national tunnel practice lead for HNTB's west region. He currently leads underground engineering for the Sound Transit West Seattle and Ballard Links Extension, and previously served as the technical oversight engineer for WSDOT on the SR 99 project. He can be reached at mwongkaew@HNTB.com.

YANG JIANG, Ph.D., P.E., S.E., is a bridge and tunnel practice consultant with HNTB Corporation in Bellevue, Wash. Jiang is the engineer of record and lead engineer for the SR 99 tunnel and the independent verification lead for the Eurasia Tunnel. He can be reached at YJiang@HNTB.com.

TONY BAUER, P.E., is the HNTB engineering manager for VTA's BSV Phase II project. He can be reached at abauer@HNTB.com.

PAUL HETU serves as the HNTB construction manager for VTA's BSV Phase II project in the tunnel and trackwork contract segment, which is currently in the procurement phase and scheduled to break ground in 2022. He can be reached at phetu@hntb.com.

[Geostrata - February/March 2022 - LARGE-DIAMETER TUNNELS – An Emerging Urban Transportation Solution \(readgeo.com\)](#), pp.

The Elizabeth River's New Immersed Tube Tunnel

Making Use of Advanced Geotechnical Testing and Soil Property Assessment Aid Design

Todd Grifka, Rodney Sedillo and Ian Chaney



Towing of immersed tube element.

The Midtown Tunnel Project team had to design safe, yet economical slope geometries for the subaqueous dredge slopes for a new roadway tunnel using immersed tube construction techniques. The design of safe slopes for this project was of paramount importance, because a dredge slope failure could cause complete failure of the existing adjacent immersed tube, sloughing slopes would create a costly maintenance issue during construction, and divers and equipment would be working within the dredge prism.

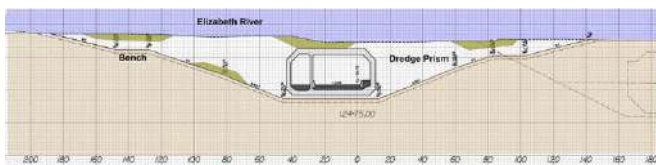


Figure 1. Dredge slope geometry and immersed tube element.

The subsurface materials were extremely weak, so to achieve safe and economical slope geometries, accurate and reliable assessments of the shear strength of the cut slopes were required. This was accomplished by employing a robust subsurface exploration focused around cone penetration testing, vane shear testing, and collection of undisturbed soil samples for advanced laboratory testing. The geologic conditions presented unique challenges for developing shear strength properties for design due to variations in the stress history of the normally consolidated and lightly overconsolidated, fine-grained alluvial soils along the tunnel alignment. In addition to traditional deterministic methods of calculating the factor of safety of excavated slopes, the project included reliability-based design methods to ensure an adequate probability of success.

Project Details

The Midtown Tunnel crosses the Elizabeth River between Norfolk and Portsmouth, Va. When completed in 1962, the two-lane tunnel conveyed U.S. Rte. 58 vehicular traffic. With increased traffic demand 40 years later, planning began for an adjacent two-lane tunnel to carry eastbound traffic. The new Midtown Tunnel was designed and constructed as a two-lane immersed tube tunnel. The project was developed under Vir-

ginia's Public Private Transportation Act, with the Virginia Department of Transportation as the project owner. The developer of the project, Elizabeth River Crossings LLC, also serves as the concessionaire over the 58-year term of the comprehensive agreement with VDOT. The design/build contractor was SKW Constructors, an unincorporated joint venture among Skanska USA Civil Southeast Inc., Kiewit Construction Company, and Weeks Marine, Inc. WSP USA served as the lead designer, under contract to SKW. Major construction of the Midtown Tunnel began in October 2012, and it opened to traffic in June 2016.

Each of the 11, approximately 330-ft-long immersed tube elements was pre-cast in a dry-dock approximately 180 nautical miles from the project site, floated into position, and then carefully placed at the bottom of a subaqueous trench. These immersed tube elements, along with the cut-and cover and open approach sections, make up the entire 4,500-ft-long river crossing. As each element was placed and connected to its adjacent element, they were ballasted and backfilled to resist buoyancy and provide a protective cover against potential sunken ship impacts or dragging anchorages. To accomplish these design objectives and to place the elements within a 1/2-in. vertical tolerance, the subaqueous trench was dredged to depths of up to 60 ft below the existing mudline and up to 100 ft below the surface of the Elizabeth River. To achieve these tolerances at such depths in murky water, a tandem of specially fabricated barges with screed blades was used to level the gravel bed on which the immersed tubes would bear. Tube placement was controlled using survey towers, divers, and side-scan sonar surveys. A typical cross section of the tunnel and slopes is shown in Figure 1.

Geologic Setting

Located within the Coastal Plain physiographic province, the project's geologic setting is characterized by surficial alluvial and fluvial sediments deposited after the last ice age around 12,000 years ago. These sediments have not been affected by variations in sea level or significant erosion events; thus, these soils have very little stress history caused by natural processes. Below these recent sediments, sea level transgressions during the last glacial periods accumulated near shore terrace deposits. Geologists define these predominantly coarse-grained deposits as the Tabb Formation, and they possess widely variable and random changes in composition. Below these deposits and separated by a geologic discontinuity, older sediments of the Yorktown Formation date to the middle Pliocene and were deposited around 4 million years ago. Although the Yorktown Formation is predominantly coarse-grained, there's evidence that the formation has experienced overburden pressures above the current in-situ pressures, likely caused by higher ground levels in the past that have since been eroded and are now characterized as a geologic discontinuity.

The bottom of the subaqueous trench was founded within the Yorktown Formation throughout much of the tunnel alignment, meaning the trench's slopes were excavated through the surficial soft and loose sediments and highly variable terrace deposits. To achieve the goal of a safe design with economical slope geometries, the subsurface exploration was developed specifically to assess the soil properties along the alignment. The paramount concern here was the undrained shear strength of the fine-grained alluvial deposits and drained strengths of the Tabb Formation. The general subsurface profile along the tunnel alignment is presented in Figure 2.

Exploration

As with many design-build projects, a preliminary subsurface investigation performed by the owner during project pre-procurement was supplemented by the design-build team for the

purpose of final design. The final exploration considered all the previously collected in-situ and laboratory test results, as well as any soil property uncertainties discovered during the progression of the dredge slope design. For instance, additional soil borings and CPTs were performed between explorations that showed a variance in the stratigraphy or in the undrained shear strength. The final exploration utilized sophisticated in-situ testing and included CPTs with full-flow, ball-shaped penetrometers and mechanically controlled electronic VSTs. These tests were used to characterize changes in very low shear strength materials near the mudline. Adjacent undisturbed sampling was conducted at strategic depths to supplement and validate the in-situ testing. To improve the accuracy of the VST results, split-barrel sampling was advanced through the soil where a VST had been conducted, and the sampled soil was subjected to laboratory testing for index properties, including Atterberg limits. This approach allowed vane correction factors to be calculated and applied to the shear strengths measured in the VSTs.

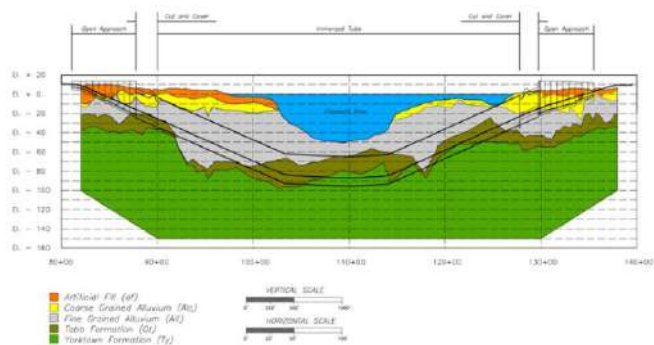


Figure 2. Generalized subsurface profile.

Dredge Slope Stability Design Methodologies

The final slope geometry used conventional deterministic-based design (i.e., allowable stress design, or ASD), where material properties are assigned values using engineering judgement based on laboratory and in-situ data, empirical correlations, and local experience to achieve an acceptable factor of safety. As a supplement to using deterministic-based material properties, the dredge slopes were further analyzed using probabilistic methods or reliability-based design. For these analyses, individual soil parameters were developed based on a statistical approach to quantify the uncertainty of each parameter using statistical assessments of the available geotechnical data set. The result of the RBD approach is to achieve a probability of success.

RBD does not rely on the engineer's biased selection of a deterministic material property value for design. Rather, RBD uses a statistical approach to consider the entire geotechnical data set to remove bias in material property selection, including measuring the uncertainty of the property as quantified through statistical derivations. Unlike ASD, where a single material property value is assigned to the analysis model, the RBD methodology uses the most likely value, typically the mean, and the variance, which measures how far the data set is from the mean value to assess a reliability index. Because direct measurement is not possible within the entirety of the stratum being analyzed, precise variability cannot be measured, but only approximated using the data set obtained from the subsurface exploration. With larger data sets, some uncertainty in the mean and variance can be reduced.

Both the ASD and RBD design methodologies utilized the same geometries and stratigraphy as determined from the field investigations and laboratory index testing. Circular and noncircular theoretical failure surfaces were modeled in the analyses. The actual mechanical analysis that utilizes limit equilibrium analyses with wedge failures, circular failures, or

optimized failures was the same in both approaches. The difference arises only in how the soil properties were determined for use, and in that the probabilistic analyses of a single slope required multiple runs to analyze the multitude of statistically-derived soil property variations.

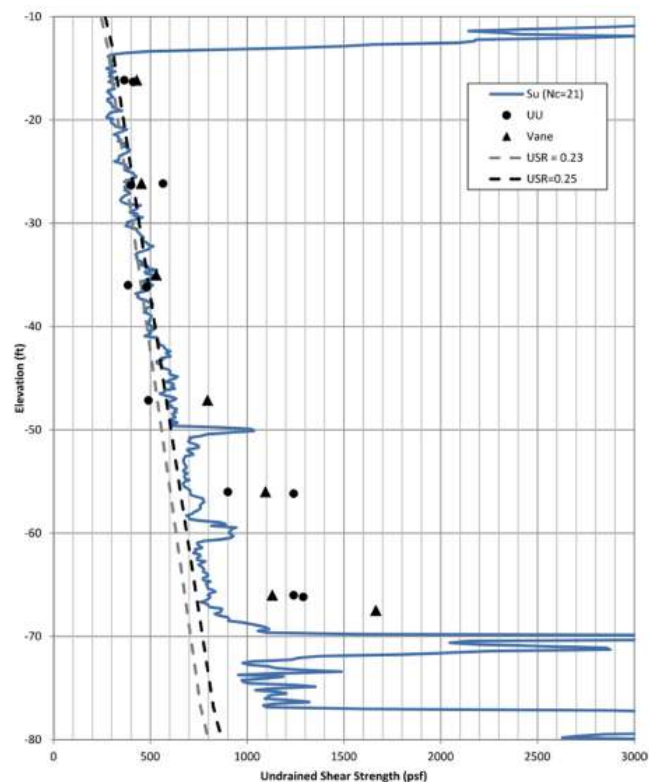


Figure 3. CPT-derived undrained shear strength correlations with in-situ and laboratory shear strengths.

Analysis Locations

Cross-section locations were chosen by carefully assessing the dredge slope heights, the variability of the soil stratigraphy within cross sections, and generalized material properties, including stress history. The length of the dredged trench was subdivided into five discrete reaches. Each reach was comprised of the dredge slope on either side of the trench, equating to 10 total analytical cross sections. The areas within each reach were deemed similar enough that the representative cross sections would be adequate to define the entire length of that reach. Uncertainty in the geometry and stratigraphy was greatly reduced by defining reach limits so these areas contained very similar attributes, thus eliminating the need to include the variability of these aspects in the analysis.

Derivation of Shear Strength Properties

Although material unit weight and hydraulic conductivity are also important when analyzing dredge slope stability, for brevity, only deviation of undrained shear strengths of clay deposits for ASD and drained shear strengths of the Tabb Formation for RBD analyses are discussed here.

Undrained Shear Strength

Undrained shear strength only applies to fine-grained material with low hydraulic conductivities, where changes in vertical effective stress cause immediate and long-term changes in pore pressure. The relatively short duration the trench would be open, coupled with the low hydraulic conductivities measured in consolidation tests, made it clear that the clay deposits would not behave in a drained manner.

When CPT profiling is used to assess the undrained strength of cohesive soils, three cone bearing factors are commonly used in practice to correlate CPT data to undrained shear strength. Although the three methods are modeled on conventional bearing capacity theory, the methods are considered empirical. The three cone bearing factors are termed the N_c , N_k , and N_{kt} methods. For each, the empirical bearing-capacity factor was selected using engineering judgment by correlating the CPT tip resistance-derived shear strength to the shear strength measured from in-situ VSTs and unconsolidated-undrained triaxial tests. The undrained shear strengths from the VSTs were used as the benchmark shear strength and considered the maximum available undrained shear strength of the soil deposit at the elevation the test was performed.



Figure 4. Full-flow ball penetrometer.

The VSTs were corrected for strain rate effects and soil anisotropy using Bjerrum's correction factor before applying the correlations. The selected cone bearing factors of $N_c = 21$, $N_k = 11$, and $N_{kt} = 14$ generally correlated well to the VSTs and UU tests. As illustrated in Figure 3, the N_c cone bearing factor yielded a closer correlation to undrained shear strength for soils at the site compared to the other two factors. The N_k and N_{kt} methods yielded higher strengths in some of the undrained strength profiles used to generate this comparison. As a secondary advantage, the N_c method does not require unit weight assessments or, in the case of the N_{kt} method, accurate pore pressure measurements during cone penetration.

While examining the plotted CPT-derived shear strength versus elevation and vertical effective stress, it became apparent that the strengths along the tunnel profile are influenced by stress history. Beneath the navigation channel, the clay deposits were found to be slightly overconsolidated due to dredging of the channel. Furthermore, some near-mudline deposits exhibited a near-zero undrained shear strength that did not increase with depth. To characterize these soils, the

tip of the CPT was replaced with a ball (Figure 4) to increase the surface area of the CPT under full-flow behavior, thus providing higher tip resolution. The results were used to optimize the slope geometries in these areas and to design intermediate benches where sloughed material could accumulate and be collected it before it reached the foundation elevation.

The CPT-derived shear strengths were plotted, and the undrained strength ratios were fit to the plots using engineering judgement. The use of a USR allows for a constant increase of shear strength with elevation to be used in the slope stability analyses. This incremental derivation of the clay's undrained shear strength is a method to approximate the strength of the deposit into a simplified model. Actual USR values used in the ASD analyses were based on the CPT data acquired within the reach where the cross section was analyzed. In most areas along the dredge alignment, this strength profile corresponds to undrained strength values ranging from about 150 psf to 300 psf at depths of 20 ft below the mudline.

Drained Shear Strength

Although CPT soundings generate many data points to correlate to a material property, such as drained shear strength, the Tabb Formation soils yielded a high degree of uncertainty. This was due to the highly variable composition of this stratum as well as the low relative thickness of the stratum compared to the other strata analyses. Additionally, this stratum was close to the bottom of the trench in some reaches, where high theoretical shear stresses can be developed in slope stability models.

The Tabb Formation within the alignment is predominantly coarse-grained, so drained shear strengths were used in the analysis for this stratum. To estimate the variability to the extent possible, CPT soundings and SPT N-value correlations were both used to populate the data set. Most likely values were corroborated using numerous empirical correlations from published sources. The variability of the drained shear strength was calculated directly within each reach. The Tabb Formation has a most likely value of 36 degrees and a coefficient of variation of 16.4 percent.

Dredge Slope Stability Results

To optimize the dredge slope geometries, both the traditional ASD and the statistical RBD analyses were used to increase the level of confidence of providing safe conditions for the divers performing the tunnel element connections. Because RBD methodology requires that the mean value and variance of each material property be input into the analysis models, the computation does not output a familiar factor of safety, but rather a reliability index that can be used to determine a probability of failure, or success.

The slopes for this project were designed with a minimum factor of safety of 1.3 and a maximum probability of failure of 1.0 percent. The resulting dredge slope geometry specified for construction was 2.5H:1V throughout much of the alignment. In areas where the deposits near the mudline exhibited extremely low shear strengths, a 10-ft-wide bench tied into the existing mudline with a 4H:1V slope (Figure 1).

Bottom Line

Many times in our profession, it's difficult to justify added exploration and design expenses to a client because the potential savings can be hard to definitively quantify. The Midtown Tunnel Project was unique in that a significant cost of constructing the immersed tube tunnel was the dredging and disposal costs of the submarine soils. What can seem like a trivial optimization, such as steepening the slopes from

3H:1V to 2.5H:1V, can result in a huge cost saving to the client. Projects that pose an opportunity to utilize extensive exploration techniques and statistical design methods to reduce cost and risk to the client can allow engineers to expand their professional abilities and make a meaningful difference.

TODD GRIFKA, P.E., M.ASCE, is a geotechnical engineer with WSP USA in Virginia Beach, Va., where he is currently a resident engineer on the Hampton Roads Bridge-Tunnel Expansion project. In this role, he's drawn extensively on the lessons learned from the Midtown Tunnel project. He can be contacted at todd.grifka@wsp.com.

RODNEY SEDILLO, P.E., is a geotechnical engineer with WSP USA in Tampa, Fla., where he's responsible for providing geotechnical engineering services to clients around the country. Sedillo provides unique approaches to solving geotechnical problems, frequently drawing upon probabilistic approaches similar to those summarized herein. He can be reached at Rodney.Sedillo@wsp.com.

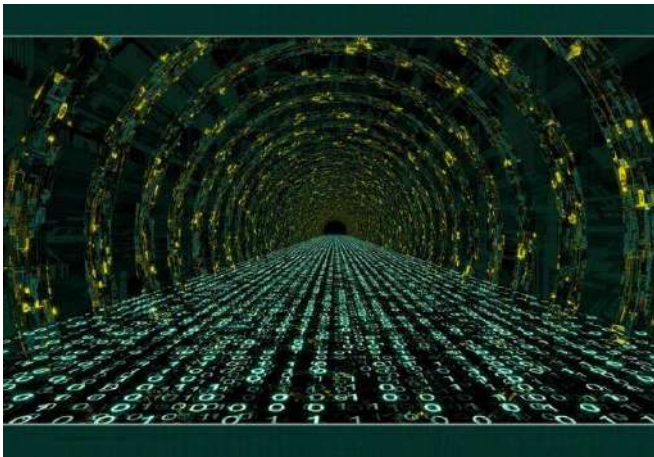
IAN CHANEY, P.E., is vice president and national director of geotechnical & tunneling for WSP USA in Virginia Beach, Va., where he's responsible for the overall direction, strategy, and management of geotechnical and tunneling services for WSP USA nationwide. He can be reached at Ian.Chaney@wsp.com.

[Geostrata - February/March 2022 - The Elizabeth River's New Immersed Tube Tunnel \(readgeo.com\)](http://readgeo.com)

Artificial Intelligence Applications for Tunneling

Addressing Geotechnical Uncertainty Governing Tunnel Projects

Michael A. Mooney and Hongjie Yu



Geotechnical uncertainty is the governing source of risk on urban tunnel projects. A typical preconstruction geotechnical site investigation for a tunnel project involves vertical and/or inclined boreholes spaced at 50-m to 75-m intervals along alignments often extending for kilometers. This leads to a sampling rate of less than 0.1 percent of the ground. The result is a very high level of geotechnical and geological uncertainty, with reliance on desktop study and understanding of geological processes to help fill in very large information gaps.

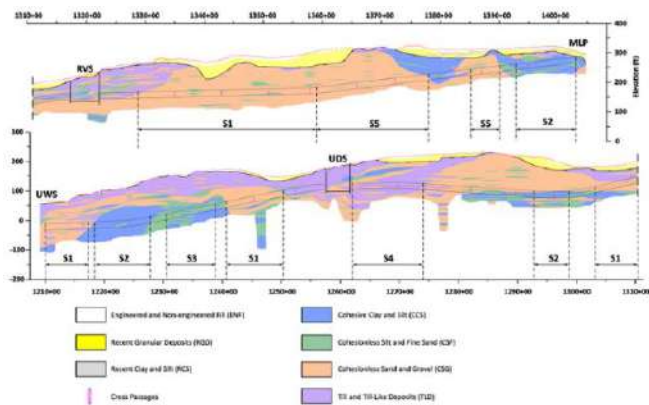


Figure 1. The geological profile for the N125 tunnel. Segments of single ESU composition, "S_i", where $i = 1, 2, 3, 4,$ or 5, were used to prepare AI machine learning models.

The resulting estimates of key geotechnical properties can have coefficients of variation on the order of unity. The estimated locations of lithological transitions can vary by tens of meters. Critical lenses of adverse ground conditions often go undiscovered prior to tunnel construction. This challenge must be addressed because urban tunneling beneath aging infrastructure and sensitive buildings allows very little room for error. Excavating 7.5-m to 15-m-diameter openings in nearsurface soil while allowing no more than 6-mm to 13-mm movements to overlying infrastructure requires clear knowledge of ground conditions and a keen understanding of ground-tunnel boring machine interaction.

An Opportunity to Know More with AI

Urban tunnel construction projects have become high-tech. TBMs outfitted with thousands of sensors provide real-time

streaming data via project networks and interactive dashboards. Existing overlying infrastructure and the ground are outfitted with extensive sensing to monitor tunnel-induced building deformation and ground movements and pressures. The collection of these data can now be automated and integrated with TBM data in real time to project stakeholders. Even the installed infrastructure components, such as precast concrete lining segments, can include embedded sensors to track movement and performance during and after construction. With such extensive data, the tunnel engineering community can indirectly tackle the great challenge of geotechnical risk that stems from very high levels of geotechnical uncertainty.

This article summarizes two ways in which AI machine learning has been effectively used to extract actionable information from tunnel project data. This includes using AI to 1) develop ground characterization models, and 2) relate ground conditions to TBM performance.

The Northgate Link Tunnel Project

The Sound Transit Northgate Link tunnel project (N125) involved the construction of twin tunnels, each 5.6 km in length, extending north from the University of Washington in Seattle. The geological profile (Figure 1) in the geotechnical baseline report, was based on 159 boreholes that categorized the ground into six major engineering soil units (ESUs). The engineered and nonengineered fill (ENF) and granular deposits (RGD) are normally consolidated. The ESUs through which the tunnel was excavated included cohesive clay and silts (CCS), cohesionless silt and fine sand (CSF), cohesionless sand and gravel (CSG), and till and till-like deposits (TLD). Each of these strata are generally overconsolidated due to several glacial advances and retreats.

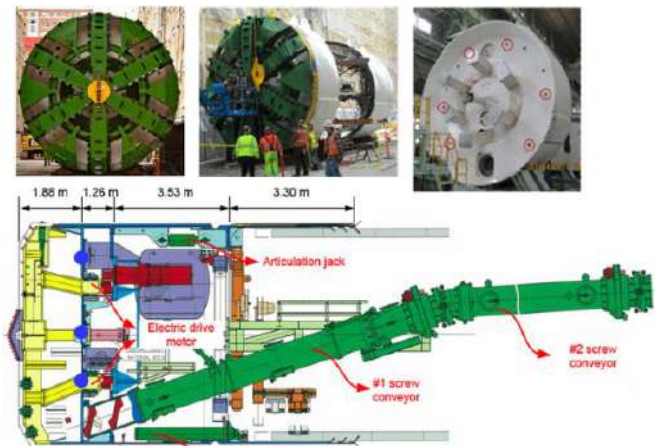


Figure 2. The Hitz earth pressure balance TBM used to excavate the northbound 6.64-m-diameter N125 tunnel in Seattle, Wash.

A Hitachi Zosen (Hitz) earth pressure balance TBM (Figure 2) was used to excavate the northbound tunnel. The TBM uses the excavated ground, combined with water, foam, and polymers as conditioning agents, to provide pressure balance against lateral earth and ground water pressures. The excavated diameter created by the TBM was 6.64 m. The TBM included more than 400 sensors recording extensive operating parameters every five seconds, including thrust jack forces, articulation jack forces, excavation chamber pressures, belt mass, cutterhead rotation speed and torque, screw conveyor rotation speed and torque, and injection rates of soil conditioning agents.

Characterizing the As-Encountered Ground

Many tunnel construction aspects could improve significantly

from accurate knowledge of the current ground conditions through which the TBM advances. This is particularly critical for closed-face TBMs used in soft ground tunnel construction where the approaching ground cannot be observed. AI machine learning can use the rich array of TBM data streaming in real time to learn the ground conditions encountered and help improve predictions of ground yet to be encountered.

It's intuitive that TBM-ground interaction, and namely the performance of the TBM, is influenced by the ground conditions. For example, the advance rate, cutterhead torque, chamber pressure distribution, and other measurable parameters will change in different ground conditions. But the specific relationships are for each ground type or combination, or which ground properties are the most informative, are not intuitive. Unfortunately, to characterize ground conditions for tunneling, there are no equivalent closed-form equations or empirical relationships like Robertson developed for CPT ground characterization. In lieu of this, AI machine learning was used to learn this relationship.

A semisupervised learning method developed by Zhou, et al. (2004) was used to build data-driven similarity among TBM data. A similarity graph was first constructed from TBM data-derived predictors, where each ring is represented by a graph node interconnected via lines of various strengths of similarity (Figure 3). ESU fractions are treated as node labels available only at tunnel rings with nearby boreholes.

Many tunnel construction aspects could improve significantly from accurate knowledge of the current ground conditions through which the TBM advances. This is particularly critical for closed-face TBMs used in soft ground tunnel construction where the approaching ground cannot be observed.

ESU data from 83 boreholes within the tunneling envelope were used to train the prediction model. These ground truth data, combined with the co-located TBM data, are referred to as "labeled data" in Figure 3. TBM data from tunnel rings where no boring logs exist are considered "unlabeled data." While all rings have TBM data-derived predictors, only 83 rings have ESU area fractions encoded by nearby boreholes. The objective of the ground characterization model is, therefore, to determine the ESU fractions at the rings without borehole data.

Figure 4 shows the general agreement in estimated ESU fractions from within the tunneling profile inferred by the AI machine learning model and estimated by the geologist before excavation. Note that neither is the actual, or ground truth, model, which remains unknown.

Furthermore, Figure 4 shows that the estimation made by the machine learning model is more heterogeneous and chaotic than the geologist's, reflecting the many small ESU lenses interspersed inside large ESU bodies. For example, between Rings 2160-2210, the machine learning model suggests the ground is mainly composed of CCS, while the geologist estimated CSF. Similarly, between Rings 1550-1620, the machine learning model predicts CSG is the dominant soil unit, but the geologist's profile depicts it as a mixture of TLD, CSF, and CSG units. Considering Seattle's repeated glaciation cycles in history, we argue that the inference by machine learning model is likely more realistic.

Another common disagreement between the two estimations is the location of ESU transitions. For example, the geologist predicts the transition from CSG to CCS occurred at Ring 387, as opposed to around Ring 340 by the machine learning model. The transition from CSG to CSF is also predicted earlier by the machine learning model by 36 rings from Ring 3007 to Ring 2971. This 50-m difference is significant, and we believe the estimation made by the machine learning model is more trustworthy. This occurs because, unlike the

geologist who only interpolates between boreholes with no guiding data, the machine learning model can take advantage of TBM data reported every millimeter of advance, allowing the model to produce a detailed characterization of the ground at the 1-m scale (when considering necessary averaging).

Using Machine Learning to Understand Advance Rate

The physics or mechanics that govern the AR of a pressure balance TBM in soft ground is complex and not well understood. Therefore, there's no closed-form equation or computational model that relates AR to ground conditions and TBM operating parameters. AI machine learning was used to extract this understanding from the data.

From the 400 parameters reported by the TBM, 107 were selected for consideration. Many of the sensed parameters are unrelated to AR and TBM-ground interaction, such as oil temperatures and hydraulic systems, and all parameters that would be dependent tell-tales of AR were also removed. For example, the screw conveyor rotation speed and mass flow rate measured on the belt conveyor will increase as a result of AR. The use of such tell-tales would produce an excellent, but useless predictor of AR.

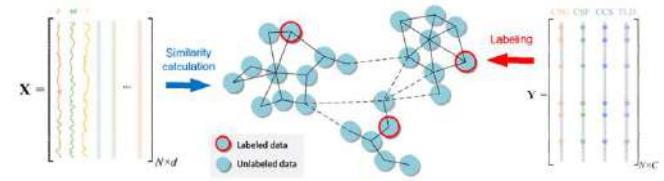


Figure 3. Schematic of a ground-characterization learning algorithm where TBM data (X) and boring log ESU fractions (Y) are used in machine learning similarity analysis.

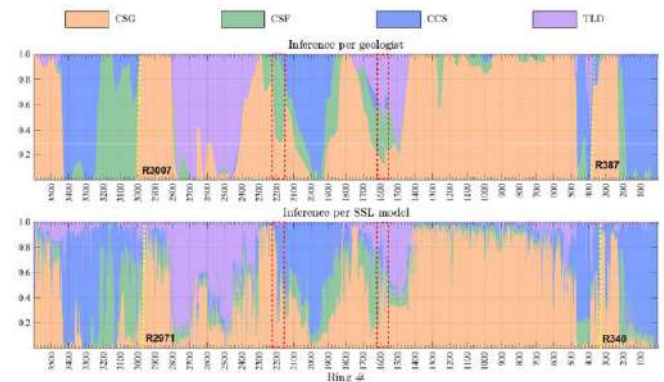


Figure 4. Comparison of an inferred ESU fraction according to the geologist and the machine learning model within the tunneling profile profiles. Each ring is 1.5 m.

The TBM data were categorized per ESU based on the geological model so that we could indirectly assess the influence of soil type on the AR. For this assessment, only segments of full-face single ESU were used in the study. A feature selection algorithm was used to identify the top 40 parameters that influence advance rate. The parameters with the greatest influence on advance rate in each of the soil groups included net thrust force, cutterhead torque, screw conveyor torque, and volume of soil conditioning used.

The support vector regression (SVR) machine learning technique was used to model the relationship between AR and 40 measurable TBM parameters. SVR-based models were created for each of the five ESUs through which the TBM excavated. SVR model training was initially performed by using 80 percent of the available TBM data. Each trained model was then tested with the remaining 20 percent of TBM data not used during training.

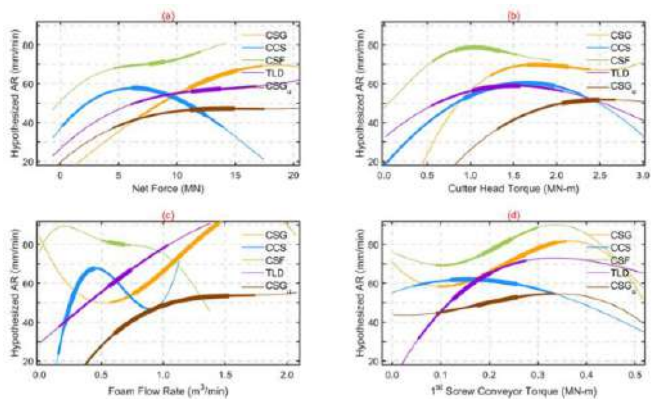


Figure 5. Sensitivity of AR to four key TBM parameters across each of the five engineering soil units. The middle 50 percent of data is reflected by the thickest line portion; 90 percent by the medium thickness.

Coefficient of determination, or R^2 , values for the trained SVR models ranged from 0.85 to 0.95, indicating that only 15-5 percent of the observed variation in the AR was not captured by the parameters used in the models. When models were applied to the test data sets, R^2 values remained very high. Also, when one ESU model was applied to data from another ESU, the R^2 values were very low, indicating the AR models are not similar across soil type. More details on the SVR method, testing, and training can be found in "Predicting EPBM Advance Rate Performance Using Support Vector Regression Modeling" by Mokhtari and Mooney (2020).

To better understand the parameter influence on AR and the influence of soil type, we systematically probed the black box SVR models to produce parameter sensitivity plots, a few of which are shown in Figure 5. The slope of each curve reflects sensitivity of AR as a function of each parameter's magnitude. For example, Figure 5a shows that AR and net thrust are positively correlated over a certain thrust range and negatively related over a different thrust range. Specifically, the CSG AR increases with increasing net thrust up to approximately 17 MN, and thereafter decreases with increasing net thrust. The sensitivity of AR to net thrust also changes. An incremental increase in CSG net thrust force at 12 MN, for example, occurs with a greater increase in AR than does a similar incremental increase in net force at 15 MN.

The sensitivity (slope), polarity (positive or negative slope), and associated ranges of net force vary with ESU. For example, the AR is always positively related with the net thrust in CSF and TLD soils, whereas there's a clear negative relationship between AR and net force in CCS soils. Generalizing to the other parameter plots shown, the soil type through which the TBM is excavating plays a significant role in the overall AR and the influence of TBM parameters on the AR. While these statistical analyses do not reveal causation, their results provide insight into when and why AR increases and decreases. Most importantly, TBM operators can use these machine learning results on the fly to optimize parameters to maximize AR.

The Broader Perspective

It's difficult to imagine that the level of geotechnical uncertainty resulting from site investigation efforts will decrease dramatically in the future. Perhaps new advances in geophysical imaging, combined with dramatic cost reduction in in-situ testing and borehole sampling, will improve what we can learn a priori. However, moving from 0.1 percent ground characterization to 70-90 percent characterization before tunnel construction does not seem feasible.

Table 1
 R^2 values and root mean squared error, also normalized by mean, statistics for the different ESU SVR models trained using 80 percent of the data and tested with 10 percent of the data from the South Transit Northgate Link tunnel project. GSG, represents a portion of unsaturated CSG, i.e. above the groundwater table.

ESU Model	Training Dataset (80%)			Test Dataset (20%)		
	R^2	RMSE (mm/min)	Normalized RMSE	R^2	RMSE (mm/min)	Normalized RMSE
CSG	0.88	10.93	0.15	0.87	11.16	0.15
CCS	0.95	6.34	0.13	0.95	6.36	0.13
CSF	0.95	4.11	0.05	0.94	4.73	0.06
TLD	0.91	6.95	0.13	0.90	7.27	0.14
CSG _u	0.85	7.19	0.17	0.84	7.24	0.17

Opens in modal lightbox

A more realistic approach is to learn from the increasing amount of real-time data made available during construction. Such analysis can provide just-in-time information that in many instances can reduce geotechnical risk that can otherwise derail tunnel projects.

With all this said, we must be careful and vigilant when using machine learning techniques. Like traditional statistical regression methods, rigorous metrics should be used to convey the accuracy of the analytical models where their accuracy is assessed using data that was not used during training. As a final cautionary note, nonlinear machine learning models are only valid over the domain of data they were trained on. Stretching their use could bring about erroneous outcomes.

MICHAEL A. MOONEY, Ph.D., P.E., M.ASCE, is a professor and the Grewcock Chair of Underground Construction & Tunneling in the Departments of Civil and Environmental Engineering, and Mechanical Engineering at Colorado School of Mines in Golden, Colo. His research includes real-time TBM monitoring, ground visioning to look ahead of TBMs, and intelligent geoconstruction. He can be reached at mmooney@mines.edu.

HONGJIE YU, Ph.D., is a postdoctoral fellow in the Center for Underground Construction & Tunneling at Colorado School of Mines in Golden, Colo. He can be reached at hyu@mines.edu.

[Geostrata - February/March 2022 - Artificial Intelligence Applications for Tunneling \(readgeo.com\)](#)

Tunneling in Tight Quarters

SEM in San Diego's Substrate

Jakob R. Walter

The tunneling industry has many techniques for creating space underground, which vary from excavation with conventional construction equipment, to drill and blast techniques, to highly specialized tunnel boring machines. The most traditional form of tunneling, which was first used thousands of years ago to create ancient Roman and Persian aqueducts, has evolved into what is now known as the Sequential Excavation Method, or SEM tunneling. SEM tunneling is an observational method that involves evaluating the type and behavior of the ground during excavation and determining the best combination of ground support components.



Figure 1. Secure pedestrian access between the Superior Courthouse of California and the Central Jail in downtown San Diego, Calif. (Model courtesy of Eric Westergren.)

During tunnel design, the ground support is prescribed based on what's known from advance geotechnical explorations. But the design also allows for additional measures and other support elements — known as "toolbox items" — that may be needed where ground conditions and behavior vary. Accordingly, required support may also be reduced where ground behavior is found to be more favorable than anticipated. Some examples of toolbox items include face dowels, permeation grouting, and pocket excavation. Viable toolbox items or other additional measures change depending on the project geotechnical conditions and initial support design for the tunnel.

Connecting a Jail and a Courthouse

SEM tunneling was successfully applied for the construction of the Courthouse Commons Tunnel in Southern California. The COCO Tunnel is a component of the Courthouse Commons Development Project located in downtown San Diego. The tunnel will provide secure pedestrian access between the Superior Courthouse of California and the Central Jail through a congested urban corridor (Figure 1). A small site was available for immediate construction access and to build a starter shaft on the east end of the alignment. The tunnel was mined from the starter shaft to the west, traversing beneath Front Street, two existing buildings, and Union Street. The shaft site accommodated a crane, two Conex boxes, the ventilation fan system, and a few minor ancillary components.

Kitty-corner from the shaft site to the northwest, a city block was available to the project team for a mechanical shop, construction staging, material storage, parking, and an area to unload excavated spoils. A building near the west end of the tunnel alignment provided indoor space for meetings with crews, as well as offices for construction and engineering staff. Despite all these resources, this downtown project setting with separated construction sites presented the team with a logistical challenge for adequate material staging, organization, and equipment coordination. These challenges varied across shifts as tunnel construction proceeded 24 hours a day, five days per week.

Design Elements and Construction Sequence

The COCO tunnel was constructed via the starter shaft (Figure 2), which was excavated within a single traffic lane and sidewalk immediately adjacent to the Central Jail. The shaft was necessary for equipment transport to the tunnel excavation area, construction personnel access, mucking out of spoils, and later construction of an elevator transfer structure from the Central Jail basement level to the tunnel. Through most of its length, the proposed tunnel is approximately 26 ft in diameter, with a cross section that looks like a modified horseshoe with a rounded invert. The total length of the tunnel is about 328 ft. The design and construction of the COCO tunnel can be categorized into five stages for simplicity. In sequential order these include pre-support, excavation round, initial lining/support, waterproofing installation, and final lining/support.



Figure 2. Canopy pipes and a collar beam in place prior to tunnel breakout from starter shaft.

Before excavation or installation of any support elements, the ground in the vicinity of the tunnel alignment required dewatering to below the final invert to prevent inflows and ground instability. The dewatering well array was designed

for the Paralic deposits of downtown San Diego, which consist of predominantly sands and gravels, based on a suite of borings and soil testing. Additional dewatering to a lower elevation was required at the starter shaft on the east end of the alignment. Dewatering of the ground in the project area was critical for SEM tunneling in this application because of the type of ground.

At the tunnel's nearest approach, the crown of the tunnel passes within 7 ft of the foundations of another existing jail facility. Due to the ongoing operations of this facility, it was of utmost importance that the jail remain in service during the tunnel construction process. The resulting pre-support for the first 200 ft of excavation, much of which passed beneath the jail, included three progressive sets of robust steel canopy pipes. These pipes measured 8 in. in diameter and were spaced 18 in. on-center. They were grouted in place to fill their interior and included grout ports so any annulus voids between the pipe and ground generated during drilling could be filled. The remainder of the tunnel length passed beneath a former decommissioned courthouse building that had been repurposed into project offices for the contractor and developer. This run of the tunnel was excavated beneath less robust ground conditions, where pre-support was installed with each excavation round to prevent raveling of the tunnel crown and face. The pre-support for the remainder of the tunnel alignment was 2-in.-diameter, 12-ft-long pipe spiles installed by a drill jumbo in quantities that varied from 3 to 25 for each round based on ground observations (Figure 3).

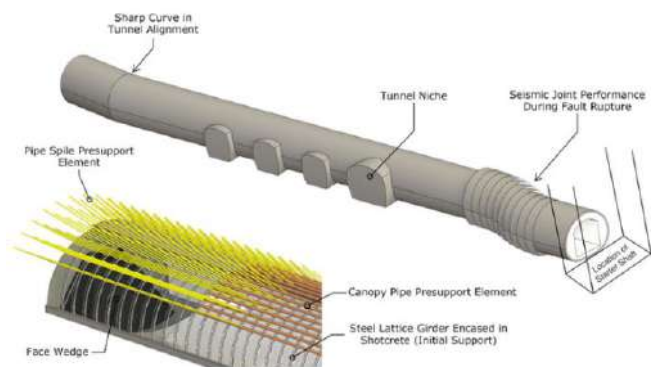


Figure 3. Rendering of tunnel alignment showing anticipated seismic joint movement during fault rupture and details of support elements. (Model courtesy of Eric Westergren.)

Tunnel excavation for SEM applications is generally segregated into multiple drifts, with the option to excavate smaller "pockets" when ground stability is a concern. The COCO tunnel was excavated with a top heading and face wedge that included approximately two-thirds of the tunnel cross section, followed by the lower bench to complete the tunnel ring (Figure 4). The entire length of the tunnel top heading was first excavated prior to the lower bench (Figure 5). Pocket excavation was most notably required on two occasions: when excavating carefully through an abandoned well structure not previously identified during geotechnical explorations, and when excavating four niches through the southern sidewall after completing the main tunnel drive.

The installation of initial support for the COCO tunnel was placed with each excavation round beneath presupport. For top heading excavation, these rounds ranged from 3 to 4 ft, while bottom heading excavation rounds were able to proceed at lengths of up to 12 ft. After a top heading round was excavated, approximately 3 in. of pneumatically applied concrete (i.e., shotcrete) was placed on all open ground to create a safe working condition. This first layer of shotcrete used to close all open ground is colloquially referred to as the "flashcrete." A steel lattice girder was then installed within the ex-

cavated round after the flashcrete reached an initial set. Finally, the entirety of the tunnel sidewalls, crown, and invert exposed by the recent excavation was covered by 10 in. of shotcrete, encasing the steel lattice girder and completing the round.

After the full length of the tunnel was excavated and supported by the initial lining, a nonwoven geotextile was applied to the inside of the shotcrete, and a PVC waterproofing membrane was applied (Figure 6). This membrane was heat-welded together throughout the underground structure and to the existing waterproofing of the adjoining structures. The final concrete lining, which later supported the full design loads of the tunnel, was then completely isolated from the groundwater that was recharged after dewatering wells were decommissioned at the end of the project. The final lining consisted of a placed reinforced concrete invert slab, followed by a semicircular crown and ribs that were placed using custom built, mechanically adjustable formwork. After waterproofing installation was completed, the final concrete invert slab was poured, followed by the remainder of the final lining using custom formwork.

Special Project Considerations and Challenges

San Diego Fault. A significant design constraint arose from the desired tunnel alignment crossing the active San Diego Fault. Analysis of the fault activity over recent geologic time designated the area as an Alquist-Priolo Earthquake Fault Zone, and it was determined that an oblique slip along a combination of the strike and dip of the fault of up to 18 in. was likely. Accordingly, a zone of systematic seismic joints (Figure 3) was incorporated into the design, utilizing primarily crushable gravel and geofoam fill between the initial and final linings. This zone, which was spatially verified based on observations of fault manifestation during excavation, was placed to allow for a fault rupture that would not compromise the final lining and waterproofing systems. Using SEM for excavation of the tunnel facilitated construction of these different cross sections.

Abandoned Brick Well. While installing the second array of canopy pipes, unexpected brick material was observed in the drilling spoils. This presented the SEM engineering and construction teams with the challenge of characterizing and addressing an unforeseen obstacle in the tunnel alignment. A system of probe drilling, video scoping, sample recovery, and environmental soil testing was employed to ultimately determine that the obstacle was a previously abandoned brick well that had been backfilled with waste and likely used as a burn pit. The well was located beneath the foundations of the in-service jail and estimated to extend from the bottom of the tunnel top heading, beyond the crown, and to the base of the building foundations.

The project team designed and implemented a campaign of consolidation grouting in which over 300 cu ft of cement grout was injected into the well structure. Once the excavation reached the identified limits of the brick structure, additional precautions were put in place to isolate foreign materials from the native ground for proper disposal. Enhanced personal protective equipment was used during this phase due to contaminants identified during sample testing, and the excavation proceeded with a pocket approach — breaking the top heading face into smaller sections to isolate the contaminated material prior to removal. Ultimately, the brick well and the undocumented fill of metal, glass, and burnt material that had been consolidation-grouted was removed without adverse effects on the integrity of the tunnel or above ground structures.



Figure 4. Excavation and mucking of spoils during top heading advance.

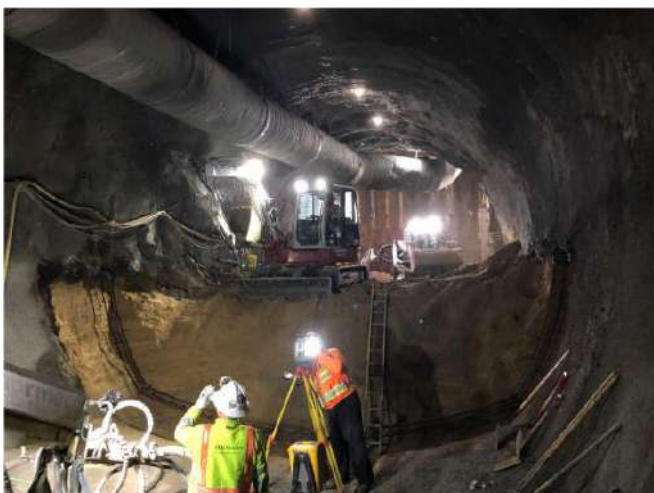


Figure 5. Lower bench excavation completed with lattice girder installed before initial support shotcrete placement; ongoing convergence monitoring with total station.



Figure 6. PVC waterproofing membrane installation following completion of initial shotcrete lining throughout entire tunnel cross section.

Ground Loss. A recurring challenge to the construction team was the manifestation of loose and raveling ground, generally where clean, poorly graded sand was encountered. In the worst of cases, this resulted in ground loss beyond

excavation limits as well as from behind previously installed shotcrete initial lining. In less dramatic cases, the ground was unable to hold wet shotcrete during flashcrete operations, which then required multiple rounds of attempts to close all open ground. As the project progressed, the construction crews developed skills to address this issue, namely with sodium-silicate mixtures and lower-impact grout sprayed on the open face before application of the thicker flashcrete.

Geotechnical Instrumentation Program

Throughout the construction phase, an integral component of the project included careful monitoring of the ground surface, surrounding buildings, tunnel interior, and underground movements at key locations. A suite of geotechnical instrumentation was thus installed in advance of the tunnel and shaft construction for monitoring before the project to establish a reliable baseline condition. The baseline included elevations on two roadways, numerous points on four buildings adjacent to and above the alignment, utility monitoring points, inclinometers, multiple point borehole extensometers, and piezometer readings.

To monitor the in-service courthouse structures adjacent to it, and the active jail facility above the tunnel alignment, liquid level and high-sensitivity settlement sensors were watched closely during dewatering and excavation activities. An additional manual survey was also performed, with leveling at critical periods when tunnel advances were made immediately below the foundation elements of the in-service jail facility. Targets on the exterior of all pertinent buildings were surveyed around the clock using robotic, automated total stations. The two AMTS devices employed on the project also surveyed surface settlement points on each street beneath which the tunnel traversed, as well as surface calibration prisms for the UMP and MPBX sensors.

Inside the tunnel, a series of convergence monitoring arrays were installed at approximately 40- to 50-ft intervals. These arrays consisted of five reflective targets spaced equally along the tunnel section circumference and were surveyed manually with each tunnel excavation advance. Monitoring of the CMAs required survey control and baseline points to be carried down the starter shaft and subsequently through the tunnel as the project progressed. Survey crew presence was constantly coordinated with the field team to also provide guidance on excavation limits during each advance.

Tunnel excavation for SEM applications is generally segregated into multiple drifts, with the option to excavate smaller "pockets" when ground stability is a concern.

Observation of the real-time instrumentation data revealed that movements did occur within the ground and at the surface as the tunnel was mined. Unexpectedly, however, the ground movements were greatest in magnitude as advances were excavated near and beyond points of interest, not when immediately under or before the points being watched. The entire suite of instrumentation was monitored holistically to understand the relation of in-ground movement (MPBX sensors) to in-tunnel convergence arrays to utility movements and building settlement. Throughout the excavation phase of the project, maximum levels of settlement, which ranged from 0.5 in. to 2 in. depending on the criticality of the feature and depth below ground surface, were never even closely approached.

SEM Into the Future

The successful excavation of the San Diego COCO Tunnel is a notable milestone in the adoption of SEM tunneling in the U.S. While this form of mining for the creation of infrastructure is common in other regions of the world, the technology remains in its infancy across the Americas. Past uses for SEM

in the U.S. have often been limited to tunnel cross passages or other ancillary tunnel works, with the use for main tunnel drives gradually growing.

Significant advantages to the Sequential Excavation Method include the ability to navigate tight turns, adjust grade, and modify cross-sectional geometry in very short distances — something that cannot be achieved with tunnel boring machines. This characteristic lends the technology to be suitable for crowded urban corridors that often have many underground obstructions and neighboring infrastructure. Furthermore, no specialized equipment is necessary for the excavation of a tunnel using the SEM method; however, the experience of the construction crews plays a vital role in the success of the tunnel excavation and support.

While SEM remains novel for many in the industry, adoption of the technology is likely to continue growing as the urban centers in the U.S. expand and become denser. As the need for more underground infrastructure in major cities spreads, those involved in the design and construction of the San Diego COCO Tunnel and other similar projects will carry on their knowledge to future SEM projects. This will develop more construction crews, engineers, and project managers who are skilled in the technology and more widespread use of SEM in the U.S. throughout the 21st century.

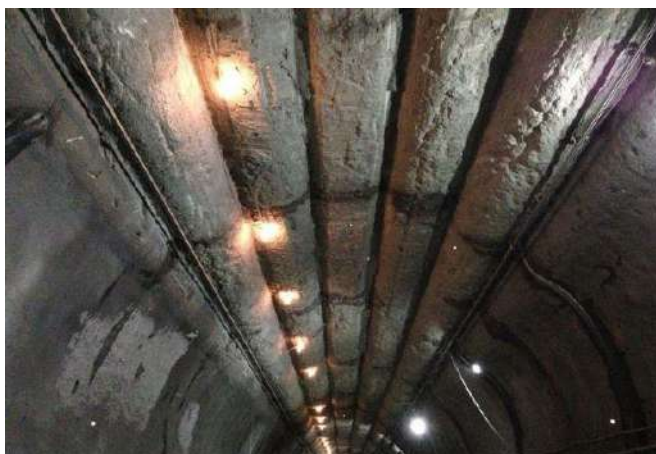
JAKOB R. WALTER, P.E., A.M.ASCE, is a senior staff engineer working for McMillen Jacobs Associates based in San Francisco, Calif. He enjoys working within California, where he can consistently frequent construction sites after advancing a project beyond the design phase. He can be reached at walter@mcmjac.com.

[Geostrata - February/March 2022 - Tunneling in Tight Quarters \(readgeo.com\)](#)

Have You Heard of Stacked Drifts?

A Tunnelling Technique That's Useful for Wide Spans Under Low Cover

Andrew G. Cushing



The Billy Bishop Toronto City Airport Pedestrian Tunnel showing stacked drifts forming the tunnel crown.

The use of "stacked drifts" in the sequential excavation method of tunnelling has been employed for over four decades and has allowed for the construction of tunnels and underground caverns approaching nearly 30-m width under clear cover thickness of 5 m or less, more typically in soft ground geology. The method essentially involves constructing a series of smaller-diameter tunnels, configured side-by-side, arched, and/or vertically "stacked." Typically, each small tunnel is backfilled with concrete and linked to adjacent tunnels with mechanical or shear interlocks to either directly form or facilitate the construction of a single, larger-diameter tunnel or underground cavity.

The method is often used when surface excavation is not permitted, and typically with low ground cover and wide span width, all factors that can contribute to difficulties and risks in underground construction. Geotechnical factors to be considered include the groundwater regime and the strength, stiffness, and permeability of the soil envelope. Low permeability soils having a degree of strength derived from cohesion (e.g., clays) are generally viewed as more ideal for stacked drift tunnelling, although excavation-induced deformation or instability in higher plasticity clays requires special attention. Permeable silty or sandy soils under a high groundwater table are typically viewed as the most challenging, generally requiring a combination of pre-excavation dewatering and ground improvement.

In addition to the routine ground surface settlement and adjacent structure movement monitoring that's typical for most conventional tunnelling projects, stacked drift tunnelling often involves internal tunnel convergence movement monitoring, both within the individual drifts themselves and within the final tunnel cavity. During construction, accurate survey control is required to ensure that the drifts achieve the required interlock and geometry. Construction quality control generally involves verification of pre-excavation ground improvement measures by core drilling and packer permeability testing, time-dependent strength development of fibre-reinforced shotcrete through sprayed test panel core drilling and beam bending tests, and other measures as required.

Design and Construction Case Histories

Several historical project examples in the U.S. and abroad can further exemplify key historical milestones using this tunnelling methodology.

nelling methodology.

Seattle, Washington

One of the earliest and perhaps most famous of the tunnels constructed by this method in the U.S. is the Mount Baker Tunnel (1983-1989), which now carries the westbound lanes of I-90 in the Seattle, Wash. area. It employed a total of 24 shield-driven drifts through stiff clay soil (Figure 1), each backfilled with concrete, with geometric shear interlock between the crown of one drift and the invert of the adjoining drift.

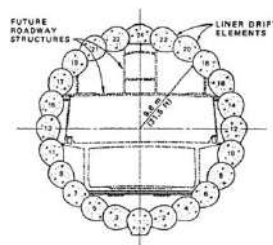


Figure 1. Mt. Baker Tunnel

The drifts were constructed bottom-up around the entire circular tunnel perimeter, resulting in a final internal diameter of 19.4 m over a 406-m length. At the portals, the minimum clear cover above the tunnel crown was only 3 m, with a minimum clear cover-to-span ratio of 0.15. In general, values of this ratio less than 0.5 are considered as "low cover" tunnelling, where no degree of soil arching can be considered. While this threshold is somewhat subjective, it also depends upon the ground conditions encountered and construction methods employed. Including about 25 mm of settlement during drift construction, the total diametric deformation after the main tunnel excavation was about 0.13 percent. Despite being constructed in the 1980s, the Mt. Baker Tunnel remains the largest-diameter, circular, soft-ground tunnel in the world. For comparison, the largest tunnel-boring machine cutter-head diameter currently is 17.6 m for the Tuen Mun - Chek Lap Kok Link highway tunnel in Hong Kong that opened in 2020.

San Juan, Puerto Rico

The Rio Pedras Station for the Tren Urbano rail project in San Juan, P.R. used mined construction, and is described by Gay, et al. (1999), and opened to the public in 2004. Temporary pre-support for both the crown and sidewalls of the station cavern was provided by a series of 15, 3-m-wide x 3-m-high x 150-m-long, sequentially-mined drifts that were subsequently backfilled with concrete to support a 19-m excavated span width in a stacked drift configuration (Figure 2 — soil grouting was performed through drift "G"). The soil cover was less than 5 m for a minimum clear cover-to-span ratio of less than 0.26. The soil within the crown was characterized as stiff, overconsolidated silty clays, while the sidewall drifts were driven within alternating layers of clean sand, silty sand, clayey sand, and clay.

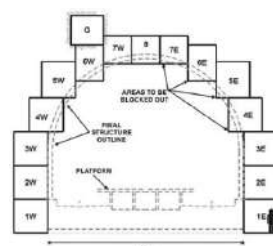


Figure 2. Rio Pedras Station

The stacked drift method of tunnelling is often used when surface excavation is not permitted, and typically with low ground cover and wide span width, all factors that can contribute to difficulties and risks in underground construction.

Boston, Massachusetts

In the late 1990s, the stacked drift method was also used for a short, 29-m length of the Central Artery/Tunnel megaproject in Boston, Mass., as a permanent underpinning measure to carry the northbound lanes of I-93 beneath the existing MBTA Red Line at South Station. A series of three stacked drifts were used to construct each of the highway tunnel side-walls to permit the excavation of a rectangular, 22-m-wide, 13-m-high opening beneath the MBTA Red Line. Soil conditions within the highway tunnel excavation profile were composed primarily of a pervious granular till (very dense sand and gravel with trace silt), with a cohesive glacial till cover and lower argillite bedrock with a highly variable weathering profile. There are two groundwater levels in the area, one at 3 m to 4.5 m below ground surface that's perched on the cohesive till layer, and a lower piezometric level in the granular till that's about 6 m to 7.5 m below ground surface, or about 26 m above the base of required excavation for the highway tunnel.

Initial access to the stacked drifts was achieved by sinking two, 35-m-deep vertical shafts, supported by 1.1-m-thick diaphragm (slurry) wall panels excavated by hydromill, one on each side of the highway tunnel. Two parallel access tunnels were then driven through the cohesive glacial till, with the crown level about 1.5 m below the bottom of the Red Line station. To facilitate excavation of the access tunnels, temporary dewatering wells were installed on each side of the Red Line station. A campaign of sodium silicate chemical grouting was then advanced using tube-a-manchettes installed through the invert of the access tunnels down to 3 m below the invert of the bottom drift. This controlled groundwater inflow during the subsequent excavation of the stacked drift walls, which was done bottom-up in three stages as shown in Figure 3. The drift walls were comprised of three cast-in-place concrete segments between 2.4 m and 3.7 m in width, each connected by mechanical couplers, over a total height of 13.4 m. The segments did not use intermediate bracing and were designed as gravity walls to resist both horizontal and vertical loads, relying on lateral friction acting at the base of each wall for overall temporary stability.

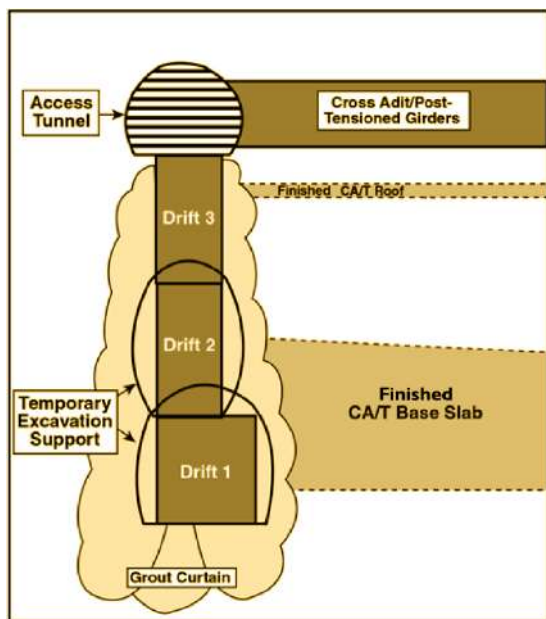


Figure 3. Stacked drifts beneath the MBTA Red Line at South Station for the Boston Central Artery Tunnel

A total of 11 cross adits were then constructed between the two upperaccess tunnels using hand-mining techniques through the cohesive glacial till between the two stacked drift walls. The adits were used to construct a series of 2.4-m-deep post-tensioned girders across the 22-m-wide highway tunnel span, with about 1 m vertical clearance to the Red Line station above. During tunnel excavation, less than 15 mm of vertical movement was reportedly measured at the MBTA Red Line structure. Vertical inclinometers within the drift walls showed negligible horizontal movement.

Milan, Italy

One of the largest span caverns ever constructed in soil was for the Venezia Station (1988-1992, opened in 1997) on the Milan Urban Link Railway Line in Italy, with a temporary internal span width of 28.8 m, a 20-m height, and a 440-m² cross-sectional area over a length of 215 m. The minimum clear cover of 4 m above the tunnel crown results in a minimum clear cover-to-span ratio of 0.14. The soils surrounding the cavern consisted of permeable sands and gravels, with a significant portion of the cavern excavated beneath the groundwater table. The "Cellular Arch" method (Figure 4) was employed because the clear cover was not deemed sufficient to use conventional tunnelling techniques reliant solely upon soil-arching theory without causing excessive surface soil deformations. The first element of construction was a driven 3.5-m-diameter pilot tunnel. Through this pilot tunnel, ground improvement injections were advanced in a 360° radial fan array beyond the future excavated cavern perimeter above the crown, beyond the sidewalls, and beneath the invert. This treatment was employed to achieve some degree of soil consolidation and cohesion, as well as to reduce the permeability of the soils beneath the water table.

Lower sidewall drifts were then excavated and incrementally supported with a primary lining of steel ribs, wire-mesh reinforcement, and sprayed shotcrete. A secondary, final lining element was then installed within these lower drifts comprising the lower sidewall and edge of the invert. Next, a series of 10, 2.1-m external diameter (1.8-m internal diameter) precast concrete microtunnels were jacked from a thrust pit within the upper crown of the cavern in 2-m incremental lengths along the entire 215-m station length.

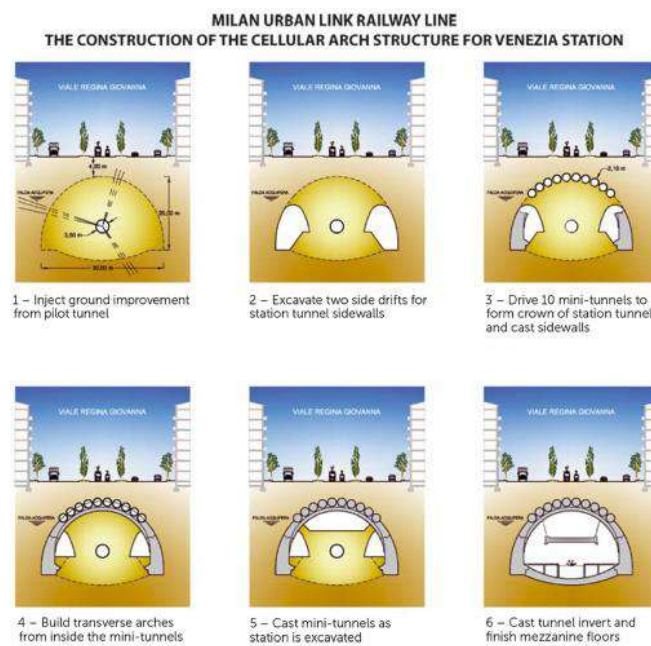


Figure 4. Construction of the cellular arch structure for Venezia Station, Milan Urban Link Railway Line, Italy

Once the lower sidewalls had been cast and the upper micro-tunnels driven into place, construction of transverse load-bearing arch cross-members were installed at 6-m longitudinal intervals, for a total of 35 intermediate cross-members and two end-members. These cross-members were constructed by cutting out the portion of each microtunnel intersected by the arch and continuing the excavation by hand down to the lower tunnel sidewall drifts. Prefabricated steel formwork was used to form each transverse arch element, with internal steel reinforcement extending through the arch and into the internal microtunnel elements, which were all then backfilled with concrete.

Hence there's a structural connection between the 10 longitudinal microtunnels and each transverse arch member. The remainder of the cavern was excavated incrementally, with an invert ranging in thickness between 1.5 m and 2 m and installed in 5-m longitudinal increments. The final element of construction was the mezzanine level that was installed within the middle of the cavern and suspended with tie rods attached to the transverse arch elements. Ignoring an initial surface heave induced by the initial grouting through the pilot tunnel, a maximum excavation-induced surface settlement of 14 mm was measured above the cavern centerline, with surface settlements at the building façade lines of up to 7 mm.

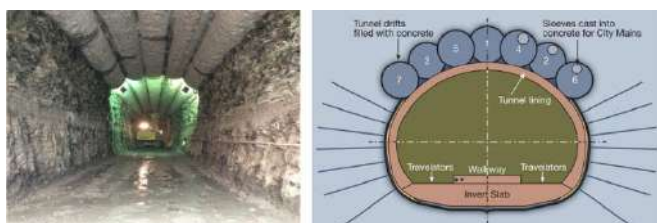


Figure 5. The Billy Bishop Toronto City Airport Pedestrian Tunnel

Toronto, Canada

The stacked drift method has been extended to excavated cavities in rock. An example is the Billy Bishop Toronto City Airport Pedestrian Tunnel (2012-2015) that was constructed in the Georgian Bay Shale, a thinly laminated shale rock mass beneath Lake Ontario. The tunnel employed a series of seven, 1.85-m-diameter interlocking secant drift bores sequentially excavated by two TBMs within the crown of the tunnel and backfilled with mass concrete (Figure 5). The resulting excavated cavity beneath the interlocking drift bore arch was approximately 10-m wide, one of the widest spans excavated within the Georgian Bay Shale within the Greater Toronto Area to date.

This method of construction was proposed by the tunnel contractor for several reasons. First, it was a precautionary safety measure to minimize potential settlement, considering that the minimum clear rock cover above the crown was less than one final cavity diameter below the overlying bed of Lake Ontario. Secondly, it utilized the knowledge of recent experiences in the excavation of the Niagara Tunnel Project (2008-2013), which provides an additional water supply to the Sir Adam Beck Hydroelectric Generating Stations in Niagara Falls, Ontario, Canada. An unshielded, 14.4-m-diameter TBM was used to construct that tunnel (currently the largest-diameter hard rock TBM in existence). Significant crown overbreak of 4-m thickness or more occurred when tunnelling encountered the Queenston Shale, a laminated and high horizontally stressed rock formation. The use of interlocking secant bores for the Billy Bishop Airport Pedestrian Tunnel is less common than the use of steel pipes installed in a tangent configuration by jacked/guided auger boring methods in both rock (in Qatar and Hong Kong, for example) and more commonly in soil.

It All Stacks Up

As the above case histories illustrate, the stacked drift method of tunnelling is typically used to construct relatively wide-open spans under relatively low soil or rock cover. As described, the method employs several technologies, including excavation of smaller drift tunnels using shield, jacked, bored, or other methods, ground improvements such as dewatering and injection grouting, and general sequential excavation of the internal soil or rock to achieve the larger tunnel or cavity geometry. The method is complementary to other mined/sequential excavation tunnelling methods, such as the so-called New Austrian Tunnelling Method, which makes extensive use of sprayed concrete (shotcrete) lining to sequentially excavate side and central drifts that are further subdivided by heading and bench levels. All such methods require extensive instrumentation and monitoring, both at the surface and internally, as the excavation progresses. Key technical inputs include drift and final geometry, soil cover, soil stiffness and type (cohesive or cohesionless), groundwater level, and viable drift excavation, dewatering, ground improvement, and final lining construction methods. With the advent of 2D and 3D finite element methods of analysis, the construction sequence can be modelled explicitly to evaluate incremental and final ground and lining stresses and movements.

► **ANDREW G. CUSHING, P. Eng., M.ASCE**, is a senior geotechnical and tunneling engineer with Arup in Toronto, Canada, where he's responsible for providing geotechnical design and advisory services for utility and metro tunnels and other large-scale infrastructure projects. He can be reached at andrew.cushing@arup.com.

[Geostrata - February/March 2022 - Have You Heard of Stacked Drifts? \(readgeo.com\)](#)

The Bearing Capacity Equation

By Mary Nodine, PE, M.ASCE



When we consider a footing on sand or on clay, Terzaghi's factors will come into play. Depth, overburden, and cohesion make three: N_q , N_γ , and N_c .

For decades, they cooperated To determine if a foundation was slated To settle, or fail dramatically. They'd shoot for a factor of safety of three.

But N_q had a competitive streak. He kept score, one fateful week Of every factor's contribution To the bearing capacity solution.

He marched up to N_γ with data in hand. "Friend," he declared, "We must make a plan. It's clear that N_c is not pulling his weight. The equation is ours! Let's take charge of our fate.

" N_c provides NOTHING for footings on sand. Add in some clay and he'll give us a hand. But ... as time goes on, the more sure I feel That drained cohesion intercepts aren't even real!"

Now N_γ , you see, was a little bit shy And she thought that N_c was a nice enough guy. But N_q had never paid her much attention (Unless a footing had massive dimensions).

For piles, N_q would ignore her outright (Since the width was so tiny compared to the height). Now, N_q was begging for her to assist! Under pressure, N_γ just could not resist.

So the factors embarked upon their selfish mission To eliminate N_c from every edition Of Holtz & Kovacs, Terzaghi and Das, Smugly declaring it no great loss.

Eraser dust flying, they scrubbed N_γ away From hand calculations, page after page. They even included in their scope The back of every envelope.

When the factors had finished their quest to delete, N_q was triumphant and clearly upbeat. The simpler equation, he thought, it was clear would improve the lives of all engineers.

But with worn-off adrenaline N_γ saw That there might be a fatal flaw. She asked, "Now that only we two remain... What do we do when the soil's undrained?"

► **MARY NODINE, PE, M.ASCE**, is a geotechnical poet and a project manager with GEI Consultants, Inc. in Woburn, MA. She can be reached at mnodine@geiconsultants.com.

[Geostrata - February/March 2022 - The Bearing Capacity Equation \(readgeo.com\)](http://readgeo.com)

ΝΕΑ ΑΠΟ ΤΙΣ ΕΛΛΗΝΙΚΕΣ ΚΑΙ ΔΙΕΘΝΕΙΣ ΓΕΩΤΕΧΝΙΚΕΣ ΕΝΩΣΕΙΣ



Σχολή Πολιτικών Μηχανικών
Εθνικό Μετσόβιο Πολυτεχνείο

ΤΟΜΕΑΣ ΓΕΩΤΕΧΝΙΚΗΣ

Διαδικτυακή διάλεξη **Δρ. Μαρίας Πανταζίδου**, Αναπληρώτριας Καθηγήτριας του Τομέα Γεωτεχνικής στην Σχολή Πολιτικών Μηχανικών Εθνικού Μετσόβιου Πολυτεχνείου.

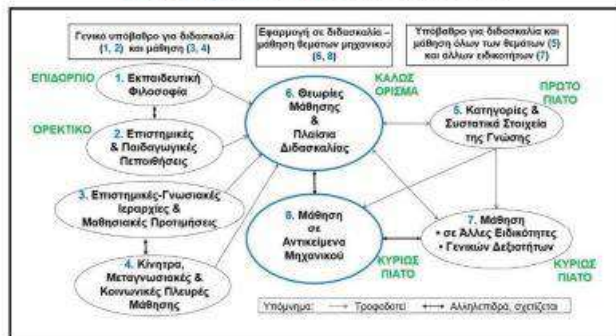
ΠΡΟΣΚΛΗΣΗ ΣΕ ΔΙΑΔΙΚΤΥΑΚΗ ΔΙΑΛΕΞΗ

Ένα εκπαιδευτικό μενού
και ένας γύρος της βιβλιογραφίας της εκπαίδευσης
για διδάσκοντες μηχανικούς

Τρίτη, 8 Φεβρουαρίου 2022, 17:00-18:00

<https://centralintra.webex.com/centralintra.php?MTID=md8474fb22e04a1b65c9b7450993883a>

Ο ΓΥΡΟΣ ΣΕ ΧΑΡΤΗ (το μενού στην επόμενη σελίδα)



από την Αναπληρώτρια Καθηγήτρια
Μαρίνα Πανταζίδου
Σχολή Πολιτικών Μηχανικών
Εθνικό Μετσόβιο Πολυτεχνείο

Περίληψη

Ο γύρος της βιβλιογραφίας της εκπαίδευσης είναι ένα συμπυκνωμένο **κείμενο** 45 σελίδων που διευκολύνει τον διδάσκοντα μηχανικό να την περιηγηθεί με τη βοήθεια του χάρτη της πρόσκλησης. Η ομιλία έχει δομηθεί ως μια συνεκτική επιλογή θεμάτων, βλέπε μενού στην επόμενη σελίδα, για να μας ανοίξει η όρεξη να δούμε τη διδασκαλία με άλλο μάτι. Οι επιμέρους στόχοι της περιλαμβάνουν και:

- (α) να μετασυστοιχούμε στη διδασκαλία μας, έστω και κατά δε, προς την υιοθέτηση ευρημάτων από την έρευνα στην εκπαίδευση,
- (β) να διαβάσουμε άρθρα από τη βιβλιογραφία της εκπαίδευσης,
- (γ) να μαζευτούμε στο ΕΜΠ σε ομάδα οι συναδέλφοι με εκπαιδευτικά ενδιαφέροντα, και
- (δ) να δημιουργήσουμε διαδιδρυματικές εκπαιδευτικές συνεργασίες.

Ένα εκπαιδευτικό μενού
και ένας γύρος της βιβλιογραφίας της εκπαίδευσης
για διδάσκοντες μηχανικούς (συνέχεια)

ΤΟ ΜΕΝΟΥ

Καμινάρισμα
Η «τυρόπιτα» της εκπαίδευσης

Ορεκτικό
Δύο παιδαγωγικές πεποιθήσεις

Κράνιο κούρα
Αυλοί σβόλοι (shunks), ερωτήσεις ανάκλησης & γυμναστική μυαλού

Κορύμβο κούρα
Μηχανική Παραμορφώσιμου Σώματος και Εδαφομηχανική με επίπεδη γη και αντάρακτο SARS-CoV-2

Δομική κούρα ως εκπαίδευση
Πώς μπορούμε όλοι να βοηθήσουμε να φαχτεί η «τυρόπιτα» της εκπαίδευσης

Για την ομιλήτρια



Η Μαρίνα Πανταζίδου είναι Αναπληρώτρια Καθηγήτρια στον Τομέα Γεωτεχνικής της Σχολής Πολιτικών Μηχανικών ΕΜΠ. Έχει πολυετή ακαδημαϊκή και επαγγελματική εμπειρία στις Ηνωμένες Πολιτείες και στην Ελλάδα στο αντικείμενο της περιβαλλοντικής γεωτεχνικής, με ιδιαίτερη έμφαση στους τομείς χαρακτηρισμού και αποκατάστασης χώρων ρυπασμένων από επικίνδυνα απόβλητα. Τα ερευνητικά της ενδιαφέροντα περιλαμβάνουν αριθμητική και φυσική προσομοίωση της κίνησης στο υπέδαφος οργανικών ρύπων που δεν αναμειγνύονται με το νερό, λήψη αποφάσεων σε θέματα περιβαλλοντικής αποκατάστασης και διδακτική της επιστήμης του μηχανικού. Τα τελευταία 20 χρόνια συμμετέχει ενεργά σε επιτροπές για τη διδασκαλία θεμάτων πολιτικού μηχανικού και από το 2017 είναι πρόεδρος της Τεχνικής Επιτροπής για την Εκπαίδευση TC306 της International Society for Soil Mechanics and Geotechnical Engineering (ISSMGE), που διοργάνωσε στην Αθήνα, διαδικτυακά, το 5^ο Διεθνές Συνέδριο για την Εκπαίδευση στη Γεωτεχνική Μηχανική στις 23-25 Ιουνίου 2020.



International Society for Soil Mechanics and Geotechnical Engineering

**ISSMGE News & Information Circular
February 2022**

<https://www.issmge.org/news/issmge-news-and-information-circular-february-2022>

1. Council Meeting - 1st May 2022

The ISSMGE Board, together with the organisers of the 20ICSMGE, have agreed that the next Council Meeting will be a hybrid event. Full details on attendance and participation will be circulated to the officers of the member societies by the 15th March 2022.

2. 20ICSMGE / 7iYGEC NEW DATES MAY 2022

New dates have been confirmed for the conferences in Sydney as follows;

7iYGEC - Friday 29 April - Sunday 1 May 2022
20ICSMGE - Sunday 1 May - Thursday 5 May 2022.

Registration is now open via the conference website <https://icsmge2022.org/registration.php>.

3. TIME CAPSULE PROJECT UPDATE

The Time Capsule Project (TCP) has attracted strong support, see <https://www.issmge.org/the-society/time-capsule> for an update.

In March 2022, a team of **discoverers** will work their way through the material placed online. This work will be an important element of the ISSMGE Time Capsule to be launched at the 20th ICSMGE in Sydney.

Individual members of the ISSMGE are welcome to indicate their interest in being part of the team of discoverers via the time capsule contact form available at: <https://www.issmge.org/the-society/time-capsule>.

4. VIRTUAL UNIVERSITY

The following have been added to the website:

[Performance assessment of soils and structures by numerical analysis](#) Prof. Toshihiro Noda

[How to perform reliability analyses on a spreadsheet](#) Dr Lei Wang

[Collapse of Fujinuma Dam by the 2011 Great East Japan Earthquake and its reconstruction](#) - Prof. Fumio Tatsuoka and Dr. Antoine Duttine

[Probability Analysis in Civil Engineering](#) Prof. Jie Zhang

5. NEWS FROM IAEG - ENGINEERING GEOLOGICAL MODELS

The International Association for Engineering Geology and the Environment (IAEG) Commission 25 (C25) is in the final stages of preparing Guidelines for the Development and Application of Engineering Geological Models on Projects. The Guidelines build on the initial C25 report on Engineering Geological Models (Parry et al. 2014) and will establish best practice based on the application of the technique on actual projects. To read the full press release please click [here](#).

6. BULLETIN

The latest edition of the ISSMGE Bulletin (Volume 15, Issue 6, December 2021) is available from the website <https://www.issmge.org/publications/issmge-bulletin/vol-15-issue-6-december-2022>.

7. ISSMGE FOUNDATION

The next deadline for receipt of applications for awards from the ISSMGE Foundation is the 31st May 2022. Click [here](#) for further information on the ISSMGE Foundation.

8. CONFERENCES

For a listing of all ISSMGE and ISSMGE supported conferences, and full information on all events, including deadlines, please go to the [Events page](#) at <https://www.issmge.org/events>. However, for updated information concerning possible changes due to the coronavirus outbreak (ie. postponements, cancellations, change of deadlines, etc), please refer to that specific events website.

As might be expected, many events have been rescheduled and we update the Events page whenever we are advised of

changes.

The following are events that have been added since the previous Circular:

8th International Symposium on Deformation Characteristics of Geomaterials - 03-09-2023 - 06-09-2023

Faculty of Engineering, University of Porto, Porto, Portugal; English; Organiser: TC101-ISSMGE, endorsed by SPG and FEUP; Contact person: Cristiana Ferreira; Address: FEUP-DEC, Rua Dr. Roberto Frias, s/n; Phone: (+351)2250817521 Email: is-porto2023@fe.up.pt; Website: <http://www.fe.up.pt/is-porto2023>

SUT OSIG 9TH International Conference Innovative Geotechnologies for Energy Transition - 12-09-2023 - 14-09-2023

Imperial College London, UK; English; Organiser: Society for Underwater Technology, Offshore Site Investigation & Geotechnics Committee; Contact person: Jacqui Adams, Address: SUT, HQS Wellington, Victoria Embankment, London WC2R 2PN, Website: <http://www.sut.org>; Email: osig2023@sut.org

GeoWorld reached 25,000 registered members!



[GeoWorld](#), the largest online professional networking site for geotechnical engineers and associated fields, has now reached 25,000+ active global members becoming the largest geocommunity in the world!

GeoWorld is a free online platform for professional networking among geotechnical engineers, companies and organizations. ISSMGE is a founding member of GeoWorld and maintains its own page on the network [here](#). Over the last decade, GeoWorld has turned into a well-established network and has a growing geo-community of 25,000+ individuals, 1,000+ companies & organizations from a total of 162 countries!

GeoWorld members can easily create a professional profile, expand your network, communicate and exchange of information with other professionals. They can also connect and interact with ISSMGEs profile as well as receive the latest news happening in the profession, by joining ISSMGE TC groups.

Furthermore, GeoWorld members can also be part of the [Geotechnical Business Directory](#), which is the most comprehensive business directory in geotechnical engineering and actively supported by ISSMGE. The 2022 Geotechnical Business Directory, the eight of the series is expected to be published in the summer of 2022!

The urgent need for remote sensing in geotechnical engineering

In my late 40s I am reflecting on how I started my career in geotechnical engineering in the European Alps on a rock slope stability project. I turned up as a 19-year-old and was asked to help assess a rock slope above a new tunnel portal. The engineering geologist, with a long white beard, took me to the gear shed and fixed me up with a harness and some ropes, and took me up a 50 m cliff. The safety talk was basic, but I thought it adequate. Over the course of that summer, I developed some great skills and learned a lot. But now with close to 30 years of hindsight, I realise I was put into a hazardous situation.

So, what has changed? We are now more considerate of our own wellbeing, health, and safety. We consider training and the need for requisite skills well before situations where we might need them arise. Remote sensing, among other emerging or established technologies, also helps. For example, engineers no longer need to spend long periods on slope faces exposed to hazards. Do not get me wrong, I still consider the skill to read a slope or rock face in situ essential, but I no longer consider the need to be hung from a rock face for weeks to be essential. Technology has changed how we work and how we approach solutions. Digital rock mapping, developed over the past decade, greatly reduces the need to spend long periods near slope hazards, especially if those hazards are seismically triggered and unpredictable.

It is not just about capturing the information remotely to increase safety, but also about being able to share the information digitally, work collaboratively across the globe, improve quality, and get more reliable data. Based on projects where I have used these digital tools, I have noted that they are safer, cheaper, and quicker to employ compared to traditional rock mapping. Consequently, I am an enthusiastic driver of remote sensing and consider it to be a truly disruptive technology!

About the authors:



Camilla and Jan are both Principals in Ground and Underground Engineering with the global professional services firm, Aurecon. Both live in New Zealand but deliver projects across the globe. Camilla leads the Ground Engineering Team in Christchurch, New Zealand. She is a Chartered Geologist with nearly 20 years of experience working across the UK, Australia, Hong Kong and New Zealand. Her main technical skills include geohazard analysis and mitigation, geotechnical emergency response, technical team leadership and project management. Camilla has been heavily involved in the assessment, response and remediation of the multiple geohazards affecting the New Zealand people following the Canterbury and Kaikoura earthquakes of 2011 and 2016.



Jan is a Geotechnical Engineering and Earthquake Engineering Specialist and maintains a global project portfolio. He was closely involved with the complex Canterbury and Kaikoura Earthquake Sequences as a first responder with Urban Search and Rescue. He is globally recognised as an earthquake engineering specialist overseeing various engineering aspects of emergency response and recovery. Over the past decade while seconded to the NZ Central Government, he managed severely earthquake damaged buildings and land by innovating with digital tools and applying smart technologies.

Both, Camilla and Jan, enjoy peer reviews, expert witness work, forensic engineering, and champion technical mastery. Together they wrote multiple publications on the application of smart materials and technology for sustainable horizontal infrastructure, civil structures, and buildings. Both are regularly invited as keynote speakers at international conferences on speaking about innovation, resilience, sustainability and state of the art digital tools.

About these articles:

To debate past, current and future issues in Geotechnical Engineering, the Time Capsule Project is welcoming and publishing short articles on the ISSMGE website.

We challenge you to write 200-400 words on any topic that will generate debate within the Geotechnical Engineering profession. [Click here to submit your message for consideration.](#)

Articles will be displayed for a limited time and views expressed need not be shared by the ISSMGE or held strongly by authors.

Final draft of the Failure Paths report

Failure paths for levees

Final



February 2022

PREPARED BY
Technical Committee on
Geotechnical Aspects of Dikes and Levees
(TC201)

Authors Part A and editors Part B and C:
Meindert Van (Deltares, The Netherlands)
Esther Rosenbrand (Deltares, The Netherlands)
Remy Tourment (INRAE, France)
Philip Smith (RoyalHaskoning DHV, United Kingdom)
Cor Zwanenburg (Deltares, The Netherlands)

Citation: Van, M.A., Rosenbrand, E., Tourment, R., Smith, P. and Zwanenburg, C. Failure paths for levees. International Society of Soil mechanics and Geotechnical Engineering (ISSMGE) – Technical Committee TC201 'Geotechnical aspects of dikes and levees', February 2022. Download ([TC201 Dykes and Levees | ISSMGE](#))

https://www.issmge.org/filemanager/article/992/9bb_TC201failure_paths_reportFinal.pdf

Mid-Term TC Report TC305

October 2017 December 2021

Name of the Technical Committee:	TC305 «Geotechnical Infrastructure for Megacities and New Capitals»
Chair:	Askar Zhussupbekov
Vice-Chair (if any):	Hoe Ling
Secretary:	Der-Wen Chang
Form filled by:	Der-Wen Chang
Number of TC members:	33
Number of chair nominated members:	3

Corresponding Members:	6
Website:	https://www.issmge.org/committees/technical-committees/impact-on-society/megacities-
Date:	31 December, 2021

<https://www.issmge.org/news/mid-term-tc-report>

First TC306 Geotechnical Engineering Education post

TC306 implemented a new "corner" of its [website](#) (a new menu on the left, called GEE posts), devoted to **Geotechnical Engineering Education posts** specifically written for geotechnical engineering instructors. Any GEE post starts as a short contribution written by a TC306 member. The submission is then discussed within the TC. The final post reflects the result of this interaction.



The first post, written by TC306 chair Marina Pantazidou, is now available online: [Contrast memorably soils and rocks](#)

Announcing the 6th McClelland Lecturer – Professor Richard Jardine

The McClelland Lecture is the honour lecture of ISSMGE TC209, with the recipient selected by a panel of peers from across the offshore geotechnical profession.

Announcing the 6th McClelland Lecturer Professor Richard Jardine

ISSMGE Technical Committee 209 Offshore Geotechnics is delighted to announce that Professor Richard Jardine of Imperial College has been invited to deliver the 6th McClelland Lecture.

Richard has contributed to offshore geotechnical engineering over most of his career. His early research pioneered laboratory-based small-strain FE modelling of foundations, included the first field observations of North Sea pile group load-displacement behaviour and paved the way for the ICP (Imperial College Pile) design method with findings that underpin international practice. Richards subsequent contributions encompass characterising geomaterial non-linearity, anisotropy, brittleness and cyclic loading through advanced laboratory testing, as well as designing new instruments and experimental protocols for field experiments, physical models and prototype research. Working with colleagues he devised new approaches to investigate and analyse very large offshore landslides and methodologies for suction bucket foundation design. Richards current focus is mainly on renewable energy applications. A key PISA JIP Academic Work Group member, he contributed to developing research-based guidelines for monopile design that are now widely adopted by industry. He leads the ALPACA research JIPs into the axial-and-

lateral, cyclic-and-monotonic behaviour of offshore piles driven in chalk and was co-leader of the recent PAGE JIP into the ageing of piles driven in sands.

Richards work has led to prestigious invited lectures including the Geotechnique, Coulomb, Bishop (ISSMGE Honour) and Rankine Lectures. He has received awards from American Society of Civil Engineers, ASTM and the French, Canadian, Chinese, Irish, Portuguese and Japanese national societies, as well as multiple UK awards including Fellowship of Royal Academy of Engineering.

Richard will deliver his lecture at the SUT's Offshore Site Investigation and Geotechnics (OSIG) 9th International Conference *Innovative Geotechnologies for Energy Transition* in September 2023.

Congratulations Richard!

Application of Unsaturated Soil Mechanics on the Analysis of Slopes

Indian Institute of Technology Mandi, Durham University, UK and Universiti Kebangsaan Malaysia (UKM) organised a 2-day training course on the "Application of Unsaturated Soil Mechanics on the Analysis of Slopes", 24-25 February 2022.

The speakers were:

Prof. David Toll, Durham University
 Dr. Arash Azizi, Portsmouth University
 Prof. D.N. Singh, IIT Bombay
 Dr. Uday Kala, IIT Mandi
 Dr. Marti Lloret-Cabot, Durham University
 Dr. Aizat Mohd Taib, UKM
 Dr. Kuo-Chieh Chao, Asian Institute of Technology
 Dr. Ashutosh Kumar, IIT Mandi
 Dr. Apiniti Jotisankasa, Kasetsart University
 Dr. Samprada Pradhan, Durham University
 Dr. Alexandros Petalas, Durham University
 Mr. Faris, UKM

The course was organised under the project theme "Understanding Landslide Susceptibility and Adaptability in South East Asia" (SEAL) (funded by UKRI-NERC). The course was attended by 160 people from 15 countries.



Geotechnical Engineers can now publish technical related content on GeoWorld, get DOIs, and reach thousands of geo-professionals

[GeoWorld](#), the professional networking platform for geotechnical engineers, recently launched [a brand-new resources section](#), which expands the classic blog functionality. **It is now possible for every GeoWorld member to share**

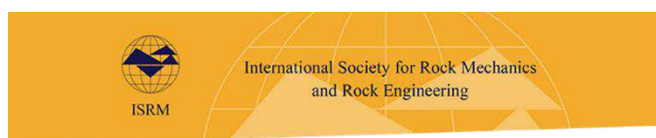
technical content based on their personal or collaborative research, attach files of datasets/reports and issue DOIs!

Besides technical content, individuals can also promote their professional activities, share their opinion or professional experiences, post updates on their professional life, share their research, promote products, services or events they or their company are offering. The possibilities are endless!

Compared to mainstream social media that require significant investment of time to reach the right audience, GeoWorld provides to its members the opportunity to reach a wide audience without a lot of effort. GeoWorld also revolutionizes the way geo-information is indexed, generated and circulated within the geo-community!

To be part of GeoWorld's large community, publish content and be listed in the Geotechnical Business Directory [create an account](#). In case you already have a Geoengineer.org account you can use it to sign in on GeoWorld and take advantage of its numerous features!

(Geoengineer.org, Feb, 21, 2022, <https://www.geoengineer.org/news/geotechnical-engineers-can-now-publish-technical-related-content-on-geoworld-get-dois-and-reach-thousands-of-geo-professionals>)



News

<https://www.isrm.net>

Second ISRM Young Members' Seminar (YMS) on 23 February 6 Feb, 2022

ISRM International Symposium 2022 - LARMS 2022 - new date for abstract submission is 20 March 10 Feb, 2022

Prof. Álvaro González García passed away 14 Feb, 2022

Prof. E.T. Brown elected as an International Member of the U.S. National Academy of Engineering 14 Feb, 2022



Scoped by ITA-AITES #60, 1 February 2022

[Major tunnel in Jiangsu opens to traffic | China](#)

[Simple and robust Paris Metro Line reaches great depths with an impressive structural concept | France](#)

[Celebrations for Lima Metro's First TBM Breakthrough | Peru](#)

[Lingering Covid forces WTC2022 postponement to September | Denmark](#)

[Civil work on Maharashtra's longest tunnel complete | India](#)

[Airport to Orewa: Aucklanders to be consulted on ambitious rail and tunnels | New Zealand](#)

[LTA awards civil contracts for Cross Island Line Phase 1 | Singapore](#)

[Glasgow Clyde Metro set for go-ahead as headline project in SNP strategy | United Kingdom](#)

[Purple Line tunneling completed between Century City and Wilshire/Rodeo! | United States of America](#)

[Brenner Lot H41 construction begins | Austria](#)

Scoped by ITA-AITES #61, 15 February 2022

[Helsinki-Tallinn tunnel can open up rail in Finland and Estonia: 'we love competition'](#)

[Metro tunnel excavation work likely to get over next month | India](#)

[Dive into the deepest structures on earth](#)

[Tunneling robot speeds installation of underground utilities | United States of America](#)

[Sydney Metro West announces shortlist for final tunnelling phase | Australia](#)

[Indonesian tunnel project proposed](#)

[Update on Massey Tunnel replacement plan | Canada](#)

[Cross River Rail's Roma Street enters new construction phase | Australia](#)

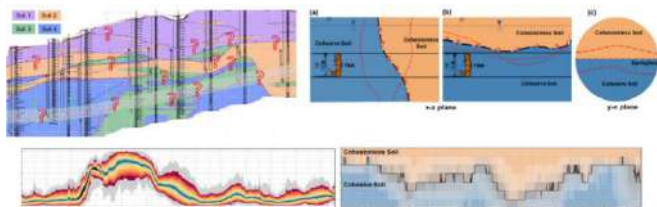
[RTS tunnel work to begin in 2 months | India](#)

[Watch: Overcoming geological challenges on the Brenner Base Tunnel | Italy-Germany-Austria](#)



Validation of Probabilistic and Artificially Intelligent Ground Models in Predicting Soil Transitions

Rajat Gangrade, PhD –Tunneling Engineer, Arup



Transitions between geological/geotechnical soil units have a critical impact on the operation and performance of a tunnel boring machine (TBM) and pose a significant risk for soft ground tunneling.

Current tunnelling practice relies on deterministic interpretations of ground conditions without accounting for ground spatial variability and uncertainty. With the increased number of claims and litigations arising due to ground uncertainty, a probabilistic interpretation of ground conditions is desired.

This talk presents two unique soft-ground tunneling case studies where soil transitions are quantified through a geo-statistics-based probabilistic assessment of ground conditions. The results from the probabilistic interpretation are validated with an artificial intelligence model of as-encountered ground conditions (developed at the Underground Construction and Tunneling Center at Colorado School of Mines) and with actual TBM data from the project sites.

The assessment aims to enhance the confidence of using probabilistic interpretations to improve ground awareness for efficient tunnel construction and supporting decision-making and active risk management on tunnel projects

Thursday 17th February 2022, Online at:
<https://youtu.be/SKnHhpvn98Y>



FIRST SUMMER SCHOOL OF THE INTERNATIONAL ASSOCIATION
FOR ENGINEERING GEOLOGY AND THE ENVIRONMENT

Aosta Valley (ITALY) and Tyrol (AUSTRIA) 4 - 15 July 2022



Aosta Valley (ITALY) and Tyrol (AUSTRIA) 4 - 15 July 2022

The school is dedicated to Ph.D. students in Earth Sciences and Engineering Geology.

NO REGISTRATION FEE IS REQUIRED

The number of participants is limited Application deadline: March 30, 2022.

For more information: www.iaeg.info
sciaeg@irpi.cnr.it

[Click here](#) to see a list of lecturers.

[Click here](#) to see the schedule.

ΔΙΑΚΡΙΣΕΙΣ ΕΛΛΗΝΩΝ ΓΕΩΤΕΧΝΙΚΩΝ ΜΗΧΑΝΙΚΩΝ

Evangelia Ieronymaki, Ph.D., M.ASCE



Evangelia ("Eva") Ieronymaki is an associate professor of geotechnical engineering at Manhattan College NY, and a research affiliate at the Massachusetts Institute of Technology. She holds bachelor's and master's degrees in civil engineering from the National Technical University of Athens in Greece, and Master of Science and Ph.D. degrees in geotechnical and geoenvironmental engineering from MIT. She's a member of the G-I Underground Engineering and Construction technical committee as well as the Technical Chamber of Greece, and is a "Future Leader" of the American Rock Mechanics Association. Her research interests focus on numerical and mathematical modeling in tunneling, soil-structure interaction, and soil behavior. She's particularly interested in developing predictive algorithms for tunnel boring machines that connect TBM advancement rates to ground surface movements.

During her Ph.D. studies, Ieronymaki collaborated closely with the Crossrail Tunnel construction consortium, performing part of her research on the construction site in London, UK. She told us it was exciting to join the project meeting at 9 a.m. every morning and how she rapidly learned the importance of quick decisions and "mental agility," which she deems is a critical characteristic for engineers. She describes successful engineers as being able to "adapt fast to find that next step or next solution without sticking with what you've done in the past." Much of Ieronymaki's current TBM research relies on the challenging task of acquiring large data sets from tunneling projects. She credits her early industry experiences as an undergraduate and graduate student researcher for providing perspective and acquiring the relevant tools and opportunities to communicate effectively with industry.

Ieronymaki teaches civil engineering courses that mix traditional theory with experimental approaches to provide students with a firmer grasp of engineering by linking the classroom to practice. She tells us that "project-based problem-solving tied to classroom lectures helps link design methodology to procedure or practice." Part of her teaching approach involves bridging a knowledge gap between classical civil en-

gineering and computer science to create "technology opportunities for numerical modeling, automatic monitoring, UAVs, image processing, and fast data extraction and processing." Her emphasis on project-based problem-solving is influenced by her educational experiences in industry and her desire to bring classroom learning to the field. Outside of work, she enjoys tennis and reading, and is especially interested in the occasional "Whodunnit" mystery novel. We asked our interviewee to tell us a little more about herself below.

What are you currently working on that excites and challenges you the most?

I'm currently working on developing predictive algorithms for estimating a) the advancement rates of Earth Pressure Balance TBMs, and b) the ground surface settlements resulting from mechanized tunneling. This research requires the development of a database with information on various tunneling projects around the world. The goal is to develop models that will be able to predict the expected advancement rates of a TBM and the ground surface movements it will cause during tunnel construction, using information about the soil and the TBM operational parameters. The results of this research will be extremely valuable to the industry because they can significantly improve the construction scheduling of TBMs, and help mitigate the risk from large ground deformations and structural damage. This research is very challenging, as it requires acquiring lots of data from the different contractors of a tunneling project, who very often do not agree on disclosing information about their part of the project.

What was the topic of your most recent technical talk? How did the audience receive it?

My most recent technical talk was at the 2018 World Tunnel Congress in Dubai, where I gave an oral presentation on a preliminary algorithm to predict ground surface response to tunneling with TBMs. The subject attracted a large audience that showed great enthusiasm, but generated many questions on the approach I am following. The research is still ongoing, and it ties with the project I described previously.

If invited to a local chapter dinner or a regional conference as a speaker, what would be the topic of your talk?

I would talk about how we can numerically predict tunnel cavity deformations when tunneling with TBMs, given data on far-field surface and subsurface ground movement. This is a model I developed and validated using data from the Crossrail tunnels in London. An alternative topic I could also talk about is a numerical method I developed for estimating the building response given greenfield ground movements due to TBM tunneling.

New Faces is an effort by the G-I Outreach and Engagement Committee to make readers aware of members under 40 years of age who are available to deliver engaging technical presentations to G-I Chapters and other professional groups. You can nominate a candidate for a future New Faces column via email to ascegioec@gmail.com, along with a brief mention of your candidate's educational background, area(s) of expertise, and employment.

By Nasser Hamdan, Ph.D., M.ASCE, and Stacey Kulesza, Ph.D., P.E., M.ASCE, Outreach and Engagement Committee, [Geostrata - February/March 2022 - Evangelia Ieronymaki, Ph.D., M.ASCE \(readgeo.com\)](#)



Network Rail senior asset engineer Manos Tsoukalas

Building monitoring and asset knowledge to improve resilience on the rail network in the South East

Network Rail's Manos Tsoukalas and Senceive's Simon Brightwell explore the impact of extreme weather on assets and the need for a resilient monitoring strategy.



<https://www.youtube.com/watch?v=q4knqZ99J4w>

At the GE Instrumentation and Monitoring 2021 conference, Network Rail senior asset engineer Manos Tsoukalas and Senceive associate director Simon Brightwell look at:

- the impact of extreme weather on assets and the need for a resilient monitoring strategy
- how monitoring is already informing engineers and asset owners to prevent failures
- how to move towards a predict and prevent strategy as asset knowledge builds.

(GROUND ENGINEERING Editorial, 16 February, 2022, <https://www.geplus.co.uk/events/watch-building-monitoring-and-asset-knowledge-to-improve-resilience-on-the-rail-network-in-the-south-east-16-02-2022>)



LLInterview Coming back to Europe George Gazetas



George Gazetas is Emeritus Professor of Geotechnical Engineering at the National Technical University of Athens, following an academic career in the US, where he taught at SUNY-Buffalo, Rensselaer (RPI), and Case Western Reserve

University. His main research interests have focused on the dynamic response of footings, piles and caissons; the seismic response of earth dams and quay-walls; soil amplification of seismic waves; and soil-structure interaction.

Much of his research has been inspired by observations after destructive earthquakes. A prolific writer and active teacher, he has been a consultant in a variety of (mainly dynamic) geotechnical problems. Recipient of several awards for his research, he has delivered prestigious lectures including the "Coulomb" (2009), "Ishihara" (2013), Kenneth Lee (2019), and "Michele Maugeri" (2019) Lectures. He was honored as the 59th Rankine Lecturer in 2019, and has received the Excellence in University Teaching Award in Greece (2015).



<https://www.instagram.com/tv/CaFxDbmDf-f/>

ΠΡΟΣΕΧΕΙΣ ΓΕΩΤΕΧΝΙΚΕΣ ΕΚΔΗΛΩΣΕΙΣ

Για τις παλαιότερες καταχωρήσεις περισσότερες πληροφορίες μπορούν να αναζητηθούν στα προηγούμενα τεύχη του «περιοδικού» και στις παρατιθέμενες ιστοσελίδες.

The 60th Rankine Lecture, 16 March 2022, Imperial College London, United Kingdom, www.britishgeotech.org

6th International Symposium on Tunnels and Shafts in Soils and Rocks, 29-03-2022 ÷ 07-04-2022, Mexico City, Mexico, www.smig.org.mx

The Second Betancourt Conference "Non-Linear Soil-Structure Interaction Calculations", April 2022, mail@georec.spb.ru, ulitsky.vladimir@gmail.com, www.georec.spb.ru

16th International Benchmark Workshop on Numerical Analysis of Dams, 6-8 April 2022, Ljubljana, Slovenia, <https://icold-bw2022.fgg.uni-lj.si>

ICEGT-2020 2nd International Conference on Energy Geotechnics, 10-13 April 2022, La Jolla, California, USA, <https://icgt-2020.eng.ucsd.edu/home>

5ISEE 5th International Seminar on Earthworks in Europe 20-22.4.2022, Prague, Czech Republic, www.c-in.eu

RaSim 10 Rockbursts and Seismicity in Mines, 24 – 29 April 2022, Tucson, USA, www.rasimsymposium.com

The overall theme of the event will be the 'Roles of hydro in the global recovery' – meaning not only recovery from the pandemic and its economic consequences, but also hydro's role in reducing further degradation of our planet from fossil fuel-based generation.

Click [here](#) to see the latest preview of the programme.

If you have any questions about the technical programme, please contact us at: Hydro2022@hydropower-dams.com



SYDNEY 7iYGEC 2021 7th International Young Geotechnical Engineers Conference A Geotechnical Discovery Down Under, 29 April - 1 May 2022, Sydney, Australia, <http://icsmge2021.org/7iygec>

SYDNEY ICSMGE 2021 20th International Conference on Soil Mechanics and Geotechnical Engineering, 1-5 May 2022, Sydney, Australia, www.icsmge2021.org

LARMS 2021 – IX Latin American Rock Mechanics Symposium Challenges in rock mechanics: towards a sustainable development of infrastructure, 15 – 18 May 2022, Asuncion, Paraguay, <https://larms2021.com>

3rd International Conference on Geotechnical Engineering - Iraq 2022, 17 to 19 May 2022, University of Baghdad, Iraq, <https://ocs.uobaghdad.edu.iq/index.php/ICGEI/ticgei>

Transport Geotechnics 2022, 19 May 2022, London, United Kingdom, <https://transport.geplus.co.uk/getr/en/page/>

2022 ICOLD 27th Congress - 90th Annual Meeting 27 May - 3 June 2022, Marseille, France, <https://ciqb-icold2022.fr/en>



Roles of hydro in the global recovery
25-27 April 2022, Strasbourg, France
www.hydropower-dams.com/hydro-2022

We are pleased that all signs are positive to go ahead with an in-person HYDRO 2022 in Strasbourg in late April. France is open to the world, and already hosting international events. Members of the hydropower community are demonstrating their strong wish to get together, and we are ready with a comprehensive programme, to make up for the lost time.

4th International Conference "Challenges in Geotechnical Engineering" CGE-2022
1 to 3 June 2022, Kyiv, Ukraine
www.cgeconf.com

Organiser: Kyiv National University of Construction and Architecture (Ukraine) and University of Zielona Gora (Poland)

Contact person: Viktor Nosenko, Vasyl Pidlutskyi, Liudmyla Skochko

Address: 31, Povitroflotsky ave., KNUCA, Kyiv, 03037, Ukraine

Phone: +38(097)3811265

Fax: +38(097) 381-12-65

Website: <http://www.cgeconf.com>

Email: info@cgeconf.com



3rd European Conference on Earthquake Engineering and Seismology (3ECEES), 19-24 June 2022, Bucharest, Romania, <https://3ecees.ro>



Workshop on soil erosion for Europe – Emerging challenges 20-22 June 2022 (WEBEX - Online)

Moderator: Panos Panagos, European Commission Joint Research Centre

Rapporteur: Diana Vieira, European Commission Joint Research Centre

Scope: Exploring the role of soil erosion in relation to land degradation, climate change, food security

The EUSO Soil Erosion Working Group (WG) organizes a workshop split in the following sessions:

1. **Sediments** (including monitoring network). Chair: Nejc Bezak (Nejc.Bezak@fgg.uni-lj.si)
2. **Farm/Field scale modelling**. Chair: Marcella Biddoccu (marcella.biddoccu@stems.cnr.it)
3. **Erosion mitigation & management practices**. Chair: Artemi Cerda (artemio.cerda@uv.es)
4. **Soil organic carbon and erosion** integration. Chair: Negrel Philippe (p.negrel@brgm.fr)
5. **Food security, nutrient losses** with erosion. Chair: Christine Alewell (christine.alewell@unibas.ch)
6. **Large scale modelling**. Chair: Pasquale Borrelli (pasquale.borrelli@unipv.it)
7. **Early Career Research on Soil Erosion**. Chair: Daniel Evans (Daniel.L.Evans@cranfield.ac.uk)
8. **Landslides and soil erosion**. Chair: Nikolaos Tavoularis (ntavoularis@metal.ntua.gr)
9. **Climate change and soil erosion**. Chair: Joris Eekhout (jeekhout@cebas.csic.es)

Overall co-ordination: Diana Vieira (Diana.SIMOES-VIEIRA@ec.europa.eu)

Participation is **free and open** (registration details will follow)

The workshop will mainly discuss issues regarding the eight mentioned topics which are of interest for this WG on "Soil erosion in relation to land degradation, climate change, food security". The outputs of the workshop will be either proceedings or a journal Special issue, together with a policy brief.

The WG on Soil Erosion currently includes 52 members. The WG may be renewed/updated in October 2022. This WG is formed in on the basis of past meetings of soil erosion modellers at JRC Ispra (March 2017), Seoul (December 2017) and a Gully erosion workshop (March 2018). In addition, 67 scientists worldwide developed the first Global Applications of Soil Erosion Modelling Tracker (GASEMT).

The WG develops links between soil erosion and emerging issues such as climate change, food security and land degradation. The WG will propose modelling approaches that can respond to new developments in European policies: Post-2020 Common Agricultural Policy (CAP), New Soil Strategy for soils, Biodiversity Strategy, Farm to Fork and Zero Pollution Action Plan.



PRF 2022 Progressive Failure of Brittle Rocks, June 20-24th, 2022, Flatrock, NC, USA, www.prf2022.org

3rd International Symposium on Geotechnical Engineering for the Preservation of Monuments and Historic Sites, 22-24 June 2022, Napoli, Italy, <https://tc301-napoli.org>

CPT'22 5th International Symposium on Cone Penetration Testing, 26-29 June 2022, Bologna, Italy, <http://cpt22.org>

IS-Cambridge 2020 10th International Symposium on Geotechnical Aspects of Underground Construction in Soft Ground, 28 - 30 June 2022, Cambridge, United Kingdom, www.is-cambridge2020.eng.cam.ac.uk

5.ICNDSMGE – ZM 2020 5th International Conference on New Developments in Soil Mechanics and Geotechnical Engineering, June 30 to July 2, 2022, Nicosia, Cyprus, <https://zm2020.neu.edu.tr>

ICONHIC2022: THE STEP FORWARD - 3rd International Conference on Natural Hazards & Infrastructure, 5 – 7 July 2022, Athens, GREECE, <https://iconhic.com/2021>

RocDyn-4 4th International Conference on Rock Dynamics an ISRM Specialized Conference, 17-19 August 2022. Xuzhou, China, <http://rocdyn.org>

ISFOG 2020 4th International Symposium on Frontiers in Off-shore Geotechnics, 28 – 31 August 2022, Austin, United States, www.isfog2020.org

16th International Conference of the International Association for Computer Methods and Advances in Geomechanics – IACMAG 30-08-2022 – 02-09-2022, Torino, Italy, www.iacmag2022.org

WTC 2022 World Tunnel Congress 2022 - Underground solutions for a world in change, 2-8 September 2022, Copenhagen, Denmark, www.wtc2021.dk

11th International Symposium on Field Monitoring in Geomechanics, September 4 - September 7, 2022, London, UK, <https://isfmq2022.uk>

7th European Geosynthetics Conference, 4 to 7 September, 2022, Warsaw, Poland, <https://eurogeo7.org>

3rd European Conference on Earthquake Engineering & Seismology, September 4 – September 9, 2022, Bucharest, Romania, <https://3ecees.ro>

Eurock 2022 Rock and Fracture Mechanics in Rock Engineering and Mining, 12÷15 September 2022, Helsinki, Finland, www.ril.fi/en/events/eurock-2022.html

IAEG XIV Congress 2022, Chengdu, China September 14-20, 2022, <https://iaeg2022.org>

28th European Young Geotechnical Engineers Conference and Geogames, 15 – 17 – 19 September 2022, Moscow, Russia, <https://www.evqec28.com/>



International Workshop on Advances in Laboratory Testing of Liquefiable Soils
17 September 2022, Kyrenia, North Cyprus
<https://nce2022.ktimo.org>

Advances in laboratory testing techniques; Novel sensors for laboratory testing; Digital image and PIV analysis; Particle-scale experimental observation.

Advances in ground investigation and field monitoring; Geophysical methods; Advanced sampling and insitu testing.

Constitutive modelling of geomaterials; Cyclic and dynamic behaviour, Anisotropy and localization; Time dependent responses

Physical modelling; Thermal behavior

Organiser : TC101

Contact person: Satoshi Nishimura

Email: nishimura@eng.hokudai.ac.jp

Website : <https://nce2022.ktimo.org>



10th International Conference on Physical Modelling in Geotechnics (ICPMG 2022), September 19 to 23, 2022, KAIST, Daejeon, Korea, <https://icpmg2022.org>

11th International Conference on Stress Wave Theory and Design and Testing Methods for Deep Foundations, 20 - 23 September 2022, De Doelen, Rotterdam, The Netherlands, <https://www.kivi.nl/afdelingen/geotechniek/stress-wave-conference-2022>

10th Nordic Grouting Symposium, 4 - 6 October, 2022, Stockholm, Sweden, <https://www.ngs2022.se/>

IX Latin American Rock Mechanics Symposium - Challenges in rock mechanics: towards a sustainable development of infrastructure, an ISRM International Symposium, 16-19 October 2022, Asuncion, Paraguay, <http://larms2022.com>



5ΠΣΑΜΤΣ

ΑΘΗΝΑ 20-22 ΟΚΤΩΒΡΙΟΥ 2022

5ο Πανελλήνιο Συνέδριο Αντισεισμικής Μηχανικής και Τεχνικής Σεισμολογίας
20-22 Οκτωβρίου 2022, Αθήνα

Ανακοινώνεται η συνδιοργάνωση εκ μέρους του Ελληνικού Τμήματος Αντισεισμικής Μηχανικής και του Τεχνικού Επιμελητηρίου Ελλάδας του 5ου Πανελληνίου Συνεδρίου Αντισεισμικής Μηχανικής και Τεχνικής Σεισμολογίας (5ΠΣΑΜΤΣ), στην Αθήνα στις 20-22 Οκτωβρίου 2022. Αποτελεί τη συνέχεια της σειράς των σχετικών συνεδρίων με τελευταίο το 4ΠΣΑΜΤΣ που διοργανώθηκε στην Αθήνα το 2019 και θα πραγματοποιηθεί στους χώρους του Royal Olympic Hotel.



2022 GEOASIA7 - 7th Asian Regional Conference on International Geosynthetic Society, October 31 – November 4, 2022, Taipei, Taiwan, www.geoasia7.org

AUSROCK Conference 2022, 6th Australasian Ground Control in Mining Conference –an ISRM Regional Symposium, 29 November – 1 December 2022, Melbourne, Australia, www.ausimm.com/conferences-and-events/ausrock/

16th ICGE 2022 – 16th International Conference on eotechnical Engineering, Lahore, Pakistan, 8-9 December, 2022, <https://16icge.uet.edu.pk/>

4th African Regional Conference on Geosynthetic – Geosynthetic in Sustainable Infrastructures and Mega Projects, 20-23 February 2023, Cairo, Egypt, www.geoafrica2023.org



14 - 16 March 2023, Kuala Lumpur, Malaysia
www.hydropower-dams.com/asia-2023



88th ICOLD Annual Meeting & Symposium on Sustainable Development of Dams and River Basins, April 2023, New Delhi, India, <https://www.icold2020.org>



UNSAT2022
8th International Conference on Unsaturated Soils
2-5 May 2023, Milos island, Greece



World Tunnel Congress 2023
Expanding Underground Knowledge & Passion to Make a Positive Impact on the World
12 - 18 May 2023, Athens, Greece
<https://wtc2023.gr>

Rapid **urbanization**, natural **hazards**, **climate** change, sustainable **energy** geo-resources, people's mobility and transportation of goods are first-priority demanding challenges that the globe is facing.

Cities and infrastructure expansion towards underground provide safe, sustainable and **green solution** facilitating the transformation of millions of people's lives into a more **resilient** lifestyle. A comprehensive understanding, **rethinking and reshaping** of the underground spaces have become even more vital and crucial in the urban transformation of **future** cities. For the latter to be attained, planning and organization of **underground development**, a **holistic approach** is required not only in terms of spatial organization or overcoming engineering challenges, but also in regards to the establishments of policies, regulations and consideration of social factors.

WTC 2023 in Athens will highlight the multiple advantages and solutions that underground space could provide, at the prospect of a whole new era of **smart technology** where sophisticated **"digital tools"** change investigation, design, construction and operation methods and **strategies** rapidly. WTC 2023 will additionally provide an ideal opportunity to showcase recent innovations and the perspective of technology to further efficiently upgrade underground infrastruc-

ture assets, transforming the industry and the **societies** it serves.

Athens (Greece) has the knowledge, and we strongly believe we have the **means** and the **responsibility** to literally make a **positive impact** on the world.

Contact Info

Phone: (+30) 210 6833600
Fax: (+30) 210 6847700
E-mail: info@athenswtc2023.gr
Visit GTS: www.eesy.gr
E-mail: eesye.gr@gmail.com



NROCK2022

The IV Nordic Symposium on Rock Mechanics and Rock Engineering
24 – 25 May 2023, Reykjavic, Iceland
www.nrock2023.com

Address

Icelandic Geotechnical Society Engjateigur 9 105 Reykjavík ICELAND

Contact Person Name Thorbjorg Thrainsdottir
Email jardtaeknifelaqid@gmail.com



The 17th Danube - European Conference on Geotechnical Engineering
7-9 June, 2023, Bucharest, Romania
<https://sites.google.com/view/17decgero>



3rd JTC1 Workshop on "Impact of global changes on landslide risk", 7 – 10 June 2023, Oslo, Norway, <https://jtc1-2023.com>



9th International Congress on Environmental Geotechnics
Highlighting the role of Environmental Geotechnics in Addressing Global Grand Challenges
25-28 June 2023, Chania, Crete island, Greece
www.iceg2022.org

From global warming to devastating calamities from increasing natural disasters — there's no denying that we're facing the worst environmental crisis of all times.

Environmental geotechnics are more than ever in the spotlight of global research, paving the way towards a green, circular economy that promotes the use of sustainable technologies and management practices.

Our civilization is sustaining the worst Environmental Crisis of all times, and the numbers are ruthless: even with strong climate action, the aftermaths of climate change are unavoidable, and the frequency of immense natural catastrophes, such as wildfires, heatwaves, droughts and flash floods will keep increasing. Aggregating these disruptive events together, and focusing on the particular role, that the next generation of Geoenvironmental Engineers will play globally, we can identify seven grand challenges, which Environmental Geotechnics is uniquely positioned to tackle:

1. Urbanization and Aging Infrastructure
2. Energy Security
3. Resource Scarcity and Preservation
4. Climate Change and Natural Hazards
5. Protecting Public Health
6. The Next Frontier: Living in extreme environments
7. Education & Post-truth Society

The 9th International Congress on Environmental Geotechnics is part of the well established series of ICEG. This conference will be held on an outstanding resort in the town of Chania of the island of Crete in Greece. The theme of the conference is "Highlighting the role of Environmental Geotechnics in Addressing Global Grand Challenges" and will highlight the leadership role of Geoenvironmental Engineers play on tackling our society's grand challenges.

ICEG will reinforce the dialogue among geoenvironmental engineering professionals and researchers envisioning new methods, tools and infrastructure to address the global grand challenges.

CONFERENCE THEMES

Landfilling

Waste characterization and properties
Stability & deformation of waste
Geotechnical recycling and reuse of waste materials
Construction and demolition wastes
Dredged sediments
Other solid wastes

Contaminant Transport And Fate

Geoenvironmental Land Remediation

Degradation and attenuation
Emerging contaminants
Contaminated land and remediation technology
In-situ remediation
Off site remediation
New remediation technologies

Climate Change Impact & Mitigation

Greenhouse gas emissions and control
Geoenvironmental risk assessment
Sustainability
Risk-based site evaluation and management

Geo-Energy

Nuclear waste
CO₂ sequestration
Shallow and deep geothermal
Methane hydrates
Underground storage facilities

Resource Mining & Extraction

Coal combustion residues
Tailings and mine wastes
Tailing ponds
Acid mine drainage
Heap leach pads

Geosynthetics for the Geo-Environment

Biogeotechnics

Engineering Barriers

(covers, liners, vertical barriers, permeable barriers)

Forensic Environmental Geotechnics

Advances in Geoenvironmental Field Characterization

Advances in Laboratory Testing & Material Characterization

Advances in Numerical Modeling

Coupled Processes in Environmental Geotechnics & Geo-Energy

Human-Induced and Natural Disaster Mitigation

Case Histories in Environmental Geotechnics and the Geoenvironment

Education in Environmental Geotechnics

Contact Information

Innovation Center on Natural Hazards and Infrastructure
Kritis 12, 15235 Athens, GREECE
Tel. +30 210 6721798
email: secretary@iconhic.com



17th Asian Regional Geotechnical Engineering Conference

14-18 August 2023, Nur-Sultan, Kazakhstan
<https://17arc.org>

Topics

- Soil characteristics and properties
- Underground space and deep excavations
- Tunneling
- Slope, debris flow and embankments
- Dams
- Shallow and deep foundations
- Soil dynamics and geotechnical earthquake engineering
- Soil improvement

- Geoenvironmental engineering
- Geotechnical reliability, risk assessment and management
- Geosynthetics and Geoproducts
- Engineering geology and rock engineering
- Forensic engineering
- Offshore and harbor geotechnics
- Geotechnical training and education
- In- situ testing and monitoring
- GeoEnergy
- Case History
- Investigation of foundations of historical structures, buildings and monuments
- Numerical analysis of soil-structure interaction
- Geotechnical Infrastructures
- Marine Geotechnics
- Mining and Geotechnics
- Design and Modeling
- Transportation Geotechnics, Engineering and Technology
- Piling foundations, technologies and testing
- Press-in piling technology
- Trenchless technology in underground constructions
- Pipelines on problematical soil ground
- Frost geotechnics
- BIM technology and geotechnical engineering
- Megaprojects and Megastructures on difficulty soil grounds
- Others

Contact Us

Conference Secretariat info@17arc.org

Registration registration@17arc.org

Abstract Submission paper@17arc.org



8th International Symposium on Deformation Characteristics of Geomaterials

3rd - 6th September 2023, Porto, Portugal

www.fe.up.pt/is-porto2023

The Technical Committee on Laboratory Stress-Strain-Strength Testing of Geomaterials (TC101) of the International Society of Soil Mechanics and Geotechnical Engineering (ISSMGE), endorsed by the Portuguese Geotechnical Society (SPG) and the Faculty of Engineering of the University of Porto (FEUP), invite you to participate in IS-PORTO 2023: 8th International Symposium on Deformation Characteristics of Geomaterials to be held from the 3rd to the 6th September 2023 in Porto.

IS-Porto 2023 aims to continue the success of previous symposia: Hokkaido 1994, Torino 1999, Lyon 2003, Atlanta 2008, Seoul 2011, Buenos Aires 2015 and Glasgow 2019. This symposium will focus on the understanding of the deformation properties of geomaterials before failure, especially on the small-strain stiffness parameters as fundamental

characteristics of geomaterials, and their implications in geotechnical design.

The main objectives of this symposium are:

Research and development in advanced laboratory geotechnical testing, including apparatus, techniques, data acquisition and interpretation.

How to deal with laboratory test equipment, methods and results to represent in situ conditions

Application of multiple information from laboratory and field testing, including geophysical testing, to integrate site characterization and ground modelling.

Laboratory load controlled tests in geomaterials that can experience softening, associated to concepts such as 'instability', collapse and 'failure'.

Demonstration of practical engineering applications: reports of collaborative studies on laboratory and field testing, sampling, theoretical and numerical analysis, project engineering and full-scale observation.

Themes

I. Experimental investigations from very small strains to beyond failure

- Advances in laboratory testing techniques (equipment and procedures).
- Advances in field testing and monitoring techniques.
- Advanced sampling.
- Data interpretation and geotechnical imaging.
- Multiscale problems in geomechanics (micro-to-macro strains).

II. Behaviour, characterization and modelling of various geomaterials and interfaces

- Constitutive modelling of geomaterials.
- Physical and numerical modelling.
- Anisotropy and localisation.
- Time-dependent response.
- Cyclic and dynamic behaviour.
- Soil stabilisation and improvement.
- Soil-plant interaction.
- Thermal behaviour.
- Non-textbook soils:
 - intermediate soils (partially drained, etc).
- Sensitive and liquefiable soils:
 - tailings and other highly brittle strain-softening soils.
- Frozen soils.

III. Practical prediction and interpretation of ground response: field observation and case histories

- Integrated site characterization: derived values to be actually used in design.
- Performance evaluation of geotechnical structures: how to improve our understanding of our "affordable" test methods that typically measure something else (hopefully reasonably related).
- Field monitoring and observational method: new systems for measuring deformations in support of alert-to-alarm criteria.

All questions related to the conference should be addressed to the Conference Secretariat:

Mr. Manuel Carvalho
Tel.: [+351 220 413 703](tel:+351220413703)
e-mail: is-porto2023@fe.up.pt

or to the Conference Chairs:

IS-Porto 2023 Chairs
Prof. António Viana da Fonseca
Dr. Cristiana Ferreira
FEUP - DEC
Rua Dr. Roberto Frias, s/n
4200-465 Porto
Portugal
e-mail: viana@fe.up.pt | cristiana@fe.up.pt



www.osig2023.com

The SUT's Offshore Site Investigation and Geotechnics (OSIG) committee is pleased to announce that its 9th international conference, 'Innovative Geotechnologies for Energy Transition', will take place from 12-14 September 2023 in London.

OSIG is the longest standing international conference series of this type. It brings together the offshore Geotechnical, Geophysical & Geoscientific industry & academic communities to share the latest research, knowledge and experience. Building on the success of previous events, the programme will encompass a wide range of technical themes, aiming to attract hundreds of international delegates. Social and networking events are also being programmed, culminating in a dinner and evening event with an exciting guest speaker.

Conference Themes

1. New regions, geology and geotechnics
2. Advances in geoscientific data acquisition
3. Advances in geoscientific processing
4. Advances in geotechnical investigation
5. Advances in AI for offshore geotechnology
6. Underground carbon capture and storage
7. Seabed slopes and slides
8. Hydrates, shallow gas and seepage
9. Seismic hazards and tsunamis
10. Data integration and ground modelling
11. Learning from offshore incidents
12. Foundation research and design

13. Optimisation and performance-based design
14. Monopile design, installation and performance
15. Jacket pile design, installation and performance
16. Suction installed foundations
17. Gravity based foundations
18. Jack up foundations
19. Floating system anchoring and foundations
20. Cyclic and seismic loading of foundations
21. Scour assessment and monitoring
22. Pipeline and cable engineering
23. Seabed interaction of dynamic cables and risers
24. Environmental and anthropogenic impacts of engineering
25. Decommissioning and clean-up
26. Engineering for climate change
27. Near coastal geotechnical engineering
28. Seabed mineral extraction



SAHC 2023 13th International Conference on Structural Analysis of Historical Constructions "Heritage conservation across boundaries", 12-15 September 2023, Kyoto, Japan, <https://sahc2023.org/>

XII ICG - 12th International Conference on Geosynthetics, September 17 – 21, 2023, Rome, Italy, www.12icg-roma.org

2023 15th ISRM Congress, International Congress in Rock Mechanics Challenges in Rock Mechanics and Rock Engineering, 9÷14 October 2023, Salzburg, Austria, <https://www.isrm2023.info/en/>

6th World Landslide Forum "Landslides Science for sustainable development", 14 to 17 November 2023, Florence, Italy, <https://wlf6.org>



World Tunnel Congress 2024 Shenzhen, China

China is the official host of the ITA-AITES World Tunnel Congress 2024 and 50th General Assembly.

The General Assembly which took place on June 30th by video-conference, has confirmed the candidacy of Shenzhen to organise the WTC 2024.



**XVIII European Conference on Soil Mechanics
and Geotechnical Engineering
25-30 August 2024, Lisbon, Portugal**

Organiser: SPG

Contact person: SPG

Address: Av. BRASIL, 101

Email: spg@lnec.pt

Website: <http://www.spgeotecnia.pt>



Brazilian expressway collapses over metro tunnel

Part of a major expressway has collapsed above a construction site in the Brazilian city of Sao Paulo where Spain's Acciona was excavating a tunnel for a new subway line.

Television images showed a lane of the Marginal Tiete expressway caving into a widening pit alongside the construction site of the tunnel under a nearby river. The Sao Paulo state metro operator said on its website that tunnels dug for the new subway project had been flooded.

No casualties have been reported and public safety officials said all 50 workers were able to exit the tunnel. Two were treated for contact with dirty water that gushed through the site.

The cause of the collapse is not yet clear and conflicting information has been given.



In a press conference, Sao Paulo Governor Joao Doria said a sewage collector owned by water utility company Sabesp was hit but in the same conference Andre De Angelo, Acciona's country director in Brazil, said there was no collision between the excavator and the sewage network. "We are looking for the causes now. It probably has to do with the rains, with erosion. The tunnelling machine was 3m away from this collector, so there was no collision," he said.

State prosecutors have opened a civil investigation.

Acciona said in a statement it has taken all required contingency measures after the incident.

Line 6 was originally due for completion in 2012, but was delayed several times as funding dried up amid a deep recession in Brazil. It is now scheduled for completion in 2025.

The planned 15km line, one of the largest infrastructure projects under construction in Latin America, will connect the Brasilandia district of northern Sao Paulo to the city centre.

Acciona won the contract worth €2.3bn (US\$2.59bn) after the previous consortium left the project.

The disastrous 31 January 2022 mudflow in the La Gasca suburb of Quito, Ecuador

On 31 January 2022 heavy rainfall triggered a disastrous mudflow in the La Gasca suburb of Quito in Ecuador. [There is a detailed set of articles about this event on the El Comercio news website.](#) In an article posted yesterday [it records the losses as 24 known fatalities, a further 12 people missing and 48 people injured.](#) This is likely to be updated during the day today.

Extremely heavy, short duration rainfall (7.5 cm in one hour has been reported) was the trigger for the mudflow. The Google Earth image below shows the La Gasca suburb and the local topography:-



Google Earth image of the area affected by the 31 January 2022 mudflow in Quito, Ecuador.

The mudflow has clearly originated on the steep slopes and channels above the city. The elevation difference between the peak and La Gasca is over 1,000 m.

There is dramatic footage of the event as it occurred on Youtube, some of which makes uncomfortable viewing. The footage below gives an idea of the nature of the event:-



<https://www.youtube.com/watch?v=uMFDuyudnQ>

There is also drone footage of the aftermath:-



<https://www.youtube.com/watch?v=uRE2jpwR39I>

The image below gives an impression of the scale of the damage:-



The aftermath of the 31 January 2022 mudflow in La Gasca, Quito. Image by: [Carlos Noriega / El Comercio](#).

Interestingly, [this area appears to have been affected by a similar mudflow on 25 February 1975](#), when a mudflow originated from the Pambachupa ravine, affecting the La Mariscal neighbourhood, close to La Gasca. On that occasion two people were killed and a further five were injured.

Perhaps surprisingly, [the municipal authorities have ruled out deforestation as being a factor in this event](#).

(Dave Petley / THE LANDSLIDE BLOG, 2 February 2022, <https://blogs.agu.org/landslideblog/2022/02/02/la-gasca-1>)

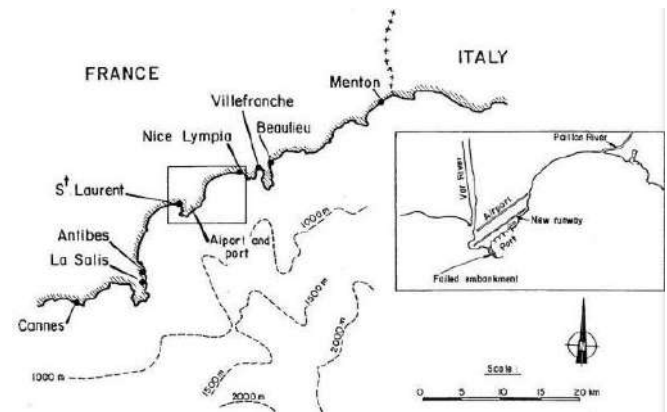


The 1979 Nice Airport landslide and tsunami

On 16 October 1979 a significant tsunami hit the coast of southern France close to Nice, between the border with Italy and the town of Antibes. In places the waves reached 3.5 m in height and travelled up to 150 m inland. Casualty figures are unclear, but estimates range between 8 and 23 fatalities.

At Nice airport, a section of fill slope failed during this event, killing seven people. This landslide involved between 2 and 3 million cubic metres of fill that was being replaced for the new port of Nice, but also involved about 7 million cubic metres of the underlying clay-silt, giving a total volume of 10

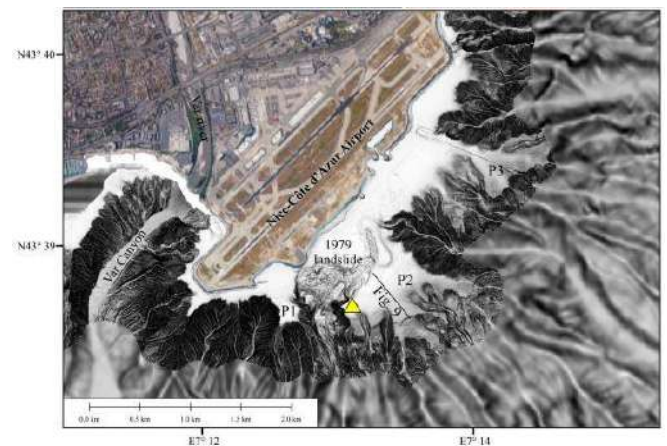
million cubic metres. The diagram below, from [Seed et al. \(1988\)](#) provides details of the location:-



The location of the 1979 Nice airport landslide. Note the section of coast that was affected by the tsunami, which extended from Antibes to the Italian border. Image from [Seed et al. \(1988\)](#).

In the hours following the disaster, two submarine cables were severed offshore from the French coast. One cable was cut after 3 hours and 45 minutes after the failure at Nice airport, and was located about 85 km from the site, whilst the other was cut 8 hours after the failure, 114 km from the slide area. These severed cables clearly indicated that there had been a massive [submarine landslide](#), which was linked to the tsunami. No seismic event had been recorded. Subsequently, a very large submarine landslide deposit has been mapped; this is estimated to have a volume of 150 million cubic metres.

In the aftermath of the disaster, two theories emerged as to the sequence of events. In one hypothesis, the landslide at Nice airport entered a submarine canyon located offshore, triggering the much larger submarine landslide. The canyon is visible in the image below:-



The sea floor topography offshore Nice airport. The location of the 1979 landslide is shown, as is the submarine canyon. Image from [Courboux et al. \(2020\)](#).

In the second hypothesis, the submarine landslide initiated naturally, triggering a tsunami. This in turn triggered the failure of the fill at Nice airport.

Intuitively, based on our current understanding of these events, the former hypothesis seems more credible to me. Interestingly, a review of the event a few years later ([Seed et al. 1988](#)) concluded that the most likely explanation was the second hypothesis, that the large scale submarine landslide occurred first.

However, more recent investigations have reversed that finding, determining with confidence that the first event was the failure at Nice airport ([Dan et al. 2007](#)). Critically, those responsible for the construction of the fill area had failed to appreciate the presence of a sensitive clay layer in the underlying sediments. In the days leading up to the disaster, heavy rainfall drove seepage of fresh water into the sediments, probably triggering failure in this weak layer, initiating the sequence of events.

Many lessons were learnt from this event. Perhaps most importantly, signs of distress were observed in the fill in the days prior to the collapse, including the development of cracks, settlement and embankment failures. Such warning signs should not be ignored.

References

Courboulex, F., Mercerat, E., Deschamps, A. et al. 2020. [Strong Site Effect Revealed by a New Broadband Seismometer on the Continental Shelf Offshore Nice Airport \(Southeastern France\)](#). *Pure and Applied Geophysics*, **177**, 3205–3224.

Dan, G., Sultan, N., Savoye, B. 2007. [The 1979 Nice harbour catastrophe revisited: trigger mechanism inferred from geotechnical measurements and numerical modelling](#). *Marine Geology* **245** (1-4), 40-64.

Seed, H., Seed, R., Schlosser, F. et al. 1988. [The landslide at the Port of Nice on October 16, 1979](#). College of Engineering, University of California.

(Dave Petley / THE LANDSLIDE BLOG, 4 February 2022, <https://blogs.agu.org/landslideblog/2022/02/04/nice-airport-1>)



Vajont Dam, a double-curved, thin-arch dam, at 262 meters high, from above

Site of the Vaiont Dam Disaster of 1963 in Italy: When this dam was completed in 1962, it was the highest dam in the world (262 m high). A landslide from Mt. Toc, above the lake and behind the dam, caused a megatsunami of water (250 m high and 50 million cubic meters) that went down the Piave River Valley and over the village of Longarone and killed between 1900-2500 people. It is a world famous site.



Photo was taken by Dr. Stratis Karantanellis, who is chair of our YEG and works at Aristotle University in Thessaloniki, Greece, while he was on a field trip with Professor Vassilis Martinos in 2018.

<https://www.multibriefs.com/briefs/IAEG/IAEG022322.php>



Tideway: Overcoming construction challenges at Victoria Embankment

Barhale regional manager Ovi Frunza highlights construction challenges at Victoria Embankment on the central section of the Thames Tideway Tunnel scheme.



<https://www.youtube.com/watch?v=LOGOh93N0NM>

At the GE Basements and Underground Structures 2021 conference, Barhale's Ovi Frunza discusses construction challenges at Victoria Embankment on Tideway's central section, including work on one of the first shafts to be completed on the project.

([geeditorial](#) / GROUND ENGINEERING, 16 February, 2022, <https://www.geplus.co.uk/events/watch-tideway-overcoming-construction-challenges-at-victoria-embankment-16-02-2022>)



Early theories why Wiltshire road buckled and cracked

Ground movement triggered by increased pore water pressure build-up is likely to have caused large cracks that have appeared in a Wiltshire road, according to a leading geotechnical specialist.

The B4069 road near Lyneham in Wiltshire has been closed since 17 February due to subsidence.

Geotechnical specialist Clive Edmonds told *NCE* that images of the damage - which show the road surface "heaved and then falling away in level" - suggest that "mass movement of the slope has been triggered probably by locally increased pore water pressure build-up in the slope profile leading to renewed landslide activity".



Large cracks have appeared in the B4069 road near Lyneham in Wiltshire



The road has been closed since 17 February

He added: "This sort of movement would account for the highly irregular switch-back look along the road alignment and cracking of the surface."

Edmonds explained that the road "coincides geologically with an area where the Jurassic age Stanford Formation (limestone) appears to overlie/overstep the Hazelbury Bryan Formation (sandstone)". Both of these are underlain by the Oxford Clay Formation.

"The road appears to run along and down the contact between the sandstone and limestone above the clay stratum going downhill away from Lyneham," he said.

"This kind of geological contact tends to be prone to past periglacial weathering effects like cambering and mass movement so is likely to have been affected in the geological past by downslope mass movement of the sandstone/limestone strata over the clay."

According to Edmonds, it will take "time and money" to safely re-instate the road.



The council is waiting a report from geotechnical specialists

"Remedial works will need to investigate and locate the slip surface at depth and design measures [will be necessary] to drain the slope to alleviate pore pressures in order to stabilise the movement noted before any re-build of the highway can be undertaken," he said.

The council has also said the issue could take up to a year to fix and cost millions of pounds, with cabinet member for transport Mark McClelland telling BBC Radio Wiltshire that the damage is "not something that can be resolved in a matter of days or weeks".



Remedial works have been undertaken on the road in the past

"It could cost hundreds of thousands or up into the millions [to fix]," he said. "There is significant damage to the road. It could be up to 12 months in total."

Wiltshire Council is currently awaiting a report from geotechnical specialists – and McClelland said it would wait until it receives this before deciding the next steps.

"The underlying ground has slipped and we need to understand why that has happened," he said. "This road has been subject to remedial works in the past and it has been a difficult road to deal with, but we've never seen anything like this before."

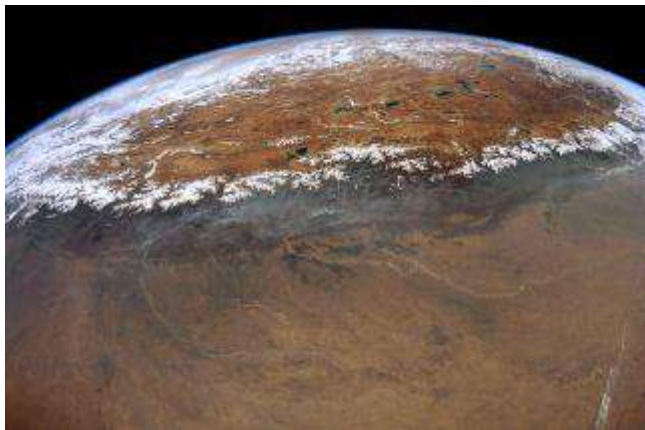
McClelland added that the road had "buckled" by around a metre in places.

(Catherine Kennedy / New Civil Engineer, 24 Feb, 2022, <https://www.newcivilengineer.com/latest/early-theories-why-wiltshire-road-buckled-and-cracked-24-02-2022>)

ΕΝΔΙΑΦΕΡΟΝΤΑ - ΓΕΩΛΟΓΙΑ

Scientists discover lost range of 'supermountains' three times longer than the Himalayas

The destruction of these ancient mountains may have fueled Earth's biggest evolution booms.



The ancient range of supermountains was up to three times longer than the Himalayas (seen here from space). (Image credit: Don Pettit/ NASA)

Twice in our planet's history, colossal mountain ranges that towered as tall as the Himalayas and stretched thousands of miles farther reared their craggy heads out of the Earth, splitting ancient supercontinents in two.

Geologists call them the "supermountains."

"There's nothing like these two supermountains today," Ziyi Zhu, a postdoctoral student at The Australian National University (ANU) in Canberra and lead author of a new study on the mountain majesties, [said in a statement](#). "It's not just their height — if you can imagine the 1,500 miles (2,400 km) long Himalayas repeated three or four times, you get an idea of the scale."

These prehistoric peaks were more than just an awesome sight; according to new research by Zhu and her colleagues published in the Feb. 15 issue of the journal *Earth and Planetary Science Letters*, the formation and destruction of these two gargantuan ranges may have also fueled two of the biggest evolutionary boom times in our planet's history — the first appearance of complex cells roughly 2 billion years ago, and the Cambrian explosion of marine life 541 million years ago.

It's likely that, as these enormous mountain ranges eroded, they dumped huge amounts of nutrients into the sea, speeding up energy production and supercharging evolution, the researchers wrote.

Rise of the giants

Mountains rise when Earth's ever-shifting tectonic plates smash two landmasses together, pushing surface rocks to soaring heights. Mountains can grow for hundreds of millions of years or more — but even the loftiest ranges are born with an expiration date, as erosion from wind, water and other forces immediately starts to whittle those peaks away.



The supercontinent Gondwana (shown in this concept image) included what are today South America, Africa, Australia, Antarctica, the Indian subcontinent and the Arabian Peninsula. (Image credit: MARK GARLICK/SCIENCE PHOTO LIBRARY via Getty Images)

Scientists can piece together the history of Earth's mountains by studying the minerals that those peaks leave behind in the planet's crust. Zircon crystals, for example, form under high pressure deep below heavy mountain ranges, and can survive in rocks long after their parent mountains vanish. The precise elemental composition of each zircon grain can reveal the conditions in the crust when and where those crystals formed.

In their new study, the researchers examined zircons with low amounts of lutetium — a rare Earth element that only forms at the base of high mountains. The data revealed two "spikes" of extensive supermountain formation in Earth's history — one lasting from about 2 billion to 1.8 billion years ago, and the second lasting from 650 million to 500 million years ago.

Prior studies had hinted at the existence of that second epic range — known as the Transgondwanan Supermountain, because it crossed the vast supercontinent of Gondwana (a single giant continent that contained the landmasses of modern Africa, South America, Australia, Antarctica, Indian and the Arabian Peninsula). However, the earlier supermountain — called Nuna Supermountain, after an earlier supercontinent — had never been detected before now.

The distribution of zircon crystals showed that both of these ancient supermountains were enormous — likely spanning more than 5,000 miles (8,000 kilometers) long, or about twice the distance from Florida to California.

That's a lot of rock to erode — and, according to the researchers, that's why these enormous mountains are so important.

Evolution in overdrive

As both mountains eroded away, they would have dumped tremendous amounts of nutrients like iron and phosphorus into the sea through the water cycle, the researchers said. These nutrients could have significantly sped up biological cycles in the ocean, driving evolution to greater complexity. In addition to this nutrient spillover, the eroding mountains may have also released oxygen into the atmosphere, making Earth even more hospitable to complex life.

The formation of the Nuna Supermountain, for example, coincides with the appearance of Earth's very first eukaryotic cells — cells containing a nucleus that eventually evolved into plants, animals and fungi. Meanwhile, the Transgondwanan Supermountain would have been eroding just as another evolutionary boom unfolded in Earth's seas.

"The Transgondwanan Supermountain coincides with the appearance of the first large animals 575 million years ago and the Cambrian explosion 45 million years later, when most animal groups appeared in the fossil record," Zhu said.

In their research, the team also confirmed previous studies that found mountain formation screeched to a halt on Earth from about 1.7 billion to 750 million years ago. Geologists refer to this period as the "boring billion," because life in Earth's seas seemingly stopped evolving (or at least evolved achingly slowly), [Live Science previously reported](#). Some scientists hypothesize that the lack of new mountain formation may have prevented new nutrients from leaking into the oceans during this time, effectively starving sea creatures and stalling their evolution.

While more research is needed to draw an airtight connection between supermountains and supercharged evolution on Earth, this study seems to confirm that our planet's most productive biological booms occurred in the shadows of some truly colossal mountains.

(Brandon Specktor / LIVE SCIENCE, 04.02.2022, <https://www.livescience.com/supermountains-drove-evolution-on-earth>)



Mysterious new substance possibly discovered inside Earth's core

The planet's core could be a mushy mix of solid and liquid.



Earth's core is weirder than first thought. (Image credit: Shutterstock)

Earth's inner core may be filled with a weird substance that is neither solid nor liquid, according to a new study.

For more than half a century, scientists believed that [Earth's](#) deepest recesses consist of a molten outer core surrounding a densely compressed ball of solid [iron](#) alloy. But new research, published Feb. 9 in the journal [Nature](#) (Superionic iron alloys and their seismic velocities in Earth's inner core, <https://www.nature.com/articles/s41586-021-04361-x.epdf>) offers a rare insight into the inner structure of the planet — and it's far weirder than previously thought.

New computer simulations suggest that Earth's hot and highly pressurized inner core could exist in a "superionic

state" — a whirling mix of [hydrogen](#), [oxygen](#) and [carbon](#) molecules, continuously sloshing through a grid-like lattice of iron.

"We find that hydrogen, oxygen and carbon in hexagonal close-packed iron transform to a superionic state under the inner core conditions, showing high diffusion coefficients like a liquid," the researchers wrote in their paper. "This suggests that the inner core can be in a superionic state rather than a normal solid state."

The planet's core is subject to bone-crushing pressures and scorching [temperatures](#) as hot as the surface of the sun, and its contents have long been a subject of speculation among scientists and science fiction authors alike. Since the 1950s, advances in the study of [earthquake](#)-generated seismic waves — which travel through the core — have enabled researchers to make more refined guesses as to what's inside the heart of the planet, but even today the picture is far from clear.

A [2021 study](#) of how a type of seismic wave called a shear (or "s") wave moved through our planet's interior revealed that Earth's inner core isn't solid iron, as was once believed, but is instead composed of various states of a "mushy" material, [Live Science previously reported](#), consisting of an iron alloy of iron atoms and lighter elements, such as oxygen or carbon.

But scientists weren't sure what this mush consisted of. Accessing the core by probe is impossible, so for the new study, the researchers turned instead to a simulation — compiling seismic data and feeding it into an advanced computer program designed to recreate the effects of the core's extreme pressures and temperatures on an assortment of likely core elements: such as iron, hydrogen, oxygen and carbon. In a regular solid, [atoms](#) arrange themselves into repeating grids, but the core simulations suggest instead that in Earth's core, atoms would be transformed into a superionic alloy — a framework of iron atoms around which the other elements, driven by powerful convection currents, are able to freely swim.

"It is quite abnormal," study first author Yu He, a geophysicist at the Chinese Academy of Sciences, [said in a statement](#). "The solidification of iron at the inner core boundary does not change the mobility of these light elements, and the convection of light elements is continuous in the inner core,"

If the simulation lines up with reality, the constant swilling of the mushy superionic materials could help to explain why the inner core's structure seems to change so much over time, and even how the powerful convection currents responsible for creating [Earth's magnetic field](#) are generated. But first, the model will have to be proven.

"We will have to wait until the experimental setting becomes ripe to replicate the inner core conditions and scrutinise the proposed models. We will then see which of the models are physical," Hrvoje Tkalčić, the head of seismology and mathematical geophysics at the Australian National University in Canberra who was not involved in the study, told Live Science in an email. "In the meantime, global seismology is making progress, with more seismological probes becoming rapidly available, and we hope to constrain some of the key parameters determining geophysical models of the inner core in this coming decade."

(Ben Turner / LIVESCIENCE, 23.02.2022, <https://www.livescience.com/earth-core-superionic>)

ΕΝΔΙΑΦΕΡΟΝΤΑ - ΠΕΡΙΒΑΛΛΟΝ

For Water Storage, small is not beautiful! This is an important research result from Ecological Society of America showing that the environmental impact of large dams is much less important than the impact of smaller storages like ponds.

Small artificial impoundments have big implications for hydrology and freshwater biodiversity

Robert Morden, Avril Horne, Nick R Bond, Rory Nathan, Julian D Olden

Abstract

Headwater streams are critical for freshwater ecosystems. Global and continental studies consistently show major dams as dominant sources of hydrological stress threatening biodiversity in the world's major rivers, but cumulative impacts from small artificial impoundments (SAIs) concentrated in headwater streams have rarely been acknowledged. Using the Murray Darling River basin (Australia) and the Arkansas River basin (US) as case studies, we examined the hydrological impacts of SAIs. The extent of their influence is considerable, altering hydrology in 280–380% more waterways as compared to major dams. Hydrological impacts are concentrated in smaller streams (catchment area <100 km²), raising concerns that the often diverse and highly endemic biota found in these systems may be under threat. Adjusting existing biodiversity planning and management approaches to address the cumulative effects of many small and widely distributed artificial impoundments presents a rapidly emerging challenge for ecologically sustainable water management.

In healthy river systems, headwater streams play a paramount role in maintaining hydrologic connectivity, harboring biodiversity, and supporting ecosystem integrity (Colvin *et al.* 2019). Despite this, debates continue over the implementation of policies and regulations seeking to protect these waters from burgeoning human enterprise. In one high-profile example, a 2015 update of the "Waters of the United States" (WOTUS) rule would have qualified both perennial and smaller non-perennial waterways in the US for water-quality protections (Marshall *et al.* 2018), but implementation of this update was halted in 2019 and further scaling back of the WOTUS definition was signed in 2020. Such regulatory actions in the US and elsewhere contrast with the large and growing body of scientific research supporting the social and ecological value of headwater streams (Meyer *et al.* 2003; Clarke *et al.* 2008; Colvin *et al.* 2019), as well as with the mounting threats to these ecosystems posed by climate change and regulating infrastructure, among other factors.

Past and planned construction of smaller scale dams is unprecedented. Recent estimates report that small- to medium-sized in-channel dams (approximately 82,891) vastly outnumber large dams around the world, and that hundreds of thousands of additional small hydropower plants may be installed to meet future energy demands (Couto and Olden 2018). Indeed, many more dams are likely to be built in coming decades due to increasing global demand for hydropower, reliable water supply, and food security (Zarfl *et al.* 2014). The widespread ecological damage and loss of important goods and services caused by large dams is well recognized (Sabater *et al.* 2018; Poff 2019; Tickner *et al.* 2020). One

recent study concluded that close to two-thirds (63%) of major global waterways have greatly reduced connectivity due primarily to large in-channel dams and to a lesser extent by a range of other anthropogenic factors (such as urbanization and floodplain structures), while the remaining one-third (37%) are considered "free flowing" (Grill *et al.* 2019).

A conspicuous omission from global assessments of river regulation by dams (eg Nilsson *et al.* 2005; Zarfl *et al.* 2014; Grill *et al.* 2019) is that headwater streams – while not directly impacted by large in-stream dams – remain at risk from the impacts of smaller dams and artificial ponds within the catchment. These smaller, diffuse sources of hydrologic interception – referred to here as small artificial impoundments (SAIs) but also often called "farm ponds", "farm dams", or "small storages" (Panel 1; Figure 1) – have received far less recognition. Awareness of the impact of smaller dams and waterbodies on hydrology and biodiversity has emerged in recent years, including the cumulative effects of dams built to support hydropower production (Walter and Merritts 2008; Couto and Olden 2018; Couto *et al.* 2021) and agriculture practices (Downing 2008; Nathan and Lowe 2012).

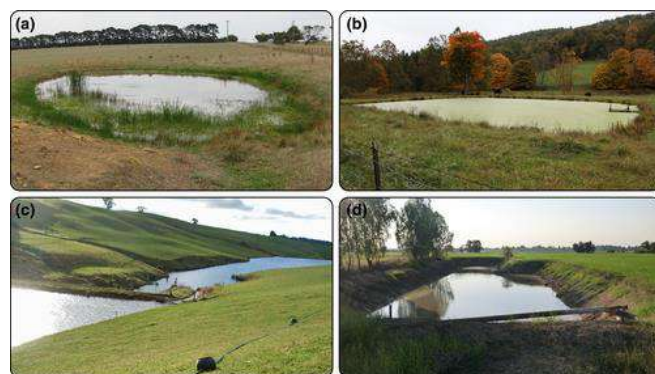


Figure 1 Examples of small artificial impoundments around the world: (a) Victoria, Australia; (b) Virginia, US; (c) Tasmania, Australia; (d) Kamphaeng Phet, Thailand.

Image credits: (a) L Lowe, (b) Chesapeake Bay Program/Flickr.com (CC BY 2.0), (c) C Wiesenfeld, (d) F Molle/Flickr.com (CC BY 2.0)

Panel 1. What are small artificial impoundments (SAIs)?

The wide range of different terms for small waterbodies is a common source of confusion (Biggs *et al.* 2017). Small *natural* impoundments are usually called "ponds" or "lakes", whereas small *artificial* impoundments are called "farm ponds", "farm storages", "small storages", "tanks", "stock ponds", or "mill ponds", and are usually constructed with a low earthen bank across a watercourse or landscape depression.

Local differences may also exist. In Australia, small *artificial* impoundments are typically called "farm dams" (Nathan and Lowe 2012), but other terms, such as "floodplain storage", "catchment dam", or "runoff dam", are sometimes used to help identify the primary source of the water. In Europe, the term "small waterbodies" appears to be a more common label when referring to a wide range of features like storages, mill ponds, and ditches (Biggs *et al.* 2017).

In this paper, we adopted the term "small artificial impoundments" (SAIs) because it apparently is the most precise and least ambiguous term. SAIs included in our analysis ranged over 400-fold in size, from as little as 250 m² to more than 100,000 m². In our case study, SAIs are typically constructed for agricultural and livestock purposes, with a smaller num-

ber managed for hydropower, recreation, aquaculture, or potable supply. Some examples of SAIs from around the world highlighting their diversity of size and construction techniques are shown in Figure 1.

The scope of SAI-related impacts is challenging to characterize at continental or global scales due to a lack of information about their number and locations in many regions (Januchowski-Hartley *et al.* 2020). Consequently, they are often excluded from investigations into how flow alteration affects freshwater ecosystems, with research and policy attention instead focusing on large in-channel structures and major water extractions. In so doing, such studies make an implicit assumption that the primary ecological impacts arise from the largest individual extractions or impoundments, rather than considering the totality of hydrological stresses in operation, including those associated with the cumulative effects of SAIs.

We examined the relative role of SAIs and larger in-stream dams in causing hydrological stress throughout a catchment, and the challenges associated with the management, and supporting policy, of SAIs into the future. Impoundments of all types can affect upstream and downstream biodiversity through multiple pathways, for instance by altering habitat conditions (Agoramoorthy *et al.* 2016; Biggs *et al.* 2017), water quality (Ibrahim and Amir-Faryar 2018), and waterway connectivity (Barbarossa *et al.* 2020). Here, we focused on the threat to downstream biodiversity using a hydrological measure of the degree of impoundment. Two specific examples, one in Australia and the other in the US, were used to demonstrate how the risk to global biodiversity from hydrological alteration, particularly in headwater streams, continues to be underestimated through disregard of the widespread, growing number and cumulative impact of SAIs.

Magnitude of hydrological stress

Global assessments of the impacts of in-stream dams have reported the “degree of regulation” (DoR), defined by the ratio of the total capacity of upstream storages with the average annual flow at a given location in the river network (Nilsson *et al.* 2005; Grill *et al.* 2019). DoR is a useful surrogate measure of the potential threat to biodiversity, with dam-induced flow changes shown to act synergistically with other impacts from dam modification (eg sediment flux, geomorphic alteration, floodplain disconnection, river corridor fragmentation; Poff *et al.* 2007; Grill *et al.* 2014). Although it is a simple metric and does not describe individual components of the flow regime, DoR provides a consistent quantitative measure of the *potential* for hydrological stress that can be readily mapped (Lehner *et al.* 2011; Grill *et al.* 2014).

To understand the role of SAIs in contributing to hydrological stress throughout a catchment, the DoR concept was applied to two case studies, the Murray Darling River basin in Australia and the Arkansas River basin in the US. These basins were selected as exemplars of the longstanding challenges facing global rivers subjected to SAIs. The Murray Darling basin is the largest river basin in Australia, covering more than 1 million km², supplying drinking water to more than 3 million people, and generating roughly 40% of Australia’s total agricultural production. The Arkansas River basin, the second longest tributary of the Mississippi River, encompasses close to 0.5 million km², and supports substantial irrigated agricultural production.

The DoR was calculated for all reaches – defined as the segments between tributaries – in the river network for both case study basins, in the first instance considering only major in-stream dams, and then accounting for the presence of SAIs. To date, a threshold DoR value to identify impacted rivers has not been estimated with any confidence; however, a DoR value of 16.7% (Grill *et al.* 2019) has been adopted as

a plausible threshold that facilitates comparisons with previous studies (see WebPanel 1 for more details).

Differences in DoR estimates are striking. In the Murray Darling River basin, when considering only major in-stream storages (Figure 2a, top), around 10% of reaches by length were flow impacted (Figure 2b, top). However, when SAIs are included, the proportion of impacted streams in the basin almost quadruples to 37%, with impacted streams represented across almost the entire basin. SAIs represent just 7% of total storage capacity, yet their influence increases the relative length of impacted waterways by 380% compared to the extent of impacts from large storages. Similarly, in the Arkansas River basin, 3.5% of reaches by length are impacted by major in-stream dams (Figure 2a, bottom), but when SAIs are included this proportion nearly triples to 9.7% (Figure 2b, bottom). In this basin SAIs represent a mere 0.03% of total storage capacity, yet they increase the relative length of impacted waterways by 280%. These differences are essentially practical in their origin: large dams are constructed on higher order streams to maximize yield, whereas SAIs are typically distributed across the landscape wherever landholders can and choose to build them.

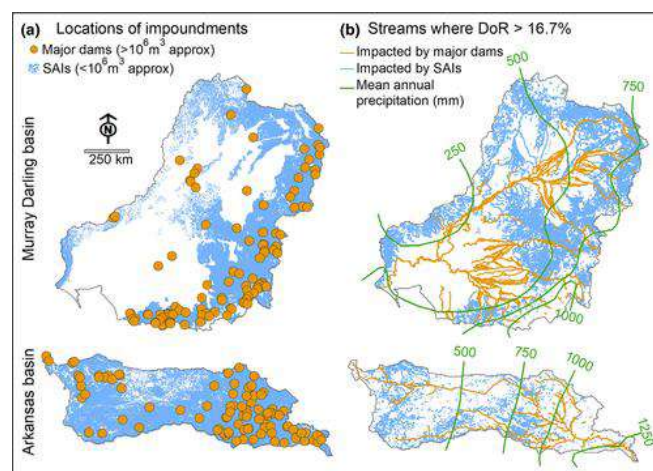


Figure 2 Impoundments and the downstream waterways in which they cause hydrologic stress. (a) Locations of major in-stream dams and small artificial impoundments (SAIs) in the Murray Darling River basin and Arkansas River basin. (b) Streams with a degree of regulation (DoR) greater than 16.7% in the Murray Darling River basin and Arkansas River basin. Precipitation data from WorldClim (Hijmans *et al.* 2005).

Climate is an important driver of our results. Areas with mean annual rainfall greater than ~1000 mm have sufficiently high rates of runoff that the DoR rarely exceeds 16.7% even with high levels of SAI development. Conversely, areas with less than ~400 mm have such low runoff that even the presence of a small number of SAIs could result in high DoR estimates. However, these areas tend to have relatively low levels of SAI development, most likely because a combination of low runoff and high evaporation make open water impoundments impractical for most agricultural purposes.

A separate hydrological analysis revealed that the effects of SAIs on downstream flow regimes are broadly similar to the effects of large dams. Using one site in southeastern Australia as an example, the effect on downstream flow regime of a hypothetical large dam was compared to a large number of SAIs with the same aggregate capacity and aggregate upstream catchment area (Figure 3). The overall percentage reduction in annual flow was somewhat higher for SAIs than for a single large storage, but the net effect on flow exceedance and numbers of low flow days were very similar. Four additional sites modeled in the same way showed comparable

results (see WebPanel 1 for modeling methods and results for other sites). In effect, if a large dam is considered a source of flow regulation, then SAIs must be viewed as a form of “distributed flow regulation”.

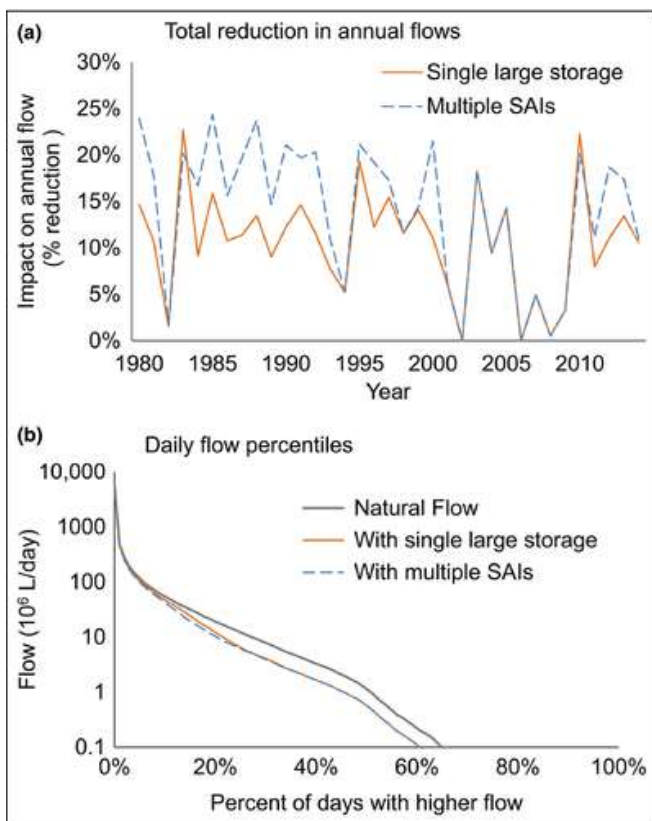


Figure 3 Comparison of impacts of a single large dam and multiple small dams, including impacts on (a) total annual flows from 1980 to 2014 and (b) daily flow percentiles. Note that in (b) the solid orange line is mostly hidden by the dashed blue line. In each scenario, streamflow from a single gauge location (above shows Mt Ida Creek, Australia, gauge 406226, catchment area 174 km²) was used as a hypothetical “natural” flow, to which the hydrological impact of impoundments was applied. The single large dam was set to a capacity of 20% of mean annual flow (DoR = 20%) with an upstream watershed area 50% of the gauged catchment. The multiple small dams were set to capacities of 2500 m³ each, with the same aggregate capacity and watershed area as the single large dam.

Spatial comparison of impacted streams with biodiversity

SAIs in both the Murray Darling River and Arkansas River basins primarily affected smaller streams and headwater streams. In some instances these streams may have higher conservation priority because they support greater numbers of threatened species than waterways affected by large dams alone. This is particularly important, as lower order streams typically compose the majority of waterways in a basin (Colvin *et al.* 2019), and widespread threats to freshwater biodiversity globally (Tickner *et al.* 2020) highlight the need to protect and restore these types of waterways.

Using the International Union for Conservation of Nature (IUCN) Red List of Threatened Species (www.iucnredlist.org) as a key measure of biodiversity, we compared numbers of threatened species across waterways of different sizes (Figure 4; see WebPanel 1 for analysis details). In both basins, almost all waterways impacted by major dams have an upstream catchment area greater than 1000 km². In contrast,

approximately half of streams impacted by SAIs have an upstream catchment area less than 100 km². For the Murray Darling River basin, the proportion of SAI-affected waterways with high numbers of threatened species is much greater for smaller (<100 km²) than larger (>10,000 km²) waterways (32% and 7% of waterways, respectively). For the Arkansas River basin, the trend is reversed (21% and 50% of waterways, respectively) due to lower order streams tending to occur in the upper catchment where there is lower rainfall (and therefore lower species counts); the inverse situation occurs in the Murray Darling basin. This underscores the need to consider how local climate and topography could lead to SAI-affected waterways having either higher or lower conservation priority.

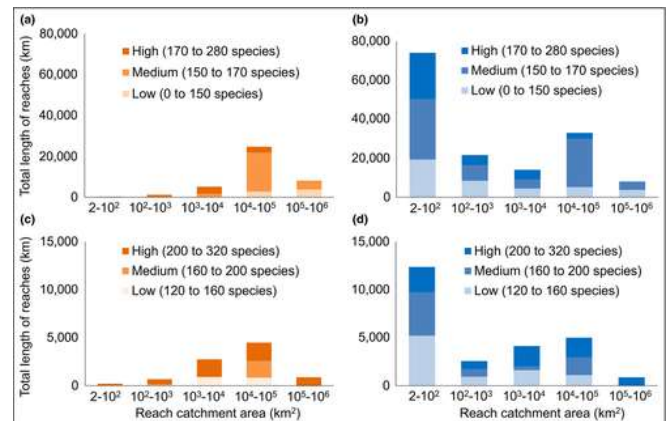


Figure 4 Total numbers of threatened freshwater species (International Union for Conservation of Nature Red List) in waterways affected (DoR > 16.7%) by large dams or large dams plus SAIs, aggregated by upstream catchment area and reach length. (a) Murray Darling River basin with large dams only; (b) Murray Darling River basin with large dams plus SAIs; (c) Arkansas River basin with large dams only; and (d) Arkansas River basin with large dams plus SAIs.

Management challenges

Efforts to restore biodiversity both upstream and downstream of large dams are ongoing worldwide. While these efforts are necessary to address the substantial environmental impacts arising downstream from such structures (Tickner *et al.* 2020), our analysis suggests that river reaches downstream of large dams may potentially represent only a small fraction of all river reaches experiencing hydrologic stress. Catchment and waterway management agencies are already overstretched, and addressing the needs of the additional waterways impacted by SAIs is undoubtedly a major task.

Challenges to current policy

While the impetus for controlling SAIs to minimize risks to biodiversity may be apparent in some areas, there may also be a complex policy mosaic and considerable local resistance. Historically, in most parts of the world, SAIs could be built with little regulation or consideration of potential environmental impacts, although some jurisdictions have in recent years introduced controls on the construction of new SAIs (Morris *et al.* 2019). Consequently, there is a tendency for many SAI owners to consider them a “right”, and therefore any attempt to regulate or limit future development can be controversial (Horne *et al.* 2017). The large number of individual SAIs requires consultation and engagement with an equally large number of individual owners. In addition, because SAIs serve a variety of purposes (Nathan and Lowe 2012), they become entwined in a range of policy areas, including agricultural water supply (Wisser *et al.* 2010), essential domestic water supply, sediment control (Ibrahim and Amir-Faryar 2018), fire management, and provision of critical

habitat and refuges (Agoramoorthy *et al.* [2016](#); Biggs *et al.* [2017](#)).

The dangers of cumulative impacts

When many individual landowners construct new SAIs, their individual impacts may be negligible but their cumulative impacts can give rise to “the tyranny of small decisions” (Kahn [1966](#)). Crucially, we have demonstrated that the storage capacity of an impoundment is not a good indicator of its potential impact, and therefore a key challenge is to ensure that the cumulative impact of existing and future SAIs is considered alongside larger dams (Couto and Olden [2018](#); Couto *et al.* [2021](#)), other current threats (such as extractions), and additional foreseeable future threats (such as climate change and land-use change).

Incomplete understanding of the problem

Knowledge of the impacts of SAIs requires, at a minimum, spatial data identifying waterbodies as small as ~200 m². This information does not exist for much of the world (McManamay *et al.* [2018](#)), although there are some exceptions, such as the US and several states in Australia. One of the highest resolution global datasets is HydroLAKES (Messenger *et al.* [2016](#)), which shows 1.42 million waterbodies; even this is insufficient, however, as the smallest identified features are around 10 ha in size, approximately the upper limit of SAIs. The scale of data processing required to capture large numbers of very small features from remote-sensing data makes generating new datasets a complex and expensive task.

Insufficient modeling tools to account for impact and assess management actions

A further issue is the difficulty in demonstrating the benefits of any remedial actions over long implementation periods (Thompson *et al.* [2018](#)). Although there exists a range of modeling tools for SAIs (Habets *et al.* [2018](#)), adaptation of these tools will be required to track the impacts and benefits of any planned management intervention. There has been some success in this regard in Australia; for example, the Murray Darling Basin Plan (Australian Government [2012](#)) includes SAIs in its annual accounting processes alongside major dams as part of the overall consumptive pool. Considerable work has been undertaken to develop new water accounting and modeling approaches to make this possible (Srikanthan *et al.* [2015](#); Morden [2017](#)).

Moving forward

Many global and continental studies overlook the impacts of SAIs, making an implicit assumption that the biggest ecological impacts arise from the biggest extractions or impoundments. Here, we have highlighted the dangers of this assumption by demonstrating that while SAIs have relatively small capacity individually, their abundance and widespread distribution can result in substantial cumulative impacts. To exclude SAIs from assessments is to underestimate the risk posed to biodiversity in smaller and headwater streams that are paramount to freshwater integrity in healthy river systems (Colvin *et al.* [2019](#)). In the future, substantial investment in the development of new information systems that catalog SAIs and implementation of environmental and hydrological monitoring is needed. Only with these data can SAIs be considered alongside other forms of anthropogenic extractions and held accountable for the hydrological impacts they generate.

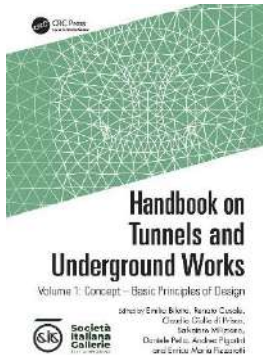
Acknowledgements

RM was funded by an Australian Government Research Training Program Scholarship and an Australian Research Council

Discovery Early Career Researcher Award (ARC DECRA) award (DE180100550). AH was funded through an ARC DECRA award (DE180100550). We thank L Lowe and C Wiesenfeld for contributing photos.

<https://esajournals.onlinelibrary.wiley.com/doi/full/10.1002/fee.2454>

ΝΕΕΣ ΕΚΔΟΣΕΙΣ ΣΤΙΣ ΓΕΩΤΕΧΝΙΚΕΣ ΕΠΙΣΤΗΜΕΣ



Handbook on Tunnels and Underground Works: Volume 1 Concept - Basic Principles of Design

**Emilio Bilotta, Renato Casale,
Claudio Giulio di Prisco,
Salvatore Miliziano, Daniele
Peila, Andrea Pigorini, Enrico
Maria Pizzarotti, Editors**

The book provides a new, global, updated, thorough, clear and practical risk-based approach to tunnelling design and construction methods, and discusses detailed examples of solutions applied to relevant case histories. It is organized in three sequential and integrated volumes:

- Volume 1: Concept – Basic Principles of Design
- Volume 2: Construction – Methods, Equipment, Tools and Materials
- Volume 3: Case Histories and Best Practices

The book covers all aspects of tunnelling, giving useful and practical information about design (Volume 1), construction (Volume 2) and best practices (Volume 3). It provides the following features and benefits:

- updated vision on tunnelling design, tools, materials and construction
- balanced mix of theory, technology and applied experience
- different and harmonized points of view from academics, professionals and contractors
- easy consultation in the form of a handbook
- risk-oriented approach to tunnelling problems.

The tunnelling industry is amazingly widespread and increasingly important all over the world, particularly in developing countries. The possible audience of the book are engineers, geologists, designers, constructors, providers, contractors, public and private customers, and, in general, technicians involved in the tunnelling and underground works industry. It is also a suitable source of information for industry professionals, senior undergraduate and graduate students, researchers and academics.

(CRC Press, 23 February 2022)



www.issmge.org/publications/issmge-bulletin/vol16-issue-1-february-2022

Κυκλοφόρησε το Τεύχος 1 / Τόμος 16 Φεβρουαρίου 2022 του ISSMGE Bulletin με τα ακόλουθα περιεχόμενα:

- **Presidential's message**
- **ISSMGE Time Capsule Project**
- **TC corner**
 - TC309/TC304/TC222: 3rd ML dialogue
 - TC107 reestablishment
- **Conference reports**
 - Engineering Challenges in Rehabilitation of Damaged Historical Monuments in Mosul, Iraq
 - Eurasian Forum on Seismology Engineering, Geotechnics and Structural dynamics, SEISMO-SIBGEOTECH-2021
 - International Conference on Geocryological Engineering Research
- **Event Diary**
- **Corporate Associates**
- **Foundation Donors**



International Journal of Geoenvironment Case Histories

An official journal of the International Society for Soil Mechanics and Geotechnical Engineering
Issue 1, Volume 7

www.geocasehistoriesjournal.org/pub/issue/view/51

[Editorial](#), Giovanna Biscontin, Ryosuke Uzuoka, Akira Murakami

[A Case Study on the Progressive Failure Mechanism of I-180 Slope Using Numerical and Field Observations](#), Binyam Mammo Bekele, Chung Song, Mark Lindemann

[Practical Design, Numerical Analysis, and Site Monitoring for Huge Arching Effect during Massive Excavation of Undercut Slope in Open-Pit Mine](#), Cheowchan Leelasukseree, Thirapong Pipatpongsa, Apipat Chaiwan, Noppadon Mungpayabal

[Ex-Post Evaluation of Countermeasures Against Residual Settlement of an Ultra-Soft Peaty Ground Due to Test Embankment Loading: A Case Study in Maizuru-Wakasa Expressway in Japan](#), Mutsumi Tashiro, Minoru Kawaida, Motohiro Inagaki, Shotaro Yamada, Toshihiro Noda

[Identification of Material Parameters by Particle Filter Using Observation Data Obtained during Construction of Rock-Fill Dam](#), Eiki Tanenaga, Kazunori Fujisawa, Akira Murakami

[Numerical Analysis of a Top-Down Constructed Deep Basement with Diaphragm Walls in Barangaroo, Sydney - A Case Study](#), Ali Parsa-Pajouh, Brad Azari, Sam Mirlatifi, Henk Buys, Ian Cullen

[Design, Construction, and Back-Analysis of a Deep Underground Parking Garage in an Urban Environment](#), Seppe Creten, Hans Verbraken, Stijn François, Christophe Bauduin

[Back Analyses of Two Deep Excavations in Hong Kong Using the Mohr-Coulomb Model with Linear Elasticity and the Hardening Soil Model](#), Charles C L Chan, Derek S M Chiu, Frankie L C Lo, Julian S H Kwan, S W Lee, Alex C O Leung



Geo-Trends Review

Issue #18 - February 2022

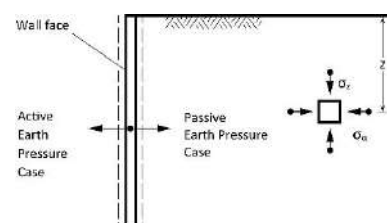
www.mygeoworld.com/geotrends/issues/18-february-2021

New TC103 Course on "Performance assessment of soils and structures by numerical analysis" by Prof. Toshihiro NODA, ISSMGE Virtual University, 03 Dec 2021



Register for free to Performance assessment of soils and structures by numerical analysis About This Course This course presents examples of performance assessment of soils and... [Read More](#)

Online Lecture Notes on Soil Mechanics - Earth Pressures, [Geoengineer.org](#) news, 26 Jan 2022 [Read More](#)



91,421 paper downloads in 2021 for the ISSMGE International Journal of Geoenvironment Case Histories! [International Journal of Geoenvironment Case Histories, ISSMGE](#), 31 Jan 2022 [Read More](#)



Annual Southwest Arizona G-I chapter Symposium, Adda Athanasopoulos-Zekkos, Geo-Institute, 16 Nov 2021

Greatly enjoyed presenting at the Annual Southwest Arizona G-I chapter Symposium on October 25, 2021, on the Lessons learned from past levee failures and the challenges these complex systems will face... [Read More](#)

Bulletin Vol. 15, Issue 6 - December 2021 circulated, ISSMGE, 10 Jan 2022 [Read More](#)

Deterministic and probabilistic case analyses of slopes, Bak Kong Low, ASCE webinar, 09 Jan 2022 [Read More](#)

Reliability-Based Design in Soil and Rock Engineering Enhancing Partial Factor Design Approaches, Bak Kong Low, Risk & Reliability, 20 Dec 2021

A new book in soil and rock engineering authored by me, published on 1 Nov 2021 by the CRC Press, 399 pages. This book is ideal for practitioners, advanced undergraduate and graduate students, r... [Read More](#)

Special issue of the ISSMGE-IJGCH: "numerical methods in geomechanics", ISSMGE, TC103, 10 Dec 2021

The special issue of the International Journal of Geotechnical Case Histories promoted by TC103, entitled "Numerical methods in Geomechanics" is on-line! Read the papers at... [Read More](#)

Four metro tunnels are completed in Hong Kong, Geoenvironment.org, news, 07 Dec 2021 [Read More](#)



Captivating Geotechnical Engineering News in 2021, Geoenvironment.org, news, 21 Jan 2022 [Read More](#)

Recognizing the YII2021 Going Digital Award winner for Geotechnical Engineering, Bentley Systems, Geo-Institute, 03 Dec 2021 [Read More](#)



Conquer Geotechnical Challenges with Confidence, Bentley Systems, Digging Deep for Safe Solutions [Connect With An Expert](#)



[Connect With An Expert](#)

New major release PLAXIS CONNECT Edition V22.00 is out!, Bentley Systems, PLAXIS, 01 Feb 2022

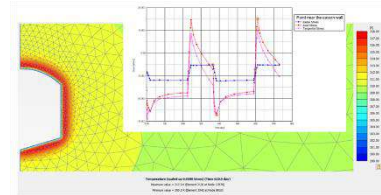


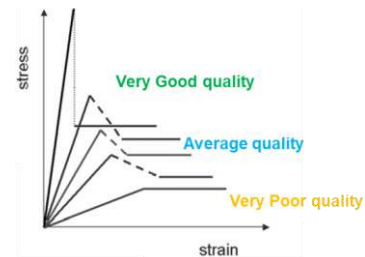
Figure 4.16 Temperature profile at the end of the 2nd depressurisation phase

PLAXIS V22 brings a major overhaul to the data structure of the material database and a more flexible and more robust way of handling project units. Due to these major changes, PLAXIS V22 will be inst... [Read More](#)

Acta Geotechnica Special Issue on "Bio-inspired Geotechnics", Julian Tao, resource, 23 Dec 2021

Call for papers for Acta Geotechnica Special Issue on Bio-inspired Geotechnics Researchers and investigators are invited to submit contributions to the special issue in Acta Geotechnica on the... [Read More](#)

How to Model Rock Engineering Problems in PLAXIS Geotechnical Analysis Software, Bentley Systems, PLAXIS, 21 Jan 2022

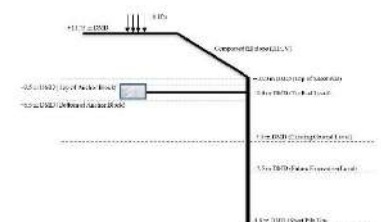


Rock engineering projects can be fascinating. Engineers working on rock need to design solutions that mobilize the natural strength of complex, largely unknown rock masses, which often play the roles... [Read More](#)

ICSE-10 proceedings now available, ISSMGE TC213, 22 Jan 2022

All papers of ICSE-10 proceedings are now available at Online Library | ISSMGE. [Read More](#)

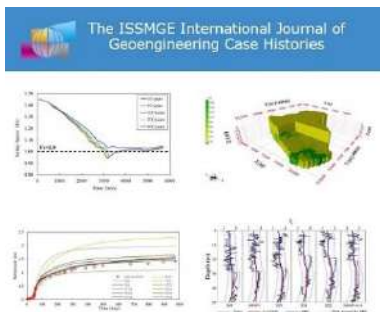
Numerical Analysis and Analytical Calculations of 3D Effects on Pullout Capacity of Anchor Blocks: Case Study in Dubai, United Arab Emirates, Geoenvironment.org, news, 15 Dec 2021, [Read More](#)



Final draft of the Failure Paths report, ISSMGE TC201, 24 Dec 2021

This report collects experiences of dike and levee failures, discusses different failed cases and summarises these experiences in failure paths that can generally be used in for... [Read More](#)

Special Issue on Engineering Practice of Risk Assessment and Management published, [International Journal of Geoenvironment Case Histories](#), TC304, 08 Nov 2021 [Read More](#)



News and Information Circular - February 2022, [ISSMGE](#), 01 Feb 2022 [Read More](#)

Integrated Resource Recovery Approach for Sustainable Solid Waste Management in Developing Countries, [Dhundi Raj Pathak](#), resource, 20 Jan 2022 [Read More](#)

The urgent need for remote sensing in geotechnical engineering, [ISSMGE](#), Time Capsule, 01 Feb 2022 [Read More](#)

TC306's GEE conferences indexed in Scopus, [ISSMGE](#), TC306, 24 Dec 2021

We are delighted to announce an important distinction for the community of geotechnical engineering education: our application for Scopus listing was approved for the series of the C... [Read More](#)

Discrete Element Method (DEM) in geotechnical engineering education, [ISSMGE](#) TC105, 20 Jan 2022

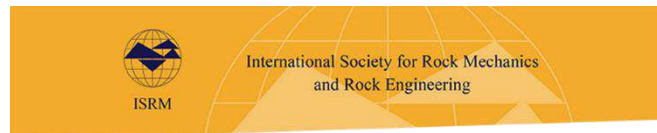
This Spring, TC105 Geomechanics from Micro to Macro is hosting a webinar series on Discrete Element Method (DEM) in geotechnical engineering education. See below. If you would like... [Read More](#)

2nd International Conference on Construction Resources for Environmentally Sustainable Technologies (CREST 2023), [DIVYESH ROHIT](#), resource, 09 Jan 2022

The organizing committee of CREST 2023 invites all interested authors to submit abstracts on the conference themes. The abstract should be of maximum 400 words in .docx and .pdf format via online subm... [Read More](#)

Support the Platinum Open Access Mission of the [ISSMGE Geocase Histories Journal](#), [International Journal of Geoenvironment Case Histories](#), [ISSMGE](#), 02 Dec 2021

Our journal is a platinum open access journal, i.e., no author or reader has to pay any costs. It is financed by forward-looking organizations that believe in equity in geotechnical engineering. If your organization is one, see the message by our Editors-in-Chief [Read More](#)



ISRM News Journal 2021 now online

The 2021 issue, volume 24, of the ISRM News Journal is now online on the ISRM website. Since 2012 the ISRM distributes the News Journal to all members in electronic version, and prints copies which are available at our sponsored symposia. The News Journal includes news from the Society life, including board and regional reports, commission work, conference and symposia reports and papers from awarded members, among other content.



https://issuu.com/isrm/docs/isrm_newsjournal_-_2021_volume_24/1?ff&hideShareButton=true



Κυκλοφόρησε το IGS Newsletter της International Geosynthetic Society με τα ακόλουθα περιεχόμενα:

IGS NEWSLETTER – February 2022

Helping the world understand the appropriate value and use of geosynthetics

<http://www.geosyntheticssociety.org/newsletters>

- New IGS Task Force Launches Inaugural Honors [READ MORE](#)

- Call for Candidates Open through 1 March 2022 IGS Council, President and Vice President Term 2022 to 2026 [READ MORE](#)
- Educate The Educators Goes Digital [READ MORE](#)
- GeoAfrica Abstract Deadline Extended [READ MORE](#)
- IGS France Welcomes New President [READ MORE](#)
- My Engineer Life With... Samira Tessarolli de Souza [READ MORE](#)
- TC-H Hosts Water And Erosion Lectures [READ MORE](#)
- Young Members Papers Competition – Beat The Deadline [READ MORE](#)
- Upcoming Webinars
- [Soil Erosion and Soil Conservation Using Geosynthetics](#) February 17 (Brisbane Time) Presented by Jane Rickson [REGISTRATION INFORMATION](#)
- Geosynthetic Solutions in Impressive Projects March 8 Presented by Max Nods, Jeroen Dijkstra, Werner Bilfinger, and Janne Kristin Pries [REGISTRATION INFORMATION](#)
- Geosynthetic Clay Liners For Dams And Dykes March 17 (repeated March 23) Presented by Kent von Maubeuge [REGISTRATION INFORMATION](#)
- Calendar of Events



<https://www.icevirtuallibrary.com/toc/jgein/29/1>

Κυκλοφόρησε το Τεύχος 1 του Τόμου 29 (Φεβρουαρίου 2022) του Geosynthetics International της International Geosynthetics Society με τα ακόλουθα περιεχόμενα:

[Mechanical and hydraulic compatibility of RAP with geosynthetics used in MSE walls](#), A. Soleimanbeigi, A. Ozocak, B. Li, E. Akmaz, A. Y. Dayioglu, B. F. Tanyu, A. H. Aydilek, W. J. Likos, 29(1), pp. 1-18

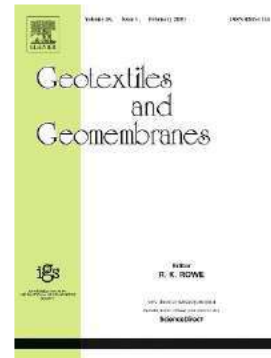
[Factors affecting geotextile filter long-term behaviour and their relevance in design](#), N. Moraci, S. Bilardi, M.C. Mandaglio, 29(1), pp. 19-42

[Self-healing of laboratory eroded defects in a GCL on silty sand](#), T.-K. Li, R. K. Rowe, 29(1), pp. 43-65

[Numerical simulation of surface blast reduction using composite backfill](#), M. Khodaparast, R. Mohamad Momeni, H. Bayesteh, 29(1), pp. 66-80

[Performance of laboratory geogrid-reinforced retaining walls under freeze-thaw cycles](#), F. Cui, C. Xiao, J. Han, S. Gao, W. Tian, 29(1), pp. 81-98

[Laboratory evaluation of dynamic shear response of sand – geomembrane interface](#), M. Samanta, R. Bhowmik, H. Khanderi, 29(1), pp. 99-112



<https://www.sciencedirect.com/journal/geotextiles-and-geomembranes/vol/50/issue/1>

Κυκλοφόρησε το Τεύχος 1 του Τόμου 50 (Φεβρουαρίου 2022) του Geotextiles and Geomembranes της International Geosynthetics Society με τα ακόλουθα περιεχόμενα:

[Editorial Board](#), Page ii

Regular Articles

[The mechanical behaviour of compacted Lambeth-group clays with and without fibre reinforcement](#), Abdullah Ekinçi, Pedro Miguel Vaz Ferreira, Mohammadreza Rezaeian, Pages 1-19

[Interface pullout resistance of polymeric strips embedded in marginal tropical soils](#), R.C. Pierozan, G.L.S. Araujo, E.M. Palmeira, C. Romanel, J.G. Zornberg, Pages 20-39

[Water exchange across a subgrade-GCL interface as impacted by polymers and environmental conditions](#), Zhi Chong Lau, Abdelmalek Bouazza, Will P. Gates, Pages 40-54

[Effect of geotextile ageing and geomembrane surface roughness on the geomembrane-geotextile interfaces for heap leaching applications](#), F.B. Abdelaal, R. Solanki, Pages 55-68

[Liquefaction and post-liquefaction resistance of sand reinforced with recycled geofibre](#), Habib Rasouli, Behzad Fatahi, Pages 69-81

[Two-dimensional soil arching evolution in geosynthetic-reinforced pile-supported embankments over voids](#), Rui Rui, Yu-qiu Ye, Jie Han, Yu-xin Zhai, ... Lei Zhang, Pages 82-98

[Analysis of cyclic shear characteristics of reinforced soil interfaces under cyclic loading and unloading](#), Meng-jie Ying, Jun Wang, Fei-yu Liu, Jing-ting Li, Shu-qi Chen, Pages 99-115

[Shaking table study on seismic behavior of MSE wall with inclined backfill soils reinforced by polymeric geostrips](#), Kaan Yünkül, Ayhan Gürbüz, Pages 116-136

[Case study and numerical simulation of PVD improved soft Bangkok clay with surcharge and vacuum preloading using a modified air-water separation system](#), Dennes T. Bergado, Pitthaya Jamsawang, Pornkasem Jongpradist, Suched Likitlersuang, ... Francisco Baez, Pages 137-153

[Interlayer bonding characterization of interfaces reinforced with geocomposites in field applications](#), F. Canestrari, F. Cardone, E. Gaudenzi, D. Chiola, ... G. Ferrotti, Pages 154-162

[Stress-strain behavior of geotextile: A proposed new indirect calculation using the static puncture test \(CBR test\)](#), José Luiz Ernandes Dias Filho, Brunner Rabello Frazão Corrêa, Paulo Cesar de Almeida Maia, Pages 163-173

[Combined influence of subsoil water content and mass per unit area on cation exchange behavior of geosynthetic clay liners](#), Yasin Karakuş, B. Enes Taşkesti, A. Hakan Ören, Pages 174-182

[Piping of silty sand tailings through a circular geomembrane hole](#), Jiying Fan, R. Kerry Rowe, Pages 183-196

Discussion & Reply

[Discussion: "Physical and numerical modelling of strip footing on geogrid reinforced transparent sand" By Jianfeng Chen,](#)

[Xiaopeng Guo, Rui Sun, Sathiyamoorthy Rajesh, Song Jiang, Jianfeng Xue, J. Geotextile Geomembr. 49 \(2\), \(April 2021\), 399-412](#), S.H. Mirmoradi, Pages 197-198

[Reply to discussion by Mirmoradi on "Physical and numerical modelling of strip footing on geogrid reinforced transparent sand"](#), Jianfeng Chen, Xiaopeng Guo, Rui Sun, Sathiyamoorthy Rajesh, ... Jianfeng Xue, Pages 199-201

ΕΚΤΕΛΕΣΤΙΚΗ ΕΠΙΤΡΟΠΗ ΕΕΕΕΓΜ (2019 – 2022)

Πρόεδρος	:	Μιχάλης ΜΠΑΡΔΑΝΗΣ, Δρ. Πολιτικός Μηχανικός, ΕΔΑΦΟΣ ΣΥΜΒΟΥΛΟΙ ΜΗΧΑΝΙΚΟΙ Α.Ε. mbardanis@edafos.gr , lab@edafos.gr
Α΄ Αντιπρόεδρος	:	Χρήστος ΤΣΑΤΣΑΝΙΦΟΣ, Δρ. Πολιτικός Μηχανικός, ΠΑΝΓΑΙΑ ΣΥΜΒΟΥΛΟΙ ΜΗΧΑΝΙΚΟΙ Ε.Π.Ε. editor@hssmge.gr , ctsatsanifos@pangaea.gr
Β΄ Αντιπρόεδρος	:	Μιχάλης ΠΑΧΑΚΗΣ, Πολιτικός Μηχανικός mpax46@otenet.gr
Γενικός Γραμματέας	:	Γιώργος ΜΠΕΛΟΚΑΣ, Δρ. Πολιτικός Μηχανικός, Επίκουρος Καθηγητής ΤΕΙ Αθήνας gbelokas@teiath.gr , gbelokas@gmail.com
Ταμίας	:	Γιώργος ΝΤΟΥΛΗΣ, Πολιτικός Μηχανικός, ΕΔΑΦΟΜΗΧΑΝΙΚΗ Α.Ε.- ΓΕΩΤΕΧΝΙΚΕΣ ΜΕΛΕΤΕΣ Α.Ε. gdoulis@edafomichaniki.gr
Έφορος	:	Γεώργιος ΓΚΑΖΕΤΑΣ, Δρ. Πολιτικός Μηχανικός, Ομότιμος Καθηγητής Ε.Μ.Π. gazetas@central.ntua.gr , gazetas50@gmail.com
Μέλη	:	Ανδρέας ΑΝΑΓΝΩΣΤΟΠΟΥΛΟΣ, Δρ. Πολιτικός Μηχανικός, Ομότιμος Καθηγητής ΕΜΠ aanagn@central.ntua.gr Παναγιώτης ΒΕΤΤΑΣ, Πολιτικός Μηχανικός, ΟΜΙΛΟΣ ΤΕΧΝΙΚΩΝ ΜΕΛΕΤΩΝ Α.Ε. otmate@otenet.gr Μαρίνα ΠΑΝΤΑΖΙΔΟΥ, Δρ. Πολιτικός Μηχανικός, Αναπληρώτρια Καθηγήτρια Ε.Μ.Π. mpanta@central.ntua.gr
Αναπληρωματικά Μέλη	:	Χρήστος ΣΤΡΑΤΑΚΟΣ, Πολιτικός Μηχανικός, ΝΑΜΑ Α.Ε. stratakos@namalab.gr Βάλια ΞΕΝΑΚΗ, Δρ. Πολιτικός Μηχανικός, ΕΔΑΦΟΜΗΧΑΝΙΚΗ Α.Ε. vxenaki@edafomichaniki.gr
Εκδότης	:	Χρήστος ΤΣΑΤΣΑΝΙΦΟΣ, Δρ. Πολιτικός Μηχανικός, ΠΑΝΓΑΙΑ ΣΥΜΒΟΥΛΟΙ ΜΗΧΑΝΙΚΟΙ Ε.Π.Ε. editor@hssmge.gr , ctsatsanifos@pangaea.gr

ΕΕΕΕΓΜ

Τομέας Γεωτεχνικής
ΣΧΟΛΗ ΠΟΛΙΤΙΚΩΝ ΜΗΧΑΝΙΚΩΝ
ΕΘΝΙΚΟΥ ΜΕΤΣΟΒΙΟΥ ΠΟΛΥΤΕΧΝΕΙΟΥ
Πολυτεχνειούπολη Ζωγράφου
15780 ΖΩΓΡΑΦΟΥ

Τηλ. 210.7723434
Τοτ. 210.7723428
Ηλ-Δι. secretariat@hssmge.gr ,
geotech@central.ntua.gr
Ιστοσελίδα www.hssmge.org (υπό κατασκευή)

«ΤΑ ΝΕΑ ΤΗΣ ΕΕΕΕΓΜ» Εκδότης: Χρήστος Τσατσανίφος, τηλ. 210.6929484, τοτ. 210.6928137, ηλ-δι. ctsatsanifos@pangaea.gr,
editor@hssmge.gr, info@pangaea.gr

«ΤΑ ΝΕΑ ΤΗΣ ΕΕΕΕΓΜ» «αναρτώνται» και στην ιστοσελίδα www.hssmge.gr